VYSOKÉ UČENÍ TECHNICKÉ V BRNĚ
BRNO UNIVERSITY OF TECHNOLOGY

FAKULTA STROJNÍHO INŽENÝRSTVÍ
FACULTY OF MECHANICAL ENGINEERING

ÚSTAV KONSTRUOVÁNÍ
INSTITUTE OF MACHINE AND INDUSTRIAL DESIGN

THE EFFECT OF SYNOVIAL FLUID CONSTITUENTS ON LUBRICATION OF HIP JOINT REPLACEMENTS

DIZERTAČNÍ PRÁCE
DOCTORAL THESIS

AUTOR PRÁCE — Ing. David Nečas
AUTHOR

ŠKOLITEL — prof. Ing. Martin Hartl, Ph.D.
SUPERVISOR

BRNO 2016

STATEMENT

I hereby declare that I have written the PhD thesis *The Effect of Synovial Fluid Constituents on Lubrication of Hip Joint Replacements* on my own according to advice of my supervisor prof. Ing. Martin Hartl, Ph.D., and using the sources listed in references.

Brno, _____ .....

David Nečas

BIBLIOGRAPHICAL REFERENCE

NEČAS, D. *The Effect of Synovial Fluid Constituents on Lubrication of Hip Joint Replacements*. PhD thesis. Brno University of Technology, Faculty of Mechanical Engineering, Institute of Machine and Industrial Design. Supervisor: prof. Ing. Martin Hartl, Ph.D.

ACKNOWLEDGEMENT

I would like to thank my supervisor prof. Ing. Martin Hartl, Ph.D. as well as the head of Tribology research group prof. Ing. Ivan Křupka, Ph.D. for their support and advice during my whole doctoral study. Special thanks must go to doc. Ing. Martin Vrbka, Ph.D. for his help and motivation. Also, I would like to thank to all my colleagues at Institute of Machine and Industrial Design for friendly and positive atmosphere. Finally, I express my huge thanks to my parents and to my great brother Daniel!

ABSTRACT

The dissertation thesis deals with the lubrication mechanisms within hip joint replacements. A systematic study of protein film formation considering various materials and operating conditions was conducted, focusing on the role of particular synovial fluid proteins while the simultaneous presence of other proteins. Since the previously applied experimental approaches did not allow to separate the individual constituents of the model fluid, an optical measurement method based on fluorescent microscopy was developed. The verification of the method is presented performing two different studies focusing on the film thickness determination and lubricant rupture ratio at lubricated contact outlet, respectively. Due to several limitations of the fluorescent microscopy, the research was supported by the use of optical interferometry method, whose usage is demonstrated in the study dealing with the protein film formation in hip joint replacements considering real conformity of rubbing surfaces. The latest part of the thesis introduces a novel methodological approach enabling to assess the role of proteins in relation to protein film thickness based on in situ observation of the contact zone. The thesis presents original results extending the knowledge in hip replacement biotribology area towards the further development of implants preventing its failure due to limited service life.

KEYWORDS

Biotribology, hip replacement lubrication, protein, albumin, γ-globulin, synovial fluid, film thickness, fluorescent microscopy, optical interferometry

ABSTRAKT

Dizertační práce se zabývá mechanismy mazání v náhradách kyčelního kloubu. Byla provedena systematická studie formování proteinového filmu při zahrnutí různých materiálů a provozních podmínek. Hlavní pozornost je přitom věnována roli jednotlivých proteinů obsažených v synoviální kapalině při současné přítomnosti dalších proteinů. Jelikož metody aplikované v předchozích studiích neumožňovaly separovat jednotlivé složky maziva, byla vyvinuta optická měřící metoda na principu fluorescenční mikroskopie. Z důvodu verifikace metody byly provedeny dvě nezávislé studie zaměřené na měření tloušťky mazacího filmu a dělení maziva na výstupu mazaného kontaktu. Z důvodu určitých limitací fluorescenční mikroskopie byla dále využita i metoda optické interferometrie, jejíž využití je ilustrováno ve studii zabývající se formováním mazacího filmu v náhradách kyčelního klubu při uvažování reálné konformity třecích povrchů. Závěrečná část práce představuje nový metodologický přístup založený na in situ pozorování kontaktní oblasti umožňující popsat roli jednotlivých proteinů ve vztahu k vývoji tloušťky mazacího filmu. Práce obsahuje originální výsledky, které přináší nové poznání v oblasti biotribologie náhrad kyčelního kloubu vedoucí k dalšímu vývoji implantátů při snaze zabránit jejich selhání v důsledku omezené životnosti.

KLÍČOVÁ SLOVA

Biotribologie, mazání náhrad kyčelního kloubu, protein, albumin, γ-globulin, synoviální kapalina, tloušťka filmu, fluorescenční mikroskopie, optická interferometrie

CONTENTS

1 INTRODUCTION

Total hip replacement is recognized to be one of the most successful and most applied surgical treatment of modern medicine. According to Heatlh at a Glance 2015: OECD indicators [1], 161 operations per 100 000 inhabitants were conducted in OECD countries in 2013, as can be seen in Fig. 1. Moreover, the number of operations still increases. Despite a rapid improvement of implant materials, hip replacements still suffer from limited longevity which is estimated to be between 10 – 20 years [2]. Since the need of revising operations substantially affects the life quality of patients, it is strongly desired to extend the durability of replacements.

The main cause of implant failure is aseptic loosening as a consequence of osteolysis [3]. During the articulation of the components, wear particles are released from the surfaces, interacting with the surrounding hard and soft tissues, leading to inflammation reactions and degradation of the tissue eventually. Therefore, recently the authors focused on in vitro testing of wear rate dependently on materials, geometry, or operating conditions [4]-[6]. It was revealed that the fundamental parameter influencing the wear of rubbing surfaces is implant material. In general, two different combinations are being implanted nowadays; hard-on-soft combination presented by very stiff femoral head (CoCrMo alloys, ceramic) and compliant acetabular cup (ultra-high molecular weight polyethylene - UHMWPE, highly cross-linked polyethylene - HXPE) and hard-on-hard combination where both components are made from metal or ceramic. From the performed studies, it is apparent that ceramic-on-ceramic implants exhibit the lowest wear rate. On the contrary, the highest wear occurs in the case when the cup is made from polymer [7].

Although the information about wear rate might be very important in relation to implant longevity, so far, little is known about the interfacial lubricating processes inside the contact. Even though, such a knowledge can lead to further development in the area of implants design or material towards the extension of the service life of replacements eventually.

The tribological performance of contact pair is substantially influenced by the prevailing lubrication regime. Sufficient separation of rubbing surfaces by fluid film can help to protect the surfaces against mutual contact potentially minimizing wear. However, it was discussed in literature that hip implants usually operate under boundary or mixed lubrication regime [8]. In terms of lubrication, one of the crucial parameters is the lubricant film thickness. In general, two different approaches can be employed for film thickness determination; numerical simulations and experimental measurements. Several studies have been conducted focusing on the numerical predictions of film thickness in hip replacements [9]-[11]. However, it must be highlighted that human synovial joints are lubricated by synovial fluid (SF) which is non-Newtonian liquid and corresponds to shear thinning behaviour [12],[13]. Moreover, it is well known that protein adsorption onto rubbing surfaces, whose simulation is particularly complicated, substantially influences film thickness and tribochemical layers [14]-[16].

The aim of the present thesis is to provide an analysis of lubricant film formation in hip joint replacements based on situ observations using optical methods. The main

attention is paid to the role of particular SF proteins (albumin, γ-globulin). So far, there is not such a study providing the information about individual protein behaviour considering model fluid containing more than one constituent. For this purpose, a novel methodological approach has to be developed.

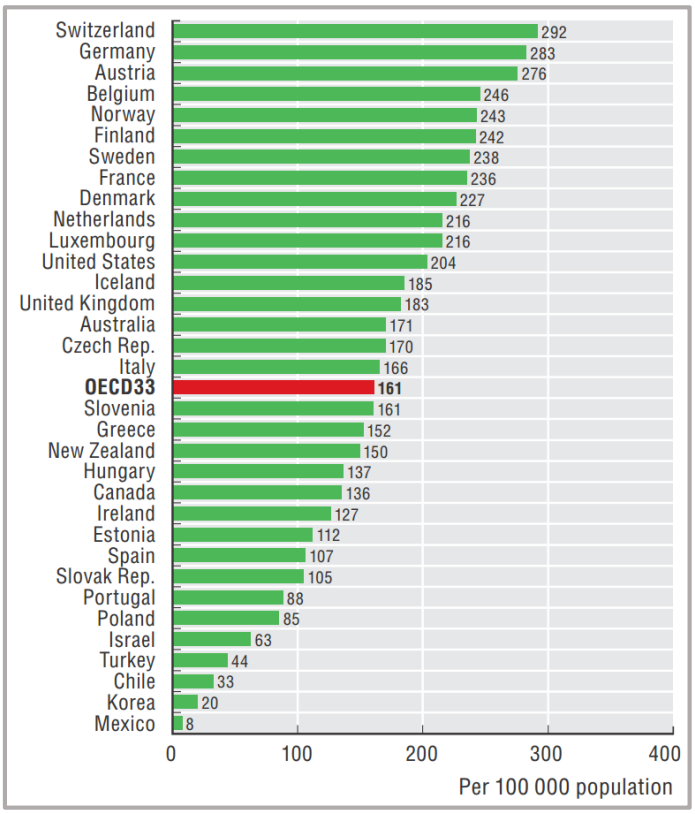

Figure 1. Hip replacement surgery in 2013 [1].

2 STATE OF THE ART

2.1 Experimental methods for film thickness investigation

An experimental investigation in tribology experienced a rapid improvement during the last few decades. Summary of the experimental methods enabling film thickness measurements inside the contact of two bodies was provided in several references [17]-[19]. Neglecting the unique approaches, often developed for specialized particular investigations, two groups of methods can be identified, in general.

The first is group is represented by the electrical techniques based on the change of electrical quantity, i.e. resistance, voltage, or capacitance. The use of electrical methods in the area of hip biotribology was introduced by Dowson et al. [20] and Smith et al. [21], who performed qualitative analysis of surfaces separation over the gait cycle in metal [20] and ceramic [21] rubbing pairs using an electrical resistivity method. One of the main drawbacks of the described approach is that the studied materials have to be conductive. Therefore, in the case of ceramic, the base material had to be coated with thin conductive layer [21] which could influence the character of film development. Although the electrical methods provide the information about the surface separation, it does not allow to observe the contact in situ disabling to describe the character of protein film formation.

Another experimental approach utilizes optical methods enabling direct contact observations. Based on the critical review, two different optical methods suitable for film thickness determination can be recognized; optical interferometry and fluorescent microscopy. As is discussed in the following chapter, optical interferometry is well-established routine technique for film thickness determination. It was proved by Hartl et al. [22] that the method provides very accurate results of the size of the gap between the two surfaces with the resolution down to 1 nm. However, due to the principle of the method, it is not possible to distinguish the individual components contained in the lubricant.

In an effort to be able to determine the role of particular constituents contained in model fluid, optical method based on the fluorescent microscopy may be a suitable solution. The results are expressed in terms of fluorescent intensity in this case [18]. By using appropriate fluorescent markers, it is possible to label the individual parts of the lubricant, so the qualitative information about the lubricant layer development can be obtained. Due to the principle of the method, fluorescent microscopy brings several advantages enhancing the measurement possibilities, such as:

- Measurement in a wide range of thicknesses from tens of nm to units of mm.
- Investigation of non-reflective, compliant materials (polymers, tissues).
- Measurement of contact bodies of high surface roughness.
- Determining of lubricant flow.

A detailed description of the mentioned experimental methods is provided in chapter 4. It should be highlighted, that the method based on fluorescent microscopy has never been used before for in-situ analysis of lubrication mechanisms in hip joint replacements. Therefore, the following part is focused on the review of the use of the method for tribological analyses.

2.2 Fluorescent microscopy in tribology

The first research work employing the fluorescent microscopy for the measurement of lubricant layer was given by Smart and Ford [23]. Mercury lamp induced fluorescence was used for the measurement of lubricant layer on rotating cylinder. It was discussed that the method enables to measure the lubricant film in the range from 0.1 µm to 1 mm dependently on calibration accuracy. In the paper, the authors detected the film thickness from 800 nm to 35 µm, according to the rotations of the steel cylinder. The knowledge was discussed in relation to starvation of rolling bearings. Global tendency of film thickness is shown in Fig. 2. It was found that the thickness of the lubricant layer in the case of turbine oil Castrol 3C and 10 000 rpm was only around 1 µm. It is expected that the film entering to the contact is too thin to ensure sufficient separation of the rubbing surfaces preventing starvation.

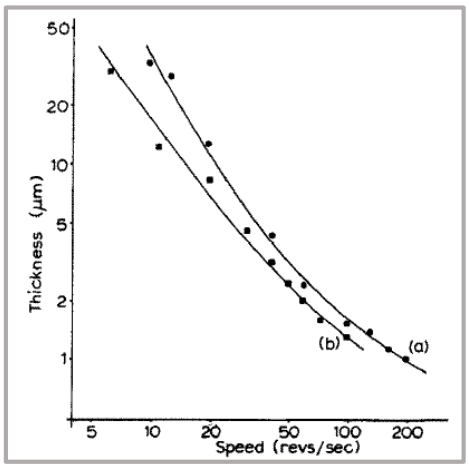

Figure 2. Development of film thickness as a function of speed for Castrol 3C oil; a) steel surface, b) chrome coated surface [23].

The following paper was introduced by Ford and Foord [24], who replaced mercury lamp by the laser of a wavelength λ = 441.6 nm. The consequence of the use of the laser as an excitation source is mainly a simpler design of the experimental setup. Publication dealt, among others, with the differences between lamp and laser excitation, while several points were highlighted:

- If the lamp is used as the excitation source, it is necessary to employ optical components from silica glass; which is unnecessary in the case of laser, when standard optical glass is usable.
- Laser of a defined wavelength is more stable and much more powerful leading to more intense emission.
- Mineral oils emit fluorescence naturally without the need of adding the fluorescent dye. In that case, the deep to which the illumination is able to penetrate, is observed. So called “excitation penetration” is much better when the oil is excited by the laser.
- In meaning of safety, laser is visible (contrary to UV lamp) simplifying the configuration of the optical system and limiting the use of protective equipment.

The authors also discussed a decay of fluorescence emission with time as a consequence of illumination. This phenomenon was observed even in the case of very stable lubricants after some time. The solution of such a problem might be the usage of the laser in a pulse regime or lowering its power, which is; however, associated with the lowering of emission. The decay of fluorescence signal with time for gas turbine oil is shown in Fig. 3.

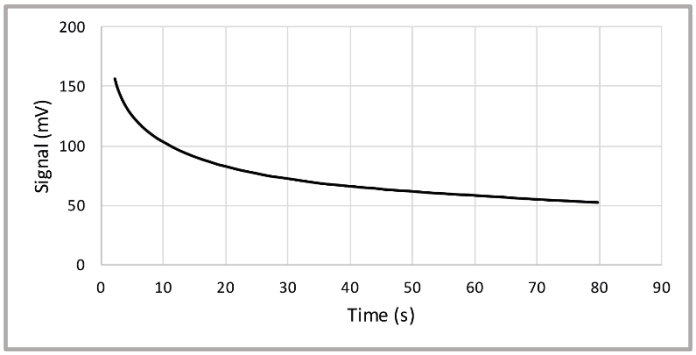

Figure 3. Decay of the fluorescence emission as a function of time for turbine oil. The figure was reproduced based on [24].

Subsequent studies employed the fluorescent method for investigation in real applications [17],[25],[26]. Poll and Gabelli [17],[25] focused on the analysis of lubricant film in the contact of shaft and rotary lip seals, the function of which is to ensure system reliability, prevent the leakage of the lubricant, and prevent the contamination of lubricant. Initially [25], a numerical model for film thickness prediction considering the viscoelastic behaviour of polymeric seals was established, partially based on the images of the contact obtained using halogen lamp induced fluorescence. The numerical model was later verified by the use of electric resistance method, while very good agreement was achieved in the whole range of investigated speeds [17]. As the resistance method suffered from limited readability, Poll et al. [26] employed the fluorescent method for direct measurement of film thickness later. The authors were able to measure the lubricant film from 0 to 10 µm with the readability equal to 0.02 microns. The issue of calibration was discussed in the study as well. The intensity/thickness dependence was obtained using steel plate and glass shaft, while the investigated configuration consisted of glass shaft and polymeric lip seal. According to authors´ recommendations, for the calibration, the glass shaft should be substituted by the steel shaft with an optical window to avoid inaccuracies coming from different tribological behaviour of glass and steel, respectively.

For the purposes of laboratory investigations, ball-on-disc experimental device, introduced by Gohar [27], is extensively used in the area of tribology. The first combination of ball-on-disc device with the fluorescent method for film thickness measurement was introduced by Sugimura et al. [28]. Mineral oils were used as the test lubricants. Although the oils emit fluorescence naturally when illuminated in UV, to enhance emission, base oils were doped by a Pyrene fluorophore, in addition. The experiments were realized under pure sliding condition, whilst the steel ball was stationary and the glass disc rotated. Two undesirable phenomena limiting the usage

of the method were discussed by the authors. The first point was the interference of light beams arising at the interfaces disabling to process a precise calibration. The authors solved this issue by replacing the steel ball by glass lens for calibration. Although the interference disappeared, it must be taken into account that the calibration may be influenced by the different optical properties of calibration and test samples, potentially affecting results accuracy. Another point apparently influencing the results was background effect caused by cavities formed at the outlet zone. This problem was not completely solved in the study.

Substantial improvement of the fluorescent method was provided by Hidrovo and Hart, who introduced dual emission laser induced fluorescence (DELIF) [29] and emission reabsorption laser induced fluorescence (ERLIF) [30] principles. In the case of DELIF (Fig. 4 - left), the lubricant is doped by two fluorescent dyes with the similar excitation, but different emission wavelengths. The method is based on ratiometric principle allowing to normalize the emission of one dye against the emission of the second one, eliminating undesirable phenomena such as illumination intensity fluctuation or background effect pronounced by Sugimura et al. [28].

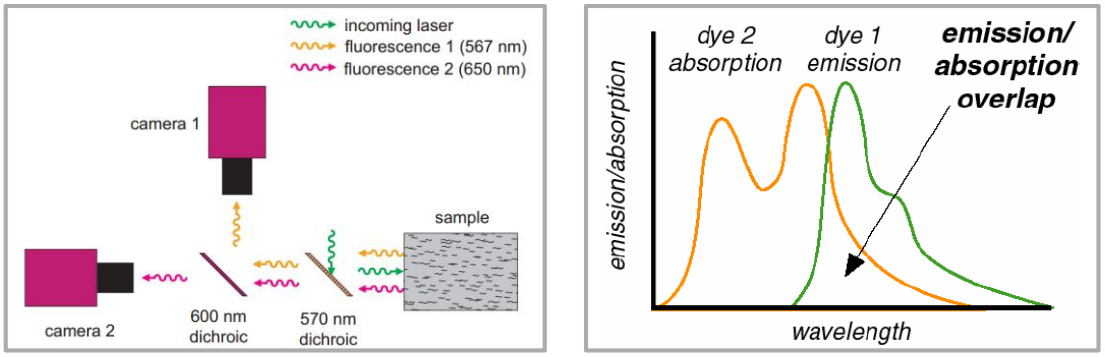

Figure 4. Left: Scheme of the DELIF principle [29]. Right: Scheme of the emission reabsorption [30].

ERLIF principle occurs when the emission wavelength of the first dye is similar to the excitation wavelength of the second dye, or vice versa, see right part of Fig. 4. In that case, two events can be observed; one dye is, in addition to external illumination, excited by the emission produced by the second dye. This effect is negligible since the emission intensity is usually considerably lower compared to the external light source intensity. However, the more substantial problem is that the emission of the second dye is lowered by the intensity being reabsorbed by the first dye. This effect must be taken into account during the data evaluation. It was highlighted that the both approaches are suitable for optically thick systems (> 5 µm). In the case of thinner films, the ratio of intensities is almost constant and the level of reabsorption is negligible. The authors were able to measure thicknesses in the range from 5 to 400 µm with 1% accuracy. The method was employed for the investigation of surface topography of the coin as well. Initially, calibration was processed using a known wedge geometry finding the dependence between the layer thickness and fluorescent intensity (Fig. 5). As the fluorophores, Pyrromethene 567 and Pyrromethene 650 were added into a base oil. Despite a very good accuracy and system stability, it should be mentioned that both the approaches were no more

applied for film thickness measurements by other authors, especially due to limitation of minimum detectable thickness and particularly complicated image processing based on the provided mathematical model.

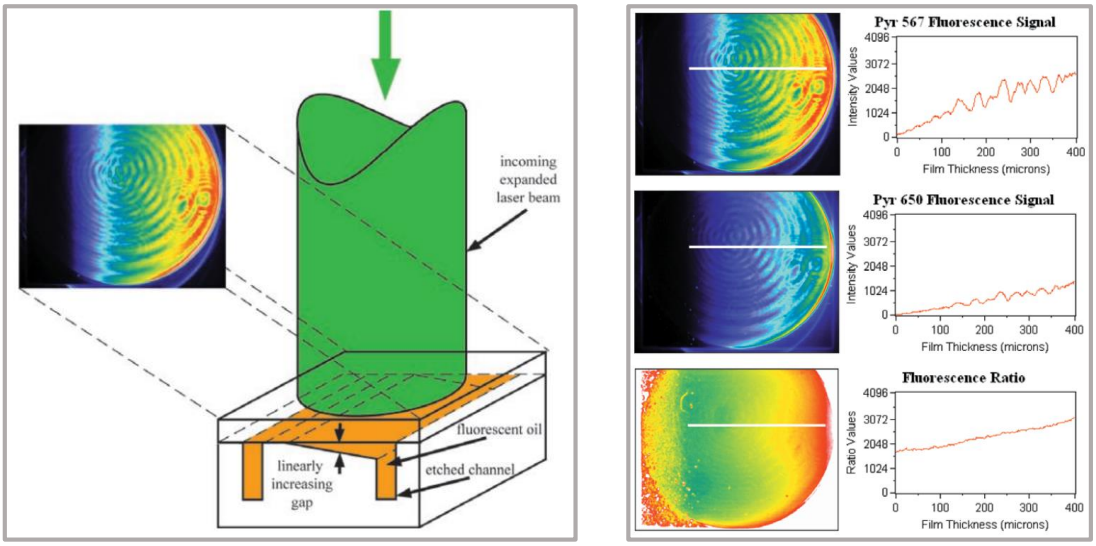

Figure 5. Left: Calibration configuration based on the known wedge geometry. Right: Dependence of film thickness on intensity for different fluorophores [30].

Azushima measured the lubricant film thickness between the tool and the workpiece sheet during drawing process [31],[32]. Topography of the surfaces after drawing was also investigated. The author clearly proved the principle of linearity between the fluorescence intensity and film thickness. The calibration consisted of the following steps. At the beginning, two glass sheets were weighted, while in a further step fluorescently doped lubricant was added between the sheets. The intensity was captured and the sheets were weighted again. From the change of the mass and the dimensions of the sheets, the thickness of the lubricant could be exactly determined. Several repetitions were conducted giving the dependence between the oil film thickness and light intensity, as is illustrated in Fig. 6.

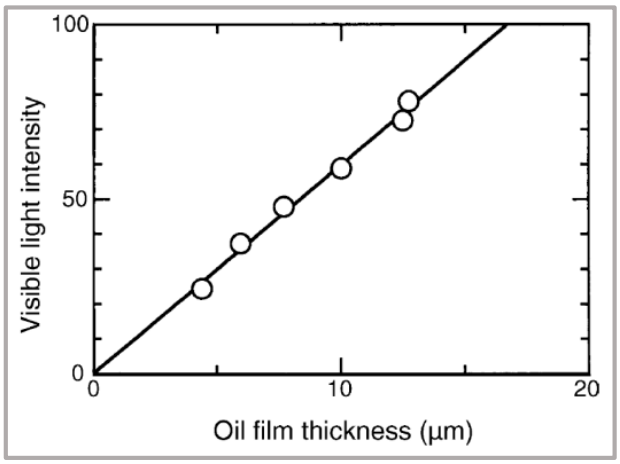

Figure 6. Dependence between the oil film thickness and light intensity [31],[32].

The use of the laser induced fluorescence (LIF) for determination of lubricant film thickness in an elastohydrodynamic (EHD) contact was presented by Reddyhoff et al. [33]. It was discussed that the knowledge about the formation of film inside the contact can help to predict friction in EHD contact, which is beneficial, since it is known that friction determines power losses and; therefore, the efficiency of machines eventually. The contact was formed between the steel ball and the glass disc, while the contact operated under fully flooded conditions. Initially, the method was verified measuring the film intensity and comparing the results with those of quantitative film thickness obtained by optical interferometry. The experiments were carried out under pure rolling conditions at rolling speed equal to 75 mm/s. As a test lubricant, glycerol doped by Eosin fluorophore was employed. Applied load was 20 N and ambient temperature was considered. Image on the left of Fig. 7 shows the contact shape while the corresponding intensity of lubricant film along the highlighted profile is displayed in the graph on the right of Fig. 7, where the film thickness evaluated by optical interferometry is plotted as well. Although the fluorescent intensity was not calibrated to film thickness determination, it is evident that there is a very satisfactory correlation of the both curves.

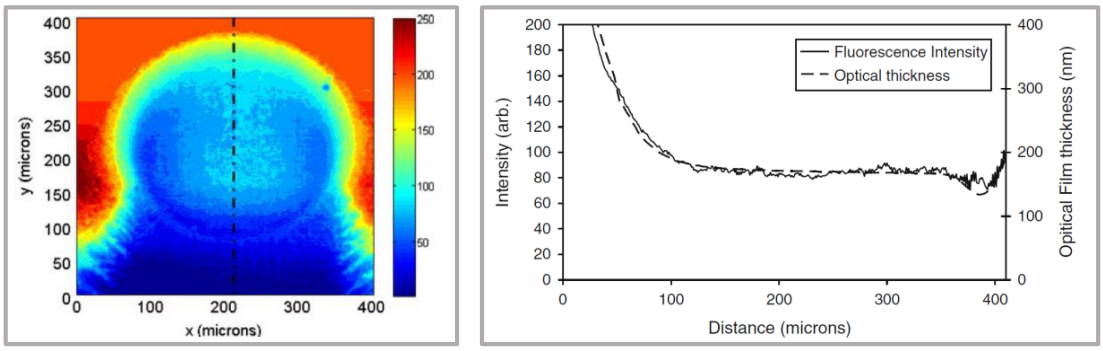

Figure 7. Left: Map of fluorescent intensity in EHD contact. Right: Film thickness in the profile (dotted dashed line in the contact image) determined by fluorescent microscopy and optical interferometry. Inlet is on the top and left, respectively [33].

Subsequently, the lubricant flow was determined by adding fluorescently doped lubricant to the contact drag, while the main attention was paid to the observation of the boundary between the stained and unstained lubricant entraining the contact. Fluorescent maps showing the progression of the doped glycerol through rolling contact with 0.5 ms intervals are displayed in Fig. 8. Total time of the progression, since there was no dye, till the flooding of the contact with dye, was 5.5 ms. It should be noted that the intensity depends on film thickness, as well as on the amount of dye presented inside the contact.

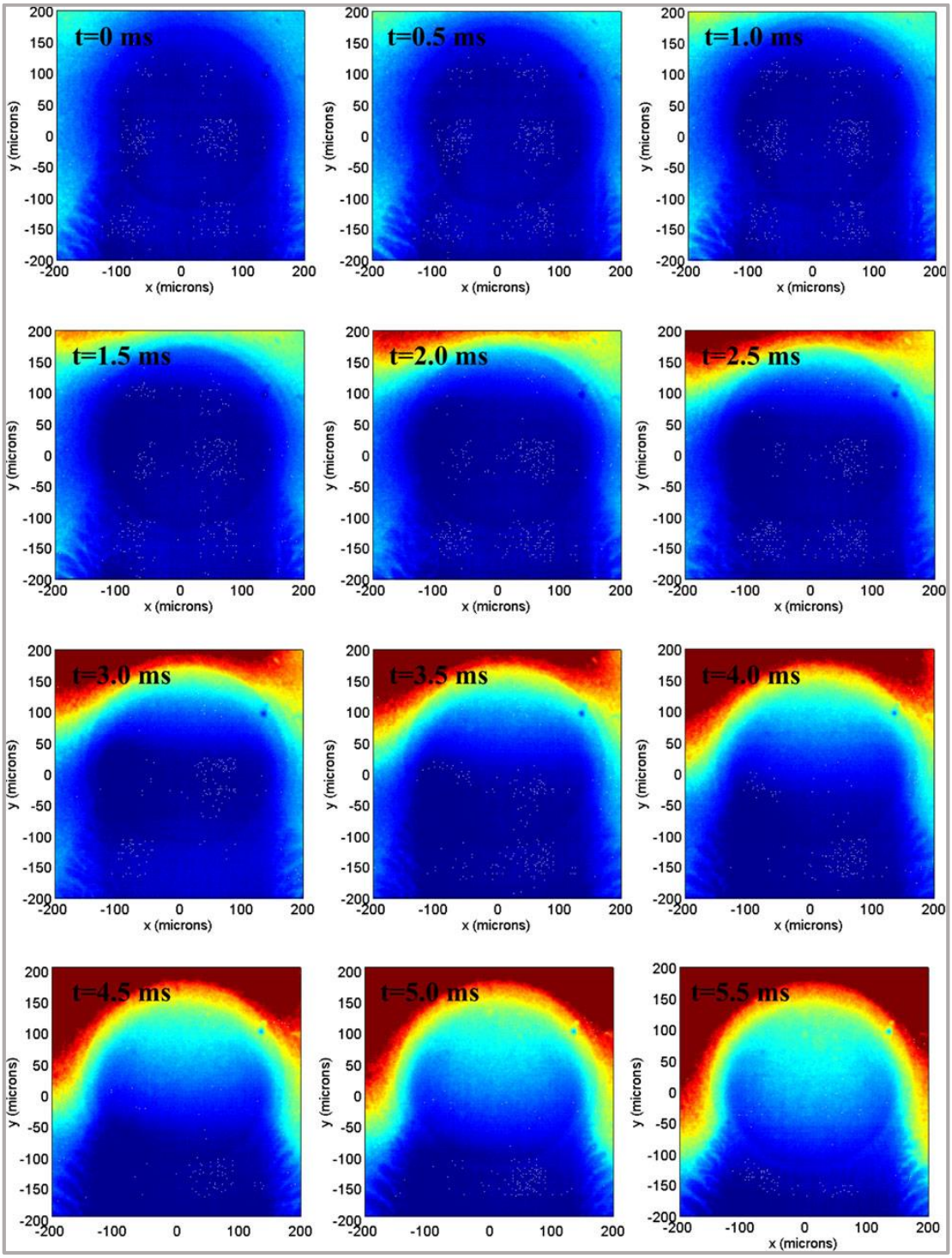

Figure 8. Flow of the stained lubricant through the contact under pure rolling conditions. Inlet is on the top of each image [33].

Another experimental approach for lubricant flow investigation, based on fluorescent method, is known as fluorescence recovery after photobleaching (FRAP). Ponjavic et al. [34] employed FRAP to investigate through-thickness velocity profiles and slip length in elastohydrodynamic lubricated (EHL) contact. Combination of the two lasers was used; 473 nm, 40 mW blue laser was employed for photobleaching,

and 488 nm, 25 mW cyan laser was used for excitation. Initially, the methodology was validated by spatiotemporal intensity distribution of plane Couette flow in a 1 μm polybutene film between two slides, while the bottom slide was stationary and the top slide velocity was 26.3 μm/s. Bleaching and exposure time were 25 ms and 180 ms, respectively. The photobleached plug initial diameter was 20 μm. Comparison of the experimental and numerical data is shown in Fig. 9. Subsequently, an EHD contact between the steel ball loaded against the glass slide was studied. Applied load of 5 N resulted to a theoretical Hertzian pressure of 315 MPa. Sliding speed was 360 μm/s leading to the expected film thickness of 170 nm. The results from experimental and numerical analysis are compared in Fig. 10.

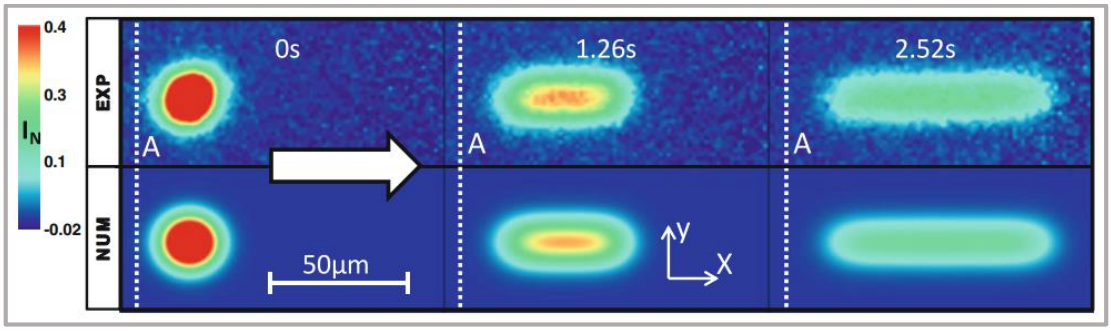

Figure 9. Validation of the methodological approach; comparison of the experimental (top) and numerical (bottom) spatiotemporal intensity distribution. White arrow indicates the shearing direction of the fluid [34].

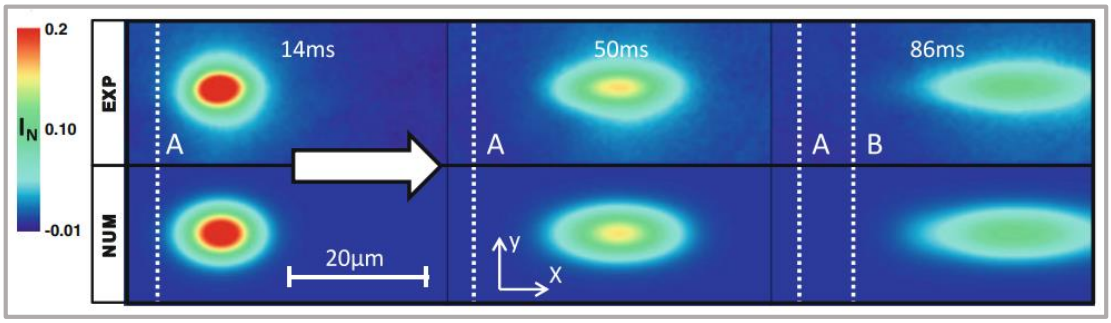

Figure 10. Photobleaching imaging velocimetry results for EHD lubricated contact [34].

Due to limitations in relation to measurement accuracy and minimum measurable film thickness, fluorescent microscopy was also successfully combined with optical interferometry several times. Qian et al. [35] investigated the lubrication failure of oil film in point EHL ball-on-disc contact at high slide-to-roll ratios (SRR). Central film thickness was measured by optical interferometry and the pool shape was observed using fluorescent microscopy. Images of the contact zone and pool shape at various speeds and SRRs are shown in Fig. 11. The authors concluded that at high SRRs, the transition from EHL to mixed or boundary lubrication regime occurs. The problem of starvation was discussed in the study as well. Due to starvation occurring in the inlet zone of the contact, thermal effects play a dominant role in the lubricated contact region, resulting to disc wear and subsequent lubricant failure.

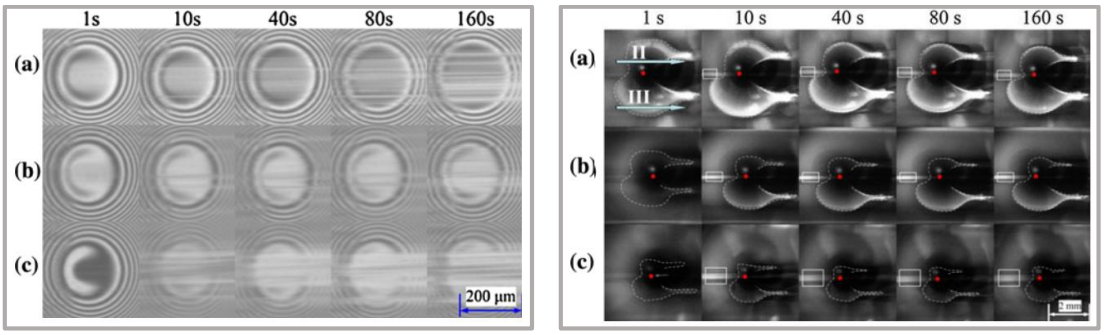

Figure 11. Images of the contact zone obtained by optical interferometry (left) and images of the pool shape obtained by fluorescent microscopy (right) under the following experimental conditions; a) u = 0.731 m/s, SRR = 1.946; b) u = 1.514 m/s, SRR = 1.974; c) u = 2.607 m/s, SRR = 1.985 [35].

The same experimental approach was consequently employed by the authors for lubricant flow analysis inside the contact under micro oil supply conditions [36]. Combination of the methods was also pronounced by Xiao et al. [37] who observed water flowing through EHD contact of the steel ball and the glass disc lubricated by hexadecane doped by a Coumarin-311. Since the water does not contain the fluorophore, a clear boundary between the fluids could be recognized.

LIF was later employed for direct measurement of film thickness in compliant contact [38]. Glass disc was sliding against polydimethylsiloxane (PDMS) pin with the radius of curvature of 12.7 mm (Fig. 12). The experiments were realized under fully flooded and starved lubrication conditions. Three various lubricants were used; pure glycerol, glycerol with distilled water in a ratio 1:1, and pure distilled water, while the dynamic viscosities were η_1 = 1.16 Pa·s, η_2 = 0.055 Pa·s, and η_3 = 0.00089 Pa·s, respectively. As a fluorophore, Eosin was added to the base lubricant as in the case of the previous study [33]. Due to low elastic modulus of the pin, very low level of load was applied, just in the range of tens of mN.

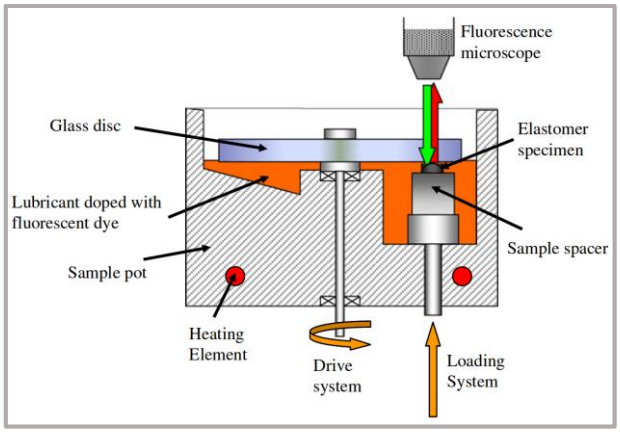

Figure 12. Scheme of the experimental configuration [38].

A measurement range in the performed study was from 200 nm to 25 µm. The results of film thickness as a function of entrainment speed under fully flooded conditions and load of 40 mN are shown in Fig. 13. In the case of glycerol, it can be clearly seen that the dependence was practically linear. The rest two lubricants

exhibited very unstable behaviour, especially at lower speeds. The tendency becomes linear at around 8 mm/s for the mixture of glycerol and water and at 25 mm/s for water, respectively.

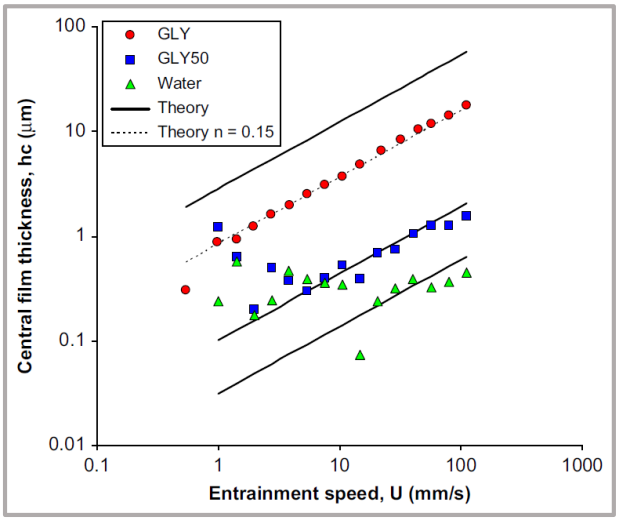

Figure 13. Development of film thickness as a function of entrainment speed for various lubricants under fully flooded conditions [38].

The authors also provided the comparison of experimental data with theoretical prediction. For mixture and water, there is a good correlation with the predicted data in the linear part of the film thickness development. Not so in the case of glycerol. As is shown in Fig. 13, the evaluated data corresponds to the prediction recalculated for lower viscosity of 0.15 Pa·s. It is expected that the deviation comes from the combination of thermal effects and hygroscopic nature of glycerol, which absorbs water vapour from the atmosphere which leads to the decrease of its viscosity. This statement was previously discussed by Bongaerts et al. [39].

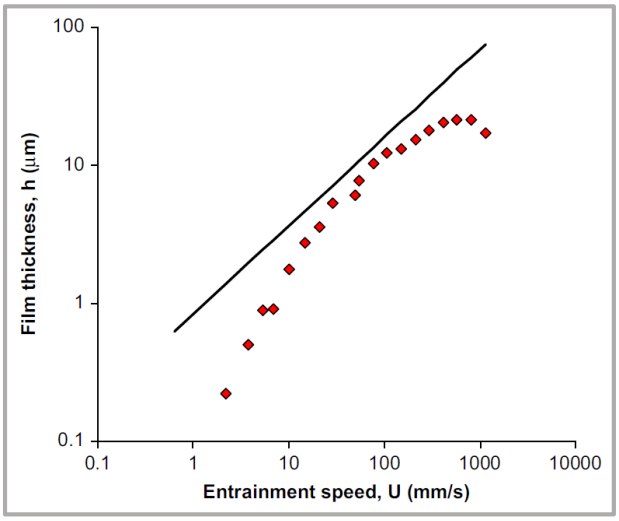

Figure 14. Development of film thickness as a function of entrainment speed for glycerol under starved conditions [38].

Film thickness results of the contact lubricated by glycerol under starved conditions and 25 mN are plotted in Fig. 14. The data are compared with fully flooded prediction considering the effective viscosity of 0.15 Pa·s. It can be seen that at high speeds a rapid divergence occurs due to starvation. In Fig. 15, contact images taken during the experiment at various speeds are displayed. The corresponding film profiles along the X and Y axis are shown in Fig. 16.

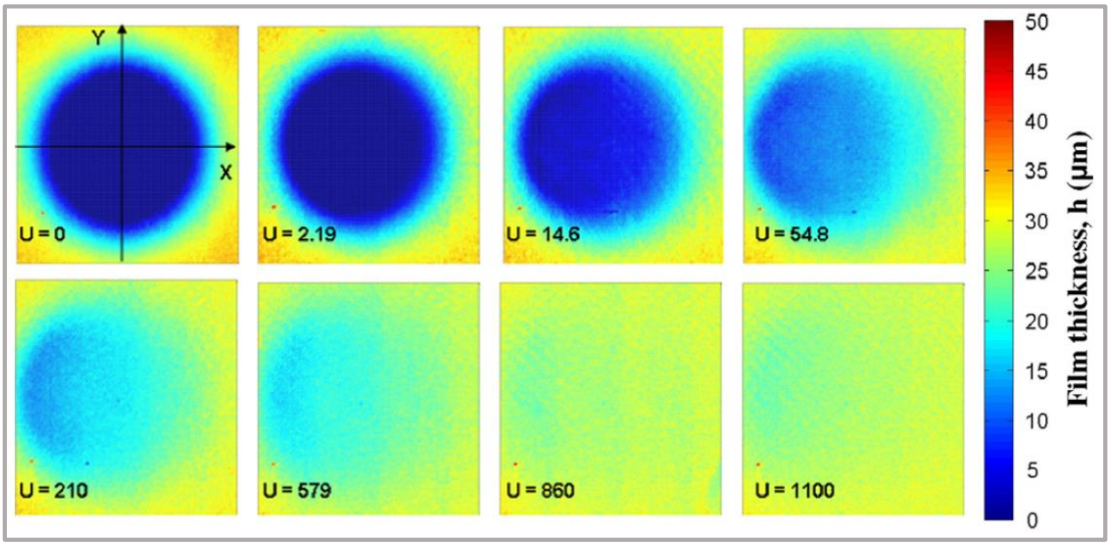

Figure 15. Film thickness maps of the contact lubricated by glycerol under starved conditions. Inlet is on the right of each image [38].

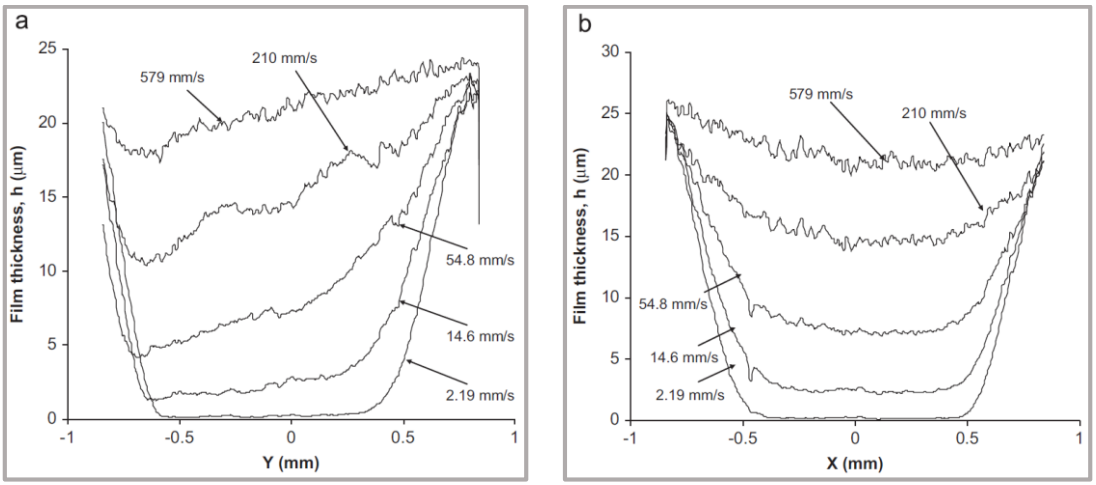

Figure 16. Profiles of film thickness along Y (a) and X (b) axis for glycerol lubricated contact under starved conditions [38].

In the consequence paper, Myant et al. [40] applied LIF investigating the effect of transient start-up and sudden halting conditions on lubricant film. The same experimental configuration (stationary PDMS pin vs. rotating glass disc), as in the previous study, was employed, and the contact was lubricated by the mixture of glycerol (90 wt%) and water (10 wt%) doped by Sulforhodamine G of an approximate concentration of 0.05 wt%. The lubricant viscosity was 40 mPa·s. In the case of start-

up motion, the end speed was 10 mm/s, while various accelerations were tested; 1000, 100, 20, 10, 6.67, and 5 mm/s^2 respectively. When sudden halting was investigated, the initial sliding speed varied from 75 to 5 mm/s, whilst sliding was maintained for around 1 min before stopping the movement to ensure stabilization of lubricant film.

The results under start-up conditions at acceleration equal to 10 mm/s^2 are shown in Fig. 17. It was observed that four different phases of film formation can be observed. Firstly, an initial contact deformation occurs immediately with the rotation of the disc. The phase is very short (≈ 0.3 s), while a slight change of the contact shape can be observed without the change of film thickness. Consequently, the surfaces are being separated by lubricant entraining the contact. During that phase a lubricant wave can be clearly observed. This phase is followed by full film formation, occurring when the wave passes through the whole contact. The lubricant film still increases. Finally, during the film relaxation phase, the film thickness is stabilized.

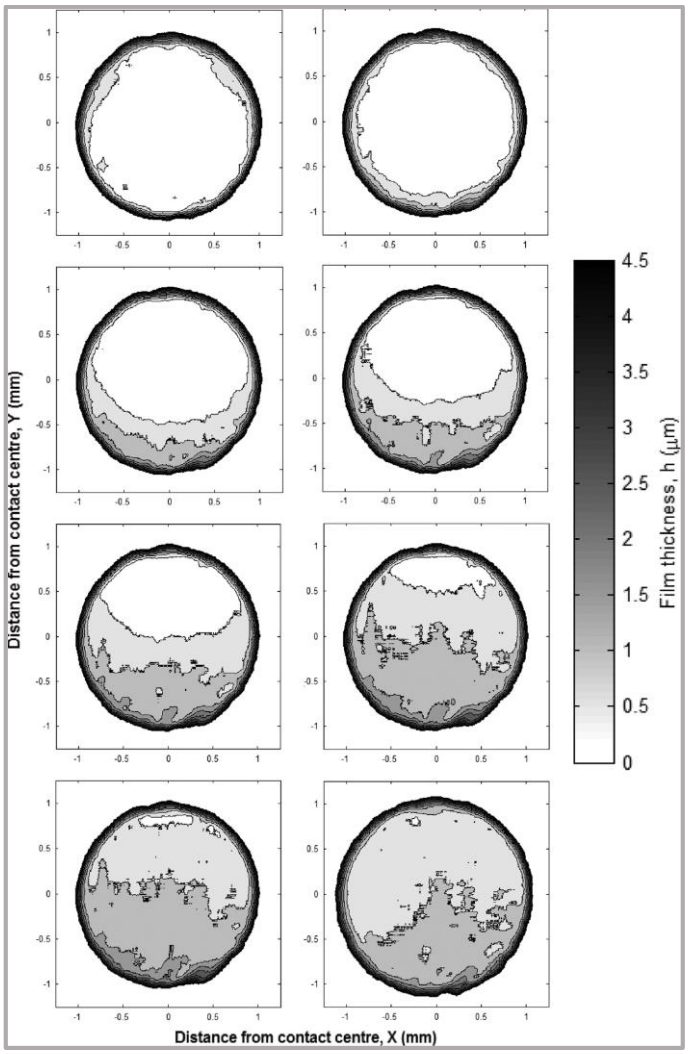

Figure 17. Maps of film thickness during start-up conditions at acceleration of 10 mm/s^2. Inlet is on the bottom of each image. Top left image is captured at time t = 0 s. Following images are taken at t = 0.13, 0.27, 0.34, 0.41, 0.55, 0.61, and 5.69 s [40].

Images of the contact under sudden halting from initial sliding speed of 75 mm/s are displayed in Fig. 18. As can be seen, film thickness decreases over several seconds. Film breakdown can be divided into two separated stages. Firstly, the contact bodies undergo rapid elastic recovery in the contact inlet and contact edges, thus leading to the entrapment of the lubricant within the central part of the contact. Consequently, the entrapped fluid is slowly squeezed out from the contact. The size of the entrapment zone was found to be dependent on the initial sliding speed.

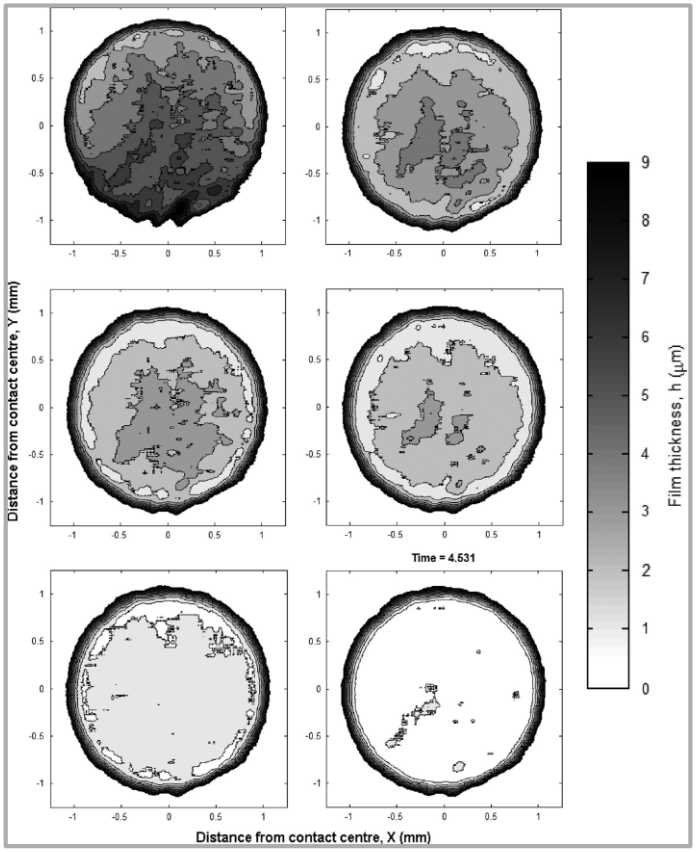

Figure 18. Maps of film thickness during sudden halting conditions from the initial sliding speed of 75 mm/s. Inlet is on the bottom of each image and the lubricant flows along Y axis. Top left image is captured at time t = 0 s. Following images are taken at t = 0.14, 0.22, 0.28, 0.77, and 5.3 s [40].

The study was followed by Fowell et al. [41], who measured the lubricant film thickness in the compliant contact in various configurations. Two non-conformal contacts were investigated; PDMS hemisphere vs. glass disc and fluorocarbon rubber (FKM) O-ring sealing vs. glass disc, respectively. Finally, the disc was substituted by concave glass lens, so the conformal setup of sealing and lens could be studied as well. As a test lubricant, mixture of glycerol (75 wt%) and water (25 wt%) doped by 0.01 wt% of Rhodamine 6G was used. Bottom part of the disc was immersed in the lubricant. Then, the lubricant is entrained to the contact as a consequence of disc/seal rotation.

PDMS/glass test was conducted under pure sliding. Radius of the pin was 12.7 mm and the pin was loaded against the disc by the force of 23.5 and 11 mN resulting to 89 kPa and 69 kPa, respectively. The range of the sliding speeds varied

from 2.4 to 1 190 mm/s for higher and from 2.4 to 221 mm/s for lower load. Film thickness maps of the contact under various loads and sliding speeds are shown in Fig. 19.

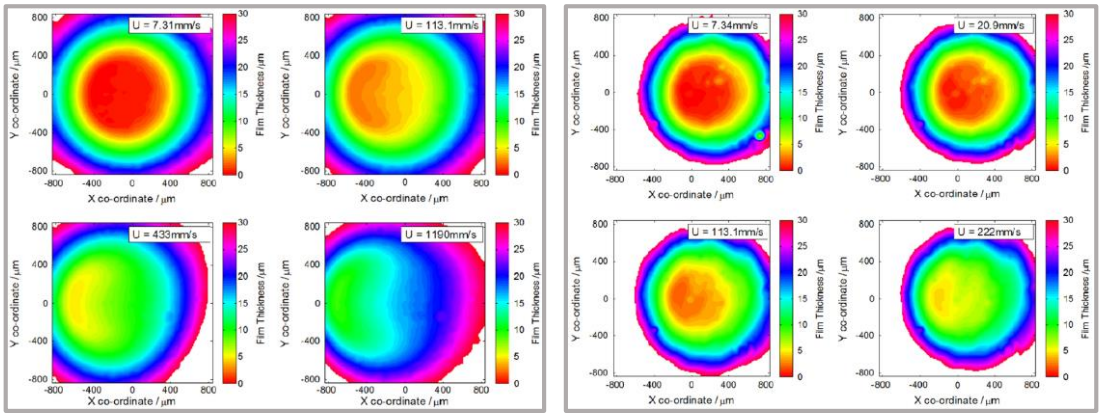

Figure 19. Film thickness maps at selected sliding speeds for PDMS pin and glass disc contact; 23.5 mN (left) and 11 mN (right) [41].

In the case of elliptical FKM O-ring and the glass disc contact, the tests were performed under pure rolling. Applied load was 5.4 N, while the estimated contact pressure reached 2.1 MPa. Speed range varied from 5.5 to 1 080 mm/s. The results showed that the film thickness increases with increasing rolling speed, in general, while the maximum thickness towards to the middle of the contact. What is in discrepancy with previous point contact is that no hydrodynamic wedge can be observed, see Fig. 20 left vs. Fig. 20 right.

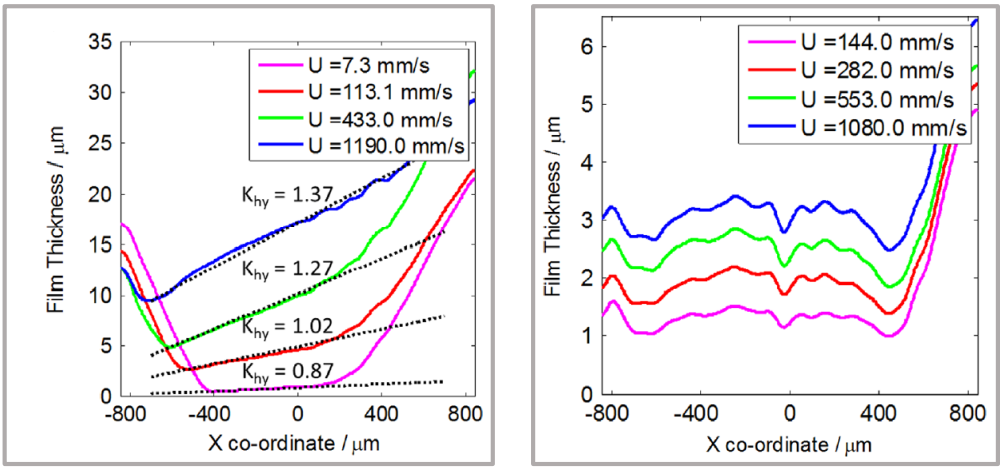

Figure 20. Profiles of film thickness along x axis for point (left) and elliptical (right) contact at selected speeds [41].

Finally, to approach the real geometry between the O-ring seal and shaft, the glass disc was substituted by glass lens to ensure high level of conformity between the counterparts. Experiments were realized under pure sliding with stationary lens and rotating barrel on which the O-ring seal was mounted. Applied load of 4.8 N and 3.63 N resulted to a contact pressures of 1.4 MPa and 1.3 MPa, respectively. The

sliding speed was changed from 9.8 to 105 mm/s. Independently of load value, film thickness was relatively thin and was less than 1 µm at all speeds. However, for both loads, the lubricant film inside the contact increased with increasing speed, while a complete separation of rubbing surfaces occurred when the speed exceeded 53.5 mm/s.

The results obtained for all the tested configurations were compared with theoretical predictions given by Hamrock and Dowson [42] and Nijenbanning et al. [43]. In the case of the first configuration, the results rather correlated to [43] at lower and were somewhere between [42] and [43] at higher load, as can be seen in Fig. 21. The results for rolling contact of O-ring seal and glass disc exhibited significant variance at lower speeds, while the data were in a good agreement with the prediction derived in [42], see Fig. 22 (left). On the contrary, conformal sliding contact between the sealing and the lens well corresponded to prediction given by Nijenbanning et al. [43], especially at higher load (Fig. 22 right). This indicates that the relative accuracy of the predictive models is strongly dependent on the applied conditions, as well as on the shape of the contact zone.

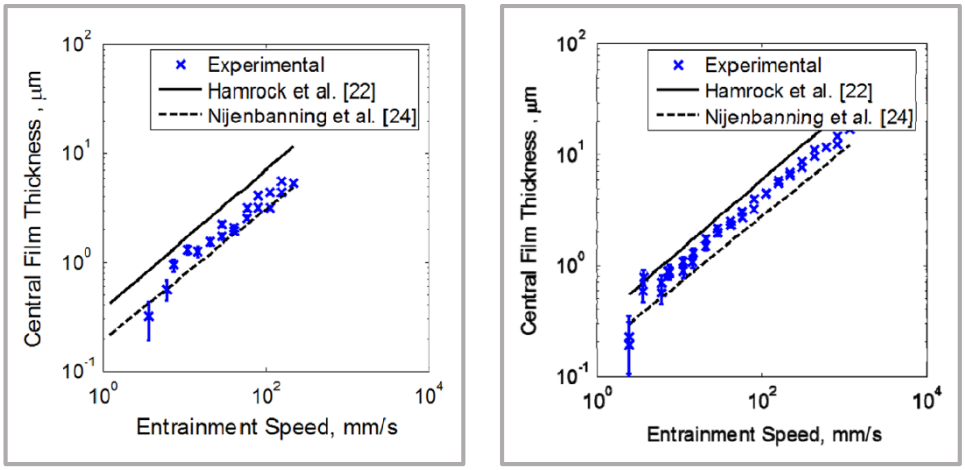

Figure 21. Development of central film thickness as a function of entrainment speed for point contact of PDMS hemisphere and glass disc loaded by 11 mN (left) and 23.5 mN (right) [41].

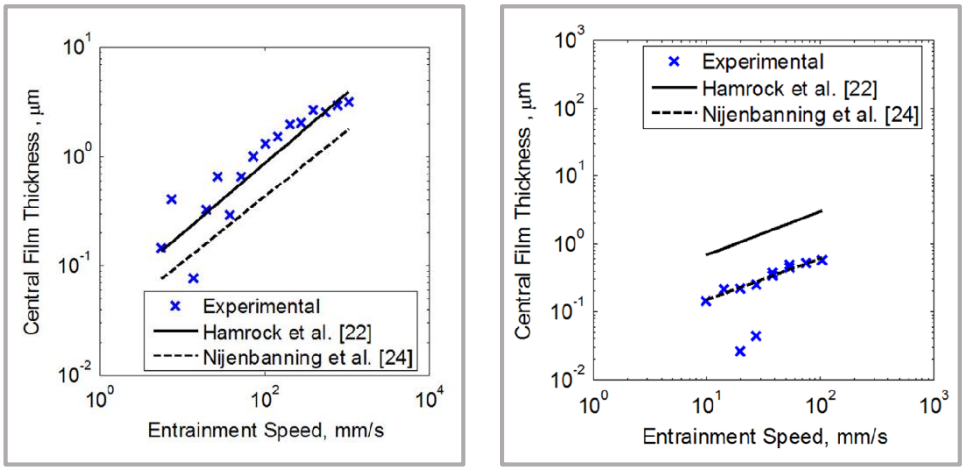

Figure 22. Development of central film thickness as a function of entrainment speed for elliptic contact of O-ring seal and glass disc (left) and O-ring seal and glass concave lens loaded by 4.8 N (right) [41].

2.3 Film thickness measurement in hip joint replacements

Initial study focused on the film thickness measurement in hip joint replacements was introduced by Mavraki and Cann [44]. The paper dealt with the fundamental aspects of implants lubrication, while the main interest was focused on the influence of proteins on coefficient of friction (COF) and film thickness. As a reference lubricant, bovine serum (BS) of various protein concentrations (25%, 50%, 100%) was used, while the results were compared with those for healthy and periprosthetic SF. Healthy fluid was represented by the solution of phosphate-buffered saline (PBS) with added albumin (A) and γ-globulin (G) in a ratio A:G = 2:1. In the case of periprosthetic fluid, the same amount of proteins was solved in 2-amino-2-(hydroxymethyl)-1,3-propanediol (Tris). To be able to determine the effect of proteins, both lubricants with the interchanged protein concentrations were also investigated.

The authors employed simplified ball-on-disc configuration while COF was measured on commercial mini traction machine (MTM) and lubricant film thickness on optical tribometer. For the evaluation of film thickness, optical interferometry method was used. Experimental conditions for both types of the tests are summarized in Tab. 1.

Table 1. Summary of the experimental conditions [44].

Parameter	MTM	Optical tribometer	Unit
Mean Hertzian pressure	0.34	0.25	(GPa)
Mean speed	5 – 50	5 – 20	(mm/s)
Load	5	5	(N)
SRR	180	0	(%)
Temperature	37	25	(°C)

The results of COF (Fig. 23, Fig. 24) showed that independently of applied lubricant, lower friction was maintained especially at slow speed regime. In terms of film thickness, the authors could observe relatively thin (< 20 nm) adsorbed protein layer while the further increase of film was attributed to hydrodynamic effect.

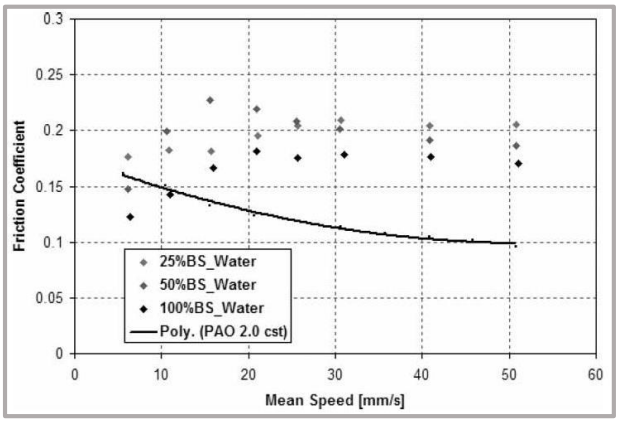

Figure 23. Development of COF as a function of mean speed for various concentrations of BS [44].

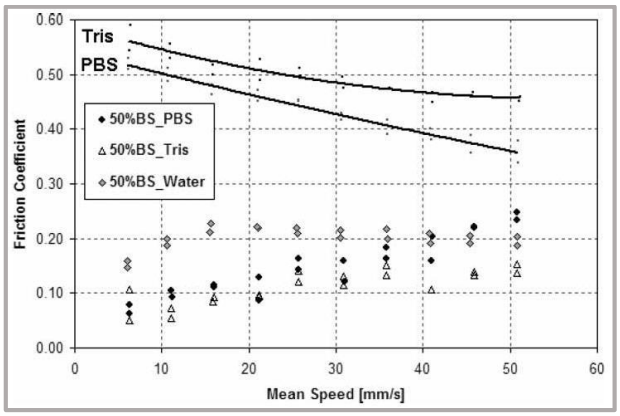

Figure 24. Development of COF as a function of mean speed for various lubricants [44].

The graph in Fig. 25 shows the dependence of film thickness on mean speed for 50% BS. As can be seen, film increases with increasing speed during the first part of the experiment. Subsequent speed sweep had a negligible effect; however, a slight tendency to increase could be still observed. The maximum film thickness at the end of the test was little bit less than 30 nm. Although there was no significant effect of lubricant on COF, the impact was evident in terms of film thickness. The film in the case of lubricant representing healthy SF was unstable and was kept between 30 and 90 nm. Periprosthetic fluid exhibited very stable layer; however, the thickness was just around 10 nm (Fig. 26).

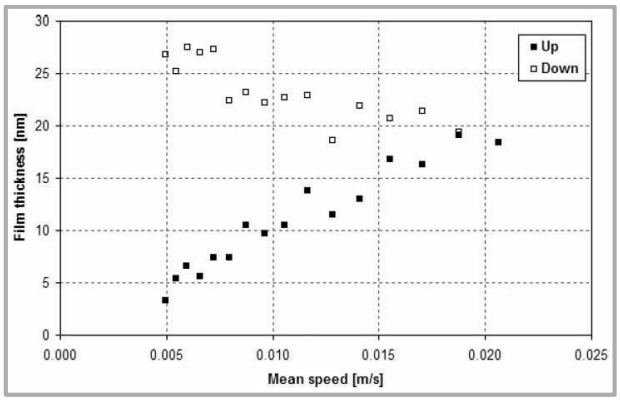

Figure 25. Development of film thickness as a function of mean speed for 50% BS [44].

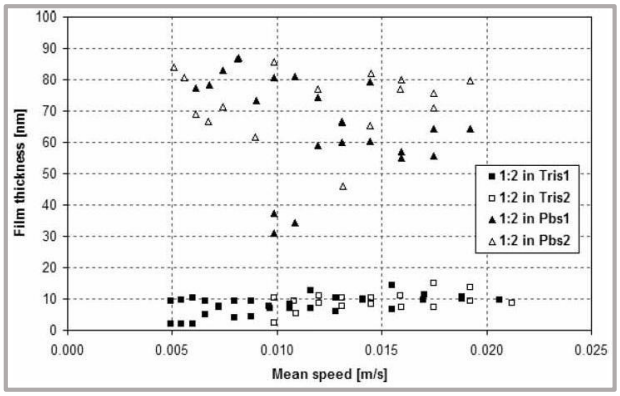

Figure 26. Development of film thickness as a function of mean speed for various lubricants [44].

The study was later extended by the same authors [12] considering the effect of high (200 MPa) and low (30 MPa) contact pressure on film thickness. For this purpose, two different configurations were investigated; ball-on-disc and lens-on-disc. The radius of the ball and the lens was 9.5 and 50 mm, respectively. Experiments were realized under pure rolling (ball-on-disc) and pure sliding (stationary ball; lens) conditions. The influence of temperature on protein film was also examined and the speed varied from 2 to 30 mm/s. The contact was lubricated by BS. According to significant variance of results, the authors emphasized that the SF, as well as BS, which is often used as its model, is the non-Newtonian fluid. Due to this fact, it is very complicated to derive predictions for film thickness estimation.

It was found that the change of the experimental conditions from pure rolling to pure sliding caused a substantial reduction of film thickness for around 70% – 80% (see Fig. 27). In general, protein film was higher at lower contact pressure. The film thickness at lower contact pressure was also very sensitive to concentration of BS, as is shown in Fig. 28. Lubricant film was approximately three times higher in the case of 100% BS compared to 25% BS. This behaviour was not observed in the ball-on-disc configuration. Finally, the authors did not observe any significant effect of increasing temperature from 25 °C to 37 °C on film thickness.

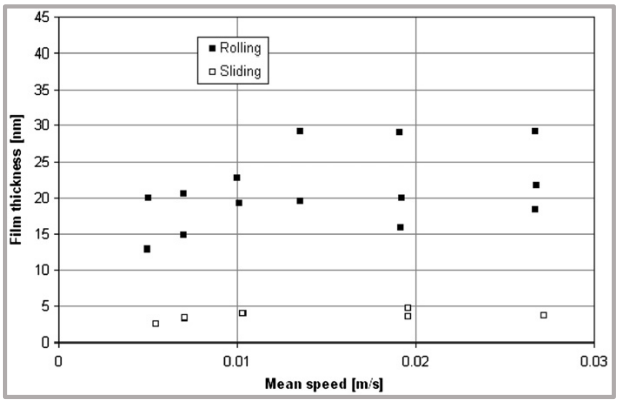

Figure 27. Development of film thickness as a function of mean speed under pure rolling and pure sliding conditions (100% BS, 37 °C, 200 MPa) [12].

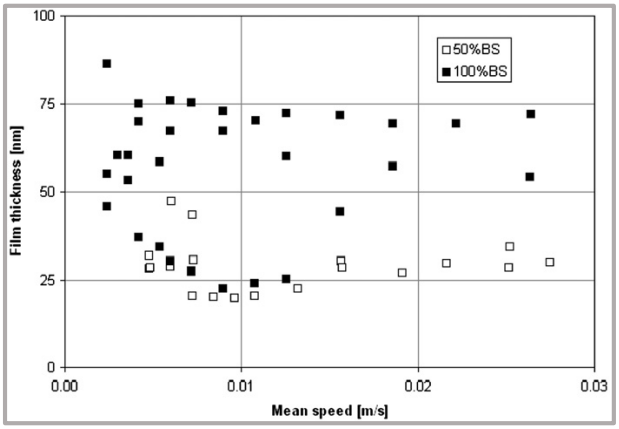

Figure 28. Development of film thickness as a function of mean speed under pure sliding conditions (50% and 100% BS, 37 °C, 30 MPa) [12].

The following paper, pronounced by Fan et al. [45], provided an extensive analysis of the effect of model fluid composition on lubricant film formation. The same experimental approach consisting of the ball-on-disc device and optical interferometry, introduced in previous studies [12],[44], was employed. For the first time, real femoral component from CoCrMo alloy was used as one of the contact bodies. The experiments were performed under pure sliding conditions with stationary ball, considering the speeds from 2 to 60 mm/s and body temperature. Several lubricants were tested, while the overview of the solutions is specified in Tab. 2.

Table 2. Test lubricants used in the performed experiments [45].

Test lubricant	Total protein concentration (g/dl)
25% BS	1.62
50% BS	3.23
100% BS	6.45
Albumin solution	1
γ-globulin solution	0.18
Albumin + γ-globulin solution	1.18

The character of protein film formation corresponded to the previously observed results [12],[44]. Adsorbed protein layer between 10 – 20 nm was detected in the most cases while the further increase of protein film was caused by hydrodynamic effect and was observed especially at lower speeds. At the end of the experiment, the total film thickness varied from 20 to 60 nm dependently on applied lubricant. In the case of BS, there was no significant influence of protein concentration on film thickness. However, complex protein solutions exhibited approximately two times higher values of protein film, see Fig. 29 vs. Fig. 30.

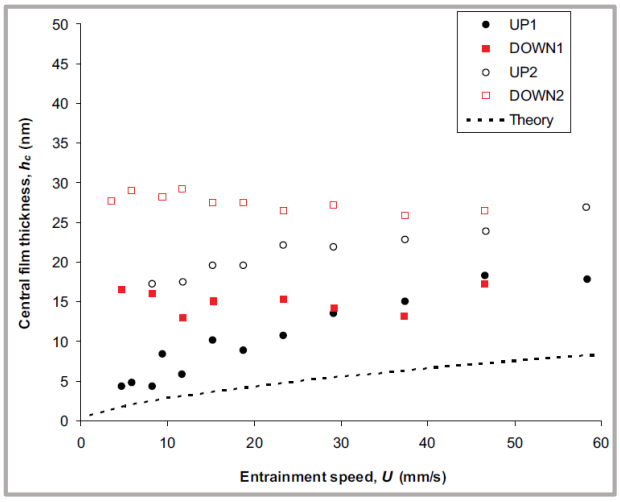

Figure 29. Development of film thickness as a function of sliding speed for 100% BS [45].

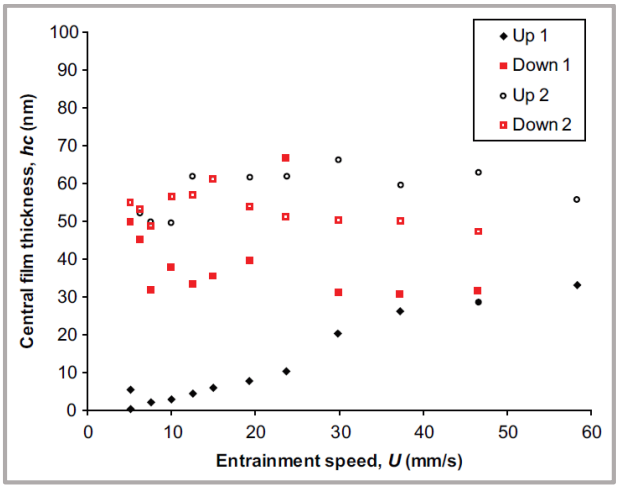

Figure 30. Development of film thickness as a function of sliding speed for solution of albumin and γ-globulin [45].

Previous studies focused mainly on the effect of mean speed, contact pressure, model fluid composition, or temperature on protein film formation. Myant et al. [46] focused on the influence of load (5 – 20 N) and time on lubricant film thickness. Moreover, static test at zero speed was conducted allowing to study protein adsorption onto surfaces. Applied load in the case of static test was 5 N while 12 cycles were performed in total. One cycle consisted of 15 seconds loading phase and following 45 seconds of unloading. The film thickness was detected at the end of each loading period. Five different test lubricants were investigated, 25% BS with total protein concentration equal to 13 mg/ml, three albumin saline solutions (protein concentrations = 10 mg/ml; 20 mg/ml; 30 mg/ml) and γ-globulin saline solution with the protein content of 6 mg/ml. From the results of the static test (Fig. 31), it is apparent that the thickest film (≈ 30 nm) was formed by γ-globulin solution, even the protein concentration was the lowest. On the contrary, lubricant containing albumin led to very thin protein film just in the range of units of nm with negligible effect of protein concentration. Thickness of BS was somewhere between the simple protein solutions and the film at the end reached around 10 nm.

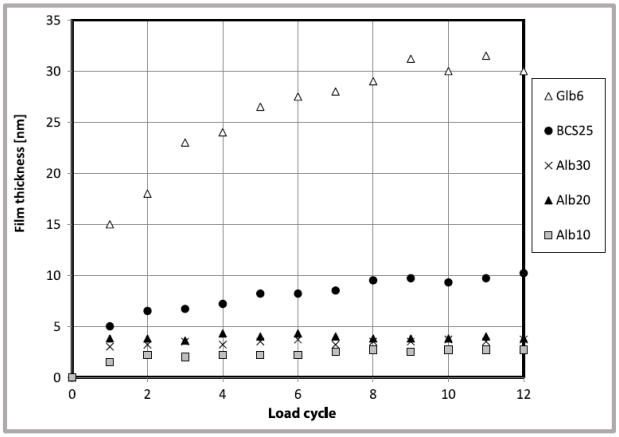

Figure 31. Development of adsorbed protein film as a function of load cycle for various lubricants [46].

Following experiment lasted 12 minutes (the same like in the case of static test), while it was carried out under constant sliding speed of 10 mm/s. Corresponding sliding distance was approximately 14.4 m. The load resulted to a mean contact pressure equal to 113 MPa. The results (Fig. 32) showed that the film thickness was the highest for γ-globulin solution, while the maximum at the end of the test was around 230 nm. Independently of protein concentration, lubricants containing albumin formed films thinner than 50 nm. What is in discrepancy with the static test is that BS results were very similar to those of albumin solutions. In meaning of character of film formation, γ-globulin film initially rapidly increased during the first three minutes and then was kept relatively constant. Albumin and BS protein layers gradually increased over a whole time of the experiment, see Fig. 32.

The last set of experiments was performed under various sliding speeds from 0 to 55 mm/s. The results exhibited significant scatter with no clear conclusions as in the previous cases. Decreasing concentration of albumin together with increasing speed led to a thicker protein film. On the contrary, BS film decreased with increasing speed. Although the results for γ-globulin were not provided, it can be summarized that the kinematic conditions and the protein content have a substantial effect on lubricant film formation.

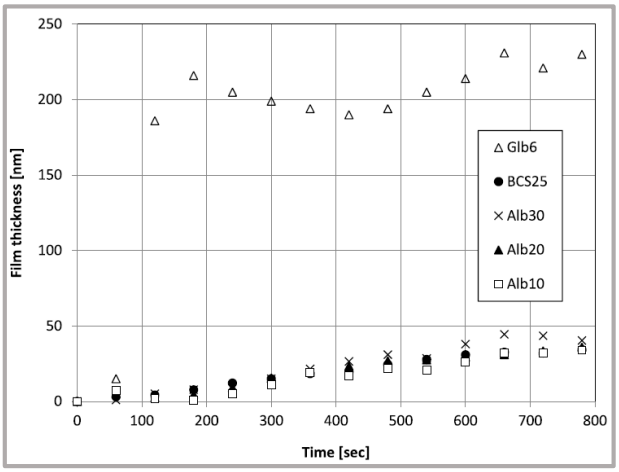

Figure 32. Development of film thickness as a function of time for various lubricants under the sliding speed equal to 10 mm/s [46].

A detailed observation of the contact lubricated by 25% BS was provided by Myant and Cann [47]. The authors observed the protein agglomerations in front of the contact while they called this gel-like suspension as a “inlet phase”, see the left part of Fig. 33. As can be seen in the graph displayed on the right of Fig. 33, very good correlation between the length of the inlet phase and the central film thickness was found. Therefore, it can be concluded that film thickness is strongly influenced by the agglomerated proteins.

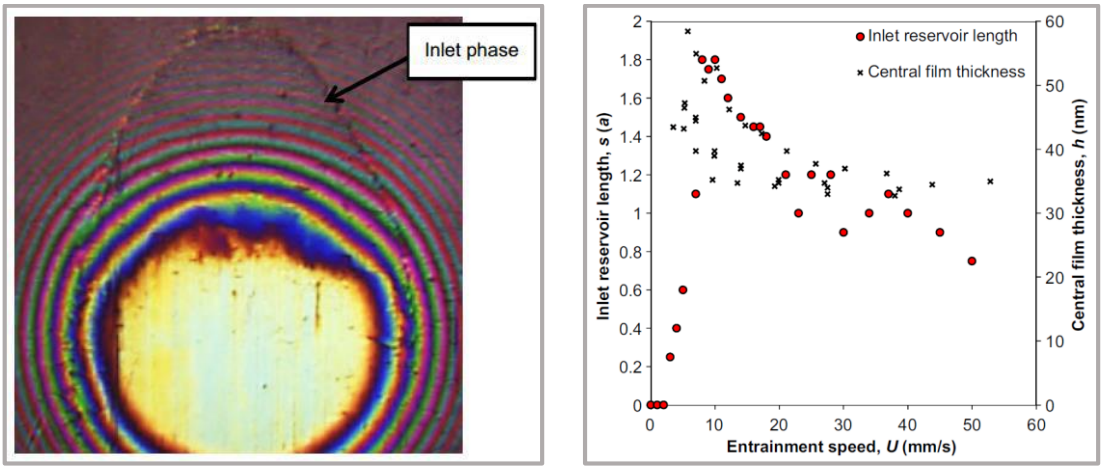

Figure 33. Left: Inlet gel-like phase of proteins in front of the contact zone. Right: Development of film thickness and inlet reservoir length as a function of sliding speed [47].

The above references focused on several factors apparently influencing the protein film formation in hip replacements. Theoretical knowledge was summarized by Myant and Cann [48]. The authors defined protein aggregation lubrication (PAL) mechanism in relation to metal-on-metal replacements, while several implications for implant tribology were highlighted and confronted with classical EHL mechanisms. For both, a reduction of contact pressure has a positive impact on film thickness. On the contrary, while the increase of sliding speed leads to an increase of lubricant film in the case of EHL, in the case of PAL, the effect is opposite; however, the composition of lubricant (i.e. protein concentration, protein ratio) must be taken into account.

In the further paper, Vrbka et al. [49] employed metal and ceramic femoral heads and the film thickness was investigated using the same experimental approach introduced above (ball-on-disc test device + optical interferometry method). Experiments were realized under various kinematic conditions (speeds, SRRs) under the constant load of 5 N. The contact was lubricated by 25% BS. Under pure rolling conditions, both materials exhibited increasing tendency of lubricant film, while metal head formed a thicker film, in general. Particularly, a maximum film thickness was approximately 100 nm for metal and only about 15 – 20 nm for ceramic at 20 mm/s (Fig. 34). Considering the slippage led to very complex character of film formation strongly dependent on positivity/negativity of SRR. When the disc rotated faster than the ball, film thickness initially rapidly increased for both heads. After reaching a maximum in the range of hundreds of nm, it started to continuously decrease and at the end of the experiment it was just in the range of units of nm. In the case of negative sliding, protein film was very thin; 20 – 25 nm at maximum for metal and 5 nm for ceramic. Further, the authors pointed out that the different conformity, compared to real synovial joints, can significantly influence protein film formation.

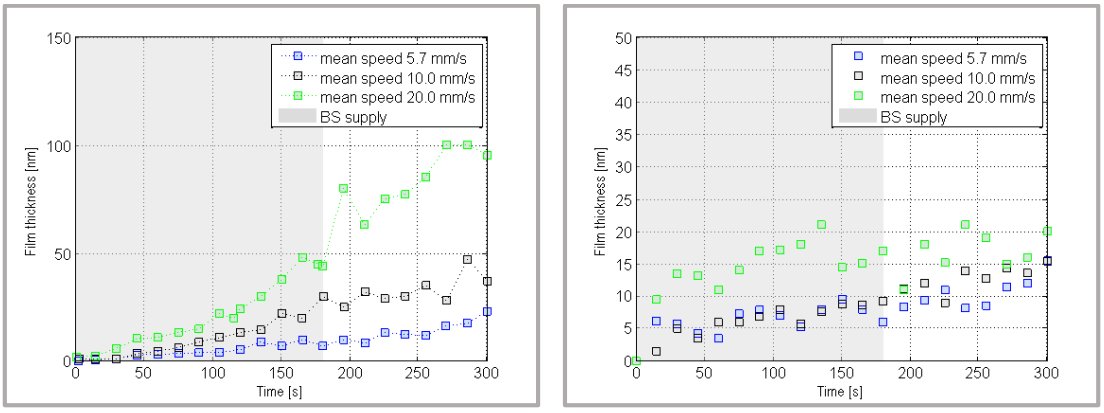

Figure 34. Development of film thickness as a function of time for metal (left) and ceramic (right) femoral head [49].

Following this implication, the authors later changed the experimental configuration from non-conformal ball-on-disc (small contact area, very high contact pressure) to more conformal ball-on-lens (larger contact area, reduction of contact pressure) [50]. The experiments were conducted under pure negative sliding; glass lens was kept stationary, and the ball rotated. The previous paper [49] showed that the film was extremely thin and could not be fully developed under negative sliding conditions. However, the change of experimental configuration caused a complete change of the film formation. Immediately after starting the experiment, the film reached almost 100 nm independently of sliding speed. After a short time, it started to gradually decrease to around 35 to 40 nm for 40 mm/s and 20 to 25 nm for 10 mm/s within a few tens of seconds. Then, the film became stabilized with not substantial change until the end of the test, see Fig. 35. The authors also focused on the effect of surface wettability. It was pronounced that the chromium layer on the bottom surface of the disc/lens exhibits a hydrophobic nature supporting the protein adsorption leading to a thicker film eventually. Subsequently, the disc coated with naturally hydrophilic silica layer was also employed, finding that the film thickness was negligible.

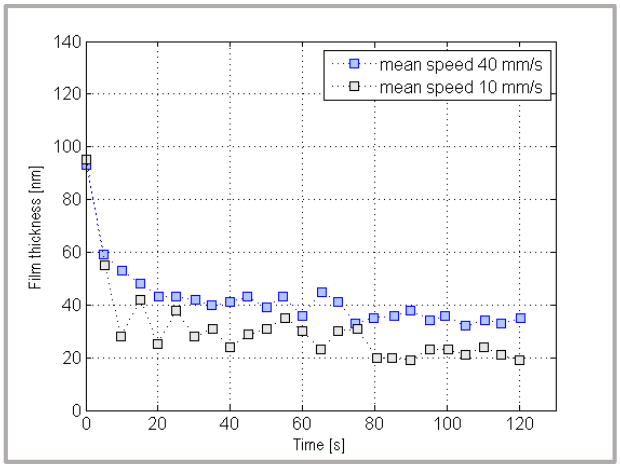

Figure 35. Development of film thickness as a function of time for various sliding speeds considering ball-on-lens experimental setup [50].

Several findings were already introduced in relation to kinematic conditions. Nevertheless, it should be emphasized that the authors previously employing ball-on-disc tribometers usually applied simple unidirectional character of motion, which does not correspond to the kinematics of real joints. Both, natural and artificial joints operate under complex multidirectional motion and transient load, dependently on gait, jump, stair climbing, etc. Therefore, Myant and Cann [51] extended the knowledge considering three different types of motions. An experimental approach was still the same consisting of ball-on-disc tribometer and optical interferometry method for film thickness evaluation. The first test was conducted under constant speed of 20 mm/s and constant sliding direction. It was followed by the experiment performed under sinusoidal speed from 0 to 20 mm/s and constant sliding direction. The last investigation was realized under sinusoidal speed from -20 to 20 mm/s with reversing sliding direction over each cycle. The results are displayed in Fig. 36. Although there was not a substantial change of film thickness development when the character of motion was changed from constant to sinusoidal speed; reversing character of motion led to a drop of the lubricant film by approximately 70%.

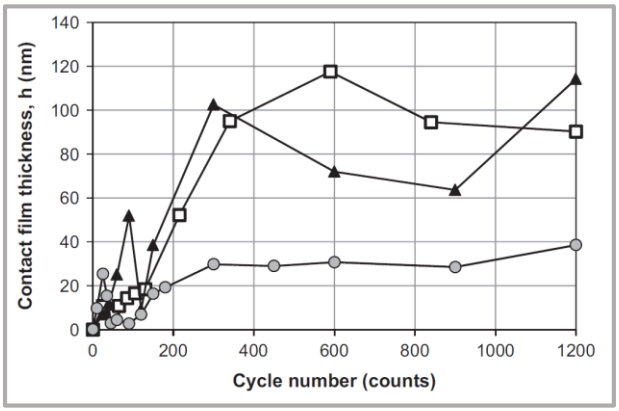

Figure 36. Development of film thickness as a function of cycle number for various motion character; constant speed and direction (white squares), sinusoidal speed and constant direction (black triangles), sinusoidal speed and reversing direction (grey circles) [51].

2.4 Analysis and conclusion of literature review

From the literature review, it is apparent that the biotribology of hip joint replacements is of a great importance due to limited service life of implants. Previously, the main attention was paid to the clarification of wear processes; however, there is still lack of information about the lubrication mechanisms in replacements. As the numerical simulations are extremely complicated due to SF nature and protein adsorption and agglomerations, the main attention is paid to the experimental investigations, while the choice of suitable experimental approach is particularly important.

Electrical methods are hardly employable, since it is desired that the studied materials have to be conductive, which is not ensured in the case of ceramic and polymer implants. Moreover, the readability and minimum detectable thickness of the lubricant layer is quite limited. In terms of optical methods, two approaches are

established, in general. Optical interferometry is very precise technique [22]; however, it provides just the information about the size of the gap between the surfaces without a knowledge about the role of particular components of the lubricant.

As little is known about the role of protein constituents on lubricating film, an optical method based on fluorescent microscopy seems to be a suitable solution [17]-[19]. The usability of the method is evident, since it enables to investigate even compliant non-reflective materials, to measure in a wide range of film thicknesses or to distinguish the individual constituents contained in the lubricant.

The method was initially used for the measurement of oil films on rotating steel cylinder discussing the knowledge in relation to rolling bearings starvation [23]. Subsequently, the principles such as LIF [24], DELIF [29], ERLIF [30], or FRAP [34] were introduced, allowing to measure film thickness inside the contact of two bodies, to study surface topography, or to determine the lubricant flow through EHL contact. The technique was also successfully combined with optical interferometry [35]-[37]. Recently, it was shown that the method enables accurate measurement of film thickness with very satisfactory readability [38],[40],[41].

For the investigation of lubricant film formation within hip joint replacements, an optical interferometry method in combination with ball-on-disc tribometers was employed several times. Based on the references, it is evident that the protein film formation is very complex phenomena depending on many factors such as mean speed [12],[44],[47],[49]; protein adsorption [14],[15]; model fluid composition [14],[45],[46]; load [46],[50]; time, rolling/sliding distance [46],[49],[51]; implant material [49],[50]; surface wettability and conformity [50]; or motion character [51]. The main differences between the SF lubrication and EHL theory were discussed in [48], where the PAL regime was defined.

It was also pointed out that the regime of lubricant supply can affect the results due to protein agglomerations observed in front of the contact zone when the contact is fully flooded [45],[47]. Nevertheless, the substance, so called inlet phase, was not observed when the lubricant was supplied continuously by a syringe pump [49],[50], indicating that the experimental conditions substantially affect the development of the protein film.

Although the importance of all the above parameters is indisputable, it should be pointed out that the absolutely fundamental factor is the composition of the model fluid in terms of protein concentration and protein ratio. Some effort was conducted to clarify the single protein solutions behaviour; however, the authors were able to investigate just simple protein solutions containing only one type of protein [45],[46] as the optical interferometry was employed for film thickness measurement.

According to author's knowledge, so far there is not such a study explaining the role of individual proteins in relation to lubricant film formation within hip replacements, considering complex model SF containing more than one constituent. The aim of the thesis coming from this fact is defined in a detail in the following chapter.

3 AIMS OF THE THESIS

The aim of the dissertation is to establish an experimental approach enabling in situ observation of lubricant film formation in hip joint replacements, focusing on the role of particular proteins contained in SF. For this purpose, fluorescent optical method will be employed since it allows to concentrate on individual parts of the model SF. After method debugging, an extensive experimental analysis of lubricant film formation will be conducted under various operating conditions. To fulfil the main goal of the thesis, solution of the following sub-goals is necessary.

- Implementation of the fluorescent method for film thickness analysis.
- Analysis of surface topography of the tested materials.
- Preparation of the model fluids containing fluorescently stained proteins.
- In-situ observation of lubricant film formation within hip implants considering various materials and operating conditions.
- Verification of the results by optical interferometry.
- Data analysis.
- Results publication and discussion.

3.1 Scientific question

How is the influence of the individual proteins contained in model SF (albumin, γ-globulin) on the development of lubricant film thickness within hip replacements regarding to implant material and kinematic conditions?

3.2 Hypotheses

- *It is expected that the contribution of γ-globulin film to total film thickness will be much more substantial than the contribution of albumin film.*
- *In terms of material, metal heads should support protein adsorption due to higher hydrophobicity; therefore, the protein film will be thicker, in general.*
- *Considering the kinematic conditions, it is suggested that the main parameter influencing the protein film development will be the level of slippage between the contact components.*
- *Respecting the PAL mechanism, an increase of speed will cause a reduction of film thickness.*

3.3 Thesis layout

The dissertation is composed of the two papers published in peer-reviewed journals and three papers published in journals with impact factor. The performed studies present the development of the methodology for the determination of protein film formation in hip joint replacements in terms of particular proteins. As the approach is based on the combination of the two methods, the first study utilizes optical interferometry method for the measurement of BS film thickness considering real conformity of rubbing surfaces [I.]. To be able to distinguish individual

constituents of model SF, a fluorescent optical method had to be developed as one of the sub-goals of the present thesis. The usage of the method for the direct measurement of film thickness in both, rigid and compliant contacts, is presented in the follow-up study [II.]. Consequently, the fluorescent technique was employed in an effort to quantify the lubricant rupture ratio at EHL contact outlet overlapping the obtained knowledge to the area of starved lubrication conditions, demonstrating the measurement possibilities of the developed technique [III.]. The latest part of the thesis demonstrates the use of the introduced methods for the purpose of the assessment of lubricant film formation within hip replacements in relation to the role of albumin and γ-globulin considering metal [IV.] and ceramic [V.] femoral components and various operating conditions.

I. VRBKA, M.; NEČAS, D.; HARTL, M.; KŘUPKA, I.; URBAN, F.; GALLO, J. Visualization of lubricating films between artificial head and cup with respect to real geometry. *Biotribology*, 2015, 1-2, 61-65.
(Author's contribution 25%)

II. NEČAS, D.; ŠPERKA, P.; VRBKA, M.; KŘUPKA, I.; HARTL, M. Film thickness mapping in lubricated contacts using fluorescence. *MM Science Journal*, 2015, 2015(4), 821-824.
(Author's contribution 40%)

III. KOŠŤÁL, D.; NEČAS, D.; ŠPERKA, P.; SVOBODA, P.; KŘUPKA, I.; HARTL, M. Lubricant rupture ratio at elastohydrodynamically lubricated contact outlet. *Tribology Letters*, 2015, 59(3), 1-9.
(Author's contribution 25%)
(Journal impact factor = 1.74)

IV. NEČAS, D.; VRBKA, M.; URBAN, F.; KŘUPKA, I.; HARTL, M. The effect of lubricant constituents on lubrication mechanisms in hip joint replacements. *Journal of the Mechanical Behavior of Biomedical Materials*, 2016, 55, 295-307.
(Author's contribution 55%)
(Journal impact factor = 2.88)

V. NEČAS, D.; VRBKA, M.; KŘUPKA, I.; HARTL, M.; GALANDÁKOVÁ, A. Lubrication within hip replacements – Implication for ceramic-on-hard bearing couples. *Journal of the Mechanical Behavior of Biomedical Materials*, 2016, 61, 371-383.
(Author's contribution 60%)
(Journal impact factor = 2.88)

4 MATERIALS AND METHODS

4.1 Experimental devices

In the present thesis, three experimental devices have been employed. The novel methodology was developed using ball-on-disc tribometer. As the fluorescent measurement method was supplemented by the optical interferometry, the use of interferometry for film thickness measurement is demonstrated using pendulum hip joint simulator which enables to investigate lubrication processes considering real conformity of surfaces. The surface topography was analyzed using optical profiler.

4.1.1 Ball-on-disc tribometer

The experiments dealing with the development of a new methodology enabling to assess the role of proteins on lubricant film formation were realized on ball-on-disc tribometer [27], where the contact is formed between the femoral head and the glass transparent disc. Both components can be driven independently by their own servomotors; therefore, various kinematic conditions can be applied. The load is applied by putting the weight on the lever. The contact of the ball and the disc is observed through optical imaging system consisting of mercury lamp illuminator, microscope, scientific complementary metal-oxide-semiconductor (sCMOS) digital camera (Andor NEO), and PC. Scheme and the photo of the test device is shown in Fig. 37, and Fig. 38, respectively.

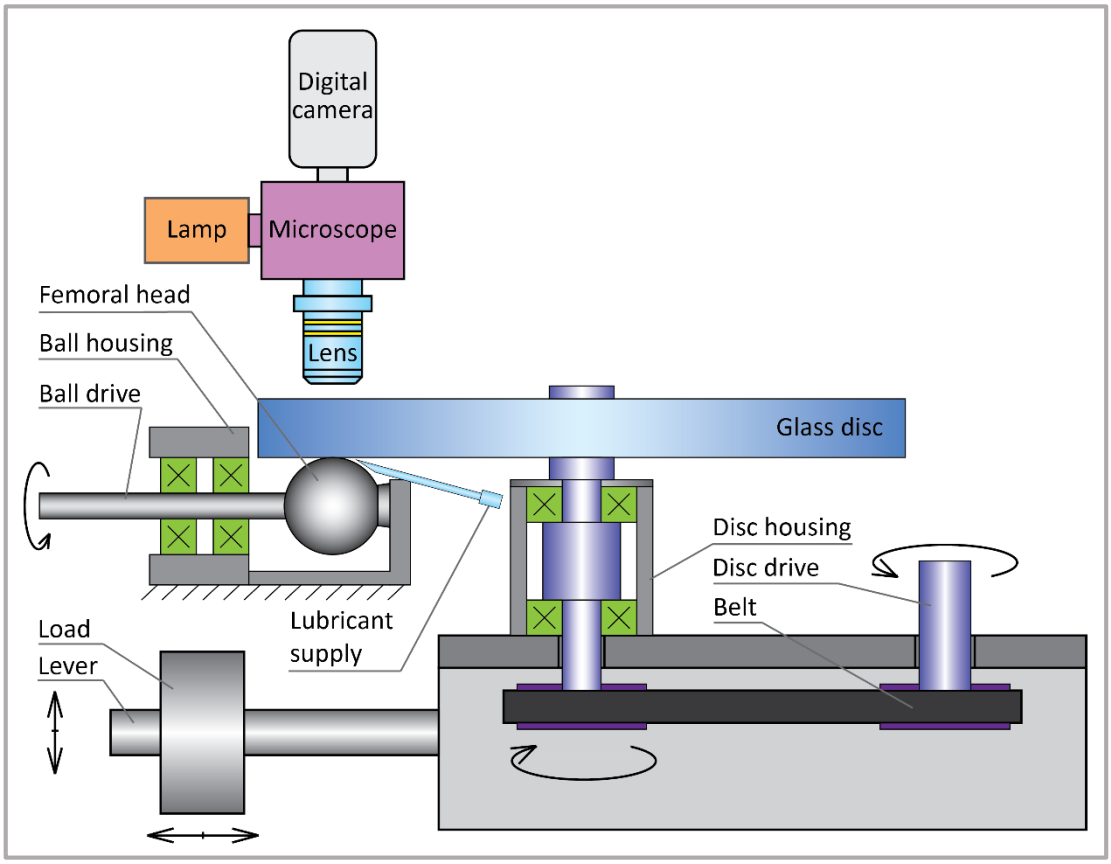

Figure 37. Scheme of the ball-on-disc optical tribometer.

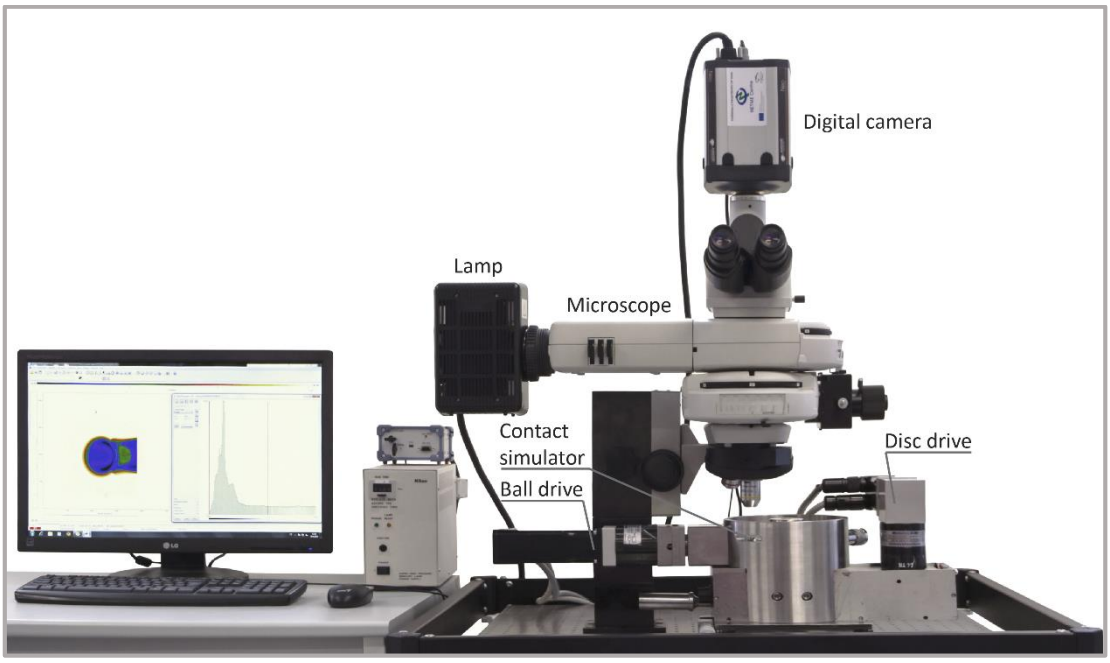

Figure 38. Photo of the ball-on-disc optical tribometer.

The simulator was also used in a modified inverted position of the test samples for the purpose of the quantification of lubricant division at the EHL contact outlet. In that case, the glass disc was substituted by the disc made from stainless steel, and the ball was placed on the top of the disc, see Fig. 39.

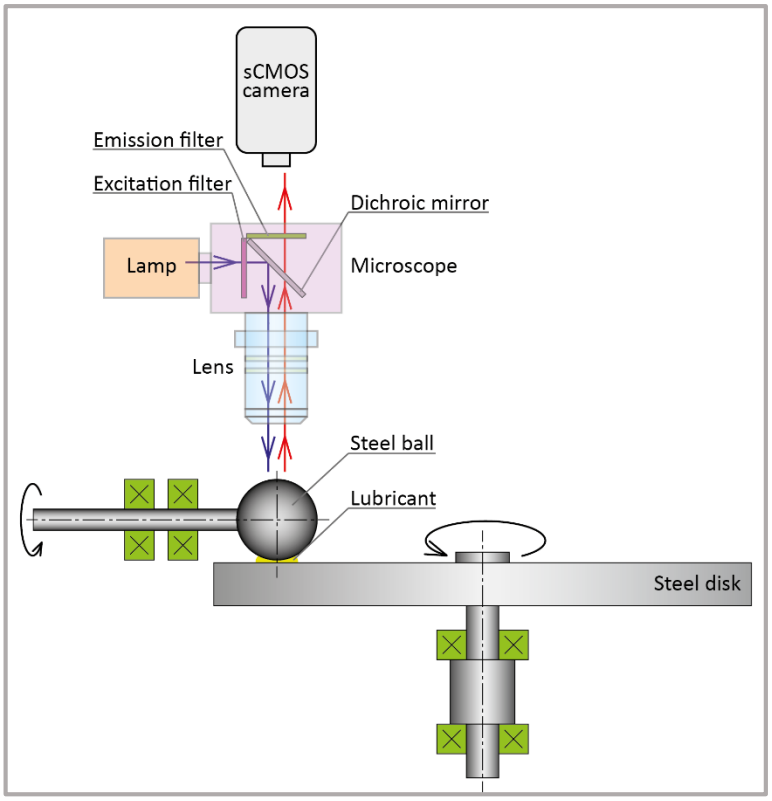

Figure 39. Inverted arrangement of the ball-on-disc optical tribometer.

4.1.2 Pendulum hip joint simulator

As the optical interferometry method was also employed in the present thesis, one of the attached papers demonstrates the use of the method for lubricant film thickness evaluation under real geometry of the joint components. The experiments were realized on pendulum hip joint simulator, originally designed by Stanton [52]. The simulator consists of base frame with fixed acetabular cup and pendulum with femoral head. The optical chain is the same as in the case of optical tribometer; however, the complementary metal-oxide-semiconductor (CMOS) colour digital camera (Phantom V710) is used in this case.

The measurement principle is based on the initial deflection of the pendulum, its releasing and consequential free oscillation in the flexion-extension plane until the motion is naturally damped due to friction between the components, which can be evaluated using angular velocity sensor [53]. The scheme of the simulator, as well as the measurement principle, is displayed in Fig. 40. Although the presented simulator enables to consider real conformity, the importance of which was indicated in literature [50], most of the experiments were realized on ball-on-disc device since all of the previous studies focusing on lubrication within hip replacements employed the same configuration; therefore, the current data could be discussed in relation to previously published results.

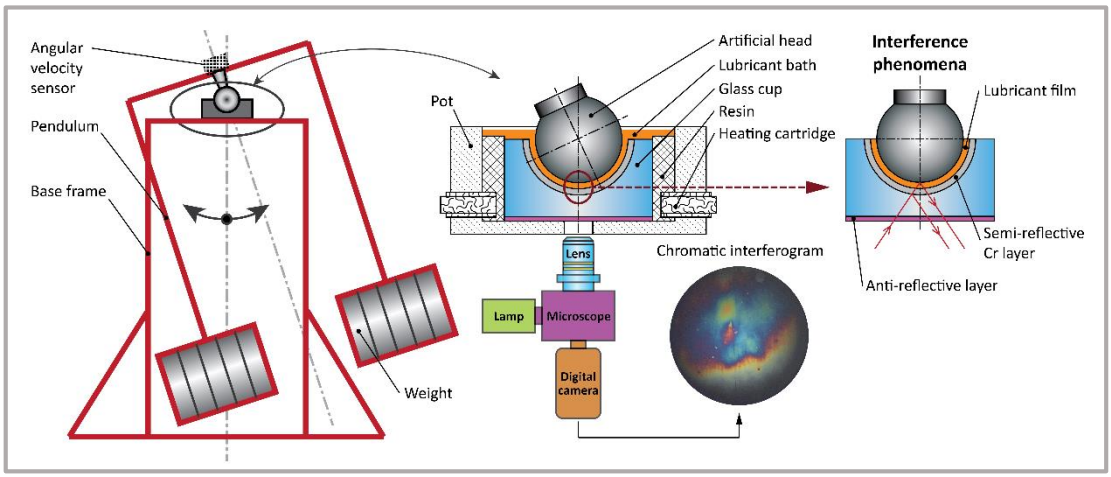

Figure 40. Principle of the measurement using hip joint simulator.

4.1.3 3D optical profiler

In the case of all tested samples, initial surface topography was analysed in a greater detail. For this purpose, a 3D optical profiler (Bruker Contour GT-X8) was employed. The measurement is based on phase shifting interferometry technique. The range of the vertical axis is down to 0.1 nm which is completely sufficient for the purposes of the present thesis, since the surface roughness of the tested balls is in the range of units of nm or higher.

4.2 Measurement methods

The main method, employed in the present thesis, is fluorescent microscopy. However, due to some limitations discussed in the following part, the experiments

are supplemented by the measurements of quantitative film thickness by optical interferometry.

4.2.1 Fluorescent microscopy

Fluorescent optical method is based on the fluorescence phenomena (Fig. 41) previously described by Haugland et al. [54] as a consequence of the three following steps:

- **Excitation:** A photon is supplied by an external light source (lamp, laser) and is absorbed by the fluorophore, creating an excited electronic single state.
- **Excited-state lifetime:** It usually lasts 1 – 10 ns. During this time, the molecule undergoes relaxation (energy dissipation) and is left in a state from which it can emit fluorescence.
- **Fluorescence emission:** A photon of energy is emitted, while the fluorophore returns to its ground state. Due to energy dissipation during the previous phase, the photon has a lower energy and; therefore, a longer wavelength than the excited photon. The difference in wavelengths or in energy is known as Stokes shift, which is an absolutely fundamental, since it allows to separate the measured emission from excitation.

As was shown in chapter 2, the method was previously employed for the direct measurement of film thickness. However, in the case of hip replacement lubrication, quantitative film thickness was not possible due to several phenomena associated with the investigated materials.

a) **Interference of light**. In the case of both tested materials (metal, ceramic), interference fringes, arising at the interface of the bottom surface of the disc and lubricant, and at the interface of the lubricant and the ball, could be observed. This phenomenon was also discussed in literature [28]. The authors solved this problem by a substitution of the test sample (steel ball) by a glass lens for calibration. However, it was later pointed out by Myant et al. [38] that the different optical properties of the calibration and test samples can lead to some inaccuracies in results.

b) **Quenching effect.** The presence of chromium in CoCrMo alloy femoral heads causes the quenching of fluorescent intensity. The phenomena was introduced in literature several times [55]-[57]. It should be highlighted that the level of intensity loss is influenced by the chromium content, as well as the type of the applied fluorophore. Therefore, it is very complicated to determine the exact effect on the thickness of the lubricant film in the specific cases. Nevertheless, the methodological approach is based on matching of the curves of film thickness given by optical interferometry with the curves describing the qualitative development of protein film obtained by fluorescence. Although the results of fluorescent intensity might be affected by the quenching due to chromium presence, the measurement uncertainty is constant in the course of entire measurements; therefore, the general information about film thickness development is relevant.

c) **Natural fluorescence of ceramics.** Contrary to metal head, a natural fluorescence was observed in the case of both tested ceramic materials. Even

if there was no fluorophore in the excited area, the materials emitted a low level of fluorescence. Moreover, so far there is not a study describing the interaction of a level of natural fluorescence and specific fluorophores. However, as in the case of quenching, the self-emitting fluorescence effect does not significantly influence the results, since the particular values of fluorescent intensity are not decisive, as the evaluation is based on qualitative increase/decrease character of intensity compared to the initial state.

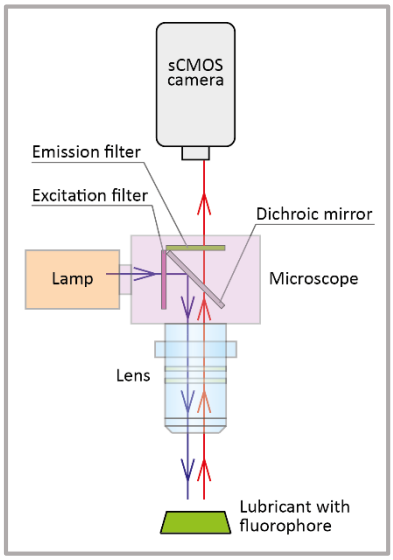

Figure 41. Principle of the fluorescent method.

In the first paper, attached to the current thesis, the use of fluorescent method for film thickness measurement in the two types of contacts is illustrated. The evaluation procedure is as follows:

a) The calibration curve is obtained from the knowledge of Hertz theory and the image of lightly loaded static contact. Moreover, to avoid light scattering, background image of lubricant is taken. Therefore, the dependence between the fluorescent intensity and the corresponding film thickness is known.
b) Capturing of the fully loaded contact zone during the running test via digital camera.
c) Matching of the contact zone images with the calibration curve; determining of the film thickness in arbitrary pixels of the images

4.2.2 Optical interferometry

Optical interferometry is well established experimental method for very accurate measurement of film thickness. If the contact of two bodies; while one of the bodies is transparent and the other one is reflective, is illuminated, then Newton rings, also known as Fizeau rings can be observed. The interference phenomenon is based on the composition of reflected light beams. The incident beam passes through the optical chain, being split on the contact surface of the transparent counterpart and lubricant. One part of the beam is reflected back to the lens, while the second one

passes through the lubricant and reflects at the interface of the lubricant and the ball. Since the travelled distance of the two beams is different, the phase is changed. Hartl et al. [22] proved that the method enables to measure the separation of the surfaces down to 1 nm with the resolution of units of nm. The evaluation is performed using the Achilles software and is based on the following steps:

a) The image of lightly loaded static contact is captured, while the calibration curves based on the shape of the contact zone can be obtained. Therefore, the dependence between the colour and the corresponding film thickness is known.
b) Capturing of the fully loaded contact zone during the running test via digital camera.
c) Matching of the captured interferograms with calibration curves; determining of the film thickness in arbitrary pixels of the images.

4.3 Test samples and experimental conditions

Test samples, as well as experimental conditions, differed according to the test type, applied simulator, or measurement method. Particular details related to the particular tests are summarized in Tab. 3. In the case of ball-on-disc tribometer, when the film thickness and protein film formation was investigated, the configuration consisted of the transparent glass disc and the ball. For the purpose of optical interferometry measurement, the disc was, moreover, coated with a thin chromium layer enhancing the contrast of interference. As one of the application of fluorescent method deals with the quantification of lubricant division at the EHL contact outlet, the configuration was modified, substituting the glass disc by the disc made from stainless steel. In the case of pendulum simulator, the contact consisted of femoral head and glass acetabular cup, which contact convex surface was, again, coated with the chromium layer ensuring sufficient contrast of light interference.

Table 3. Summary of the experimental conditions employed in the performed studies.

	[I.]	[II.]		[III.]	[IV.]	[V.]
Load (N)	532	12	12; 26; 41	30	5	
Contact pressure (MPa)	28.7	401.7	66.5; 83.8; 100	800	270	280
SRR (%)	-200	0		-150 – 150	-150; 0; 150	
Mean speed (mm/s)	5.9 – 0	10 - 500		60; 220; 450	5.7; 22	
Ball diameter (mm)	28	25.4		25.4	28	
Diametric clearance (µm)	92	-		-	-	
Ball material	CoCrMo alloy	Si_3N_4	Phenol	Stainless steel	CoCrMo alloy	BIOLOX®*forte*; BIOLOX®*delta*
Test lubricant	25% BS	Mineral oil		Mineral oils	Protein solution	

	[I.]	[II.]	[III.]	[IV.]	[V.]
Lubricant viscosity (Pa·s)	-	0.644	0.19; 0.45; 0.64; 1.4	-	
Protein content (mg/ml)	22.4	-	-	10.5	
Temperature (°C)	37	Ambient			

4.4 Staining the proteins

Protein labelling is time consuming process and desires strict compliance of the steps described below. As the fluorescent markers, Rhodamine-B-isothiocyanate (RBITC – Sigma-Aldrich 283924) and Fluorescein-5-isothiocyanate (FITC – Sigma-Aldrich F7250) were used for staining BS albumin (Sigma-Aldrich A7030) and γ-globulin from bovine blood (Sigma-Aldrich F7250), respectively. The process, employed in the present thesis, was developed at Kyushu University, while the proteins were stained at University Hospital Olomouc as a part of cooperation in the area hip replacement biotribology research. Staining of the proteins consists of the following steps:

- The exact amount of fluorescent dye is added to 300 ml of distilled water. The concentrations are 4.9 mg/300 ml for RBITC and 4.4 mg/300 ml for FITC.
- The suspension is mixed using an electromagnetic field (RBITC – 4 hours, FITC – 8 hours).
- The solution is consequently divided to 50 ml tubes.
- 1 g of albumin/γ-globulin is added to the tubes which are left in a refrigerator overnight to allow the proteins to be solved naturally.
- 50 ml suspension is divided into 4 centrifugal tubes of a volume of 12.5 ml.
- Tubes are putted into a centrifuge and are centrifuged for 60 minutes at 21 G acceleration.
- Centrifuged suspension is grouped from 4 to 2 tubes being centrifuged again for 60 minutes at 21 G.
- Determining the protein concentration in the centrifuged suspension.
- Preparation of the lubricant doses.
- Freezing the suspension to -22 °C.

To avoid any loss of fluorescence emission during labelling process, all the steps must be carried out in the dark room to prevent the contact of dyes with ambient light. It should be noted that the staining process does not cause any conformational changes of proteins; therefore, the nature of the model SF is the same as in the case of non-stained proteins.

4.5 Experiment design

In the first performed study [I], the use of thin film colorimetric interferometry method is illustrated as a tool for film thickness measurement. Due to lack of knowledge about protein film formation related to the effect of surface conformity, the experiments were realized in real ball-on-cup configuration. Before the experiment, the glass cup was casted by an epoxy resin in a dish and was pre-heated

by the cartridges to 37 °C. Subsequently, the cup was filled with the pre-heated lubricant and the pendulum arm with the head was arranged to the cup. The applied load (532 N) was designed to the strength of the glass to avoid the cup damage. When the head was in the cup, the pendulum was deflected to maximum angle (16°) and was released to oscillate freely until the stop of the movement due to friction forces between the rubbing surfaces. The frequency of the swinging, given by the design of the simulator, was 0.5 Hz. As a result, the dependence between the film thickness and pendulum rotation (mean speed) was obtained. Moreover, the signal from angular velocity sensor could be converted to the coefficient of friction. To avoid inaccuracies coming from the contamination, all the contact components were cleaned in 1% sodium dodecyl sulphate solution, rinsed in distilled water, dried by pressed air, and washed in isopropyl alcohol before testing.

The following experiments were conducted using ball-on-disc tribometer in an effort to present the ability of the fluorescent method for the direct measurement of film thickness [II]. Initially, the rigid EHD contact between the ceramic (Si_3N_4 – natural fluorescence was not observed for this material) inch ball and the glass disc was investigated, since the theoretical prediction for film thickness estimation given by Hamrock and Dowson [58] is known to be sufficiently accurate over the wide range of operating conditions. The film thickness was evaluated based on the calibration process described above. The results were expressed as a function of film thickness on rolling speed. As there was an excellent agreement between the predicted and experimental data, the ceramic ball was later substituted by the ball made from phenol in an effort to measure the film thickness within the isoviscous-elastohydrodynamic lubricated (i-EHL) contact. The effect of mean rolling speed and load on central film thickness was investigated, while the results were compared with those predicted by Hamrock and Dowson [59]. In the case of both tested configurations, the sufficient amount of lubricant was stored in a dish below the ball. Due to ball rotations, the lubricant was continuously supplied to the contact.

As was mentioned in the literature review, the first application of fluorescent method was conducted by Smart and Ford [23], who dealt with the starvation of rolling bearings. When several rolling elements are in the same contact drag, the lubrication conditions are strongly affected by the thickness of the oil film entering the contact after passing the previous contact. However, so far there was no an experimental study determining the ratio of the lubricant division at the contact outlet. Therefore, after verification of the method by film thickness measurement, the method was used to detect the division ratio of the mineral oil on both surfaces, the ball and the disc, after passing through the contact [III]. The experiments were realized in an inverted position of the ball-on-disc tribometer, as is schematically shown in Fig. 42. The lubricant was supplied to the contact drag on the disc. The rupture ratio was studied as function of SRR, mean speed, contact geometry and lubricant viscosity. The measurement was based on the detection of the fluorescent intensity of the oil film in the centre of the contact drag, while the intensity was measured twice under each conditions in a consequence ball-disc-ball-disc to avoid measurement inaccuracies. The results were compared with the numerical analysis given by Bruyere et al. [60].

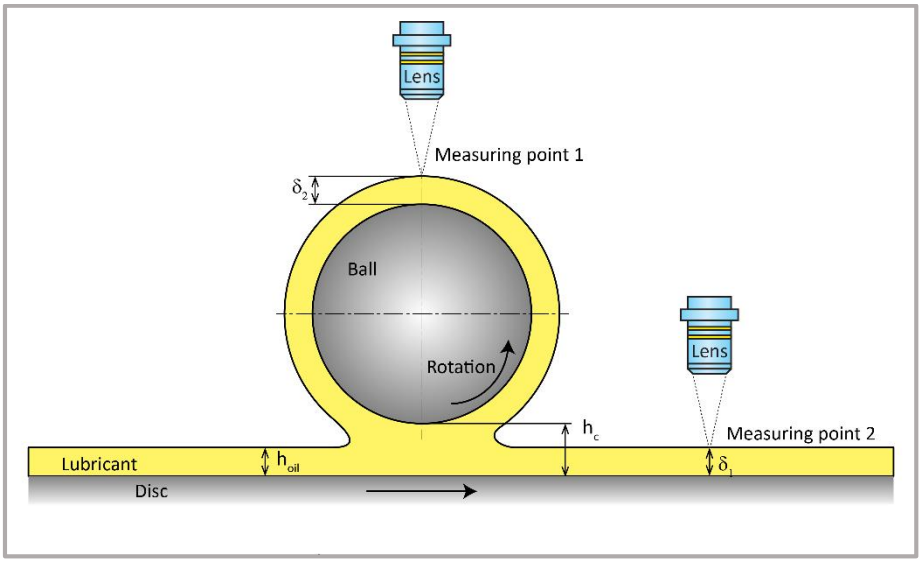

Figure 42. Illustration of the locations where the fluorescent intensity was detected [III].

The latest part of the dissertation combines the use of both optical methods in an effort to determine the lubricant film formation in hip joint replacements in relation to the contribution of particular proteins [IV]-[V]. For this purpose, the experiments had to be conducted three times under each experimental conditions. The only difference was in the applied test lubricant (fluorescently stained constituents). Due to limitations described above, the film thickness could not be measured by fluorescent microscopy directly. Therefore; initially, the film thickness was evaluated using optical interferometry, while the test lubricant contained both non-stained proteins (albumin, γ-globulin). Consequently, the test was repeated under the same conditions, while the lubricant contained fluorescently stained albumin and non-stained γ-globulin, so the intensity of albumin film could be measured while the simultaneous presence of γ-globulin. Finally, the measurement was repeated for the third time with non-stained albumin and stained γ-globulin. The lubricant was supplied in front of the contact zone through a syringe pump, while the dosing time was 3 minutes and the dosing speed was 3.5 ml/min. Al the measurements were evaluated separately and were composed to the graphs showing the development of film thickness, albumin and γ-globulin film as a function of time. The cleaning procedure before the experiment was the same as in the previous study [I].

Due to substantial quenching effect, the disc was not covered by a chromium layer in the case of fluorescent microscopy. Nevertheless, several comparative experiments with coated and uncoated discs were conducted, finding that the fluorescent intensity was generally lower in the case of coated disc; however, the tendency of the lubricant film was the same. Therefore, it can be concluded that the chromium layer does not affect the protein film formation substantially.

5 RESULTS AND DISCUSSION

Thin film colorimetric interferometry technique for film thickness measurement has a long tradition at the Institute of Machine and Industrial Design (IMID). The method was developed by prof. Hartl and prof. Křupka who established tribology research group at IMID more than twenty years ago. The usage of interferometry method is not the main contribution of the author of the present dissertation; however, it is used for the supportive measurements of film thickness, so the use of the technique is illustrated in one of the attached papers [I].

Film thickness was measured in the real geometrical configuration (ball-on-cup), since it was indicated in literature that the conformity can substantially affect the formation of protein film. 28 mm CoCrMo alloy femoral head was loaded against the glass acetabular cup and the film thickness was measured as a function of time and pendulum deflection, respectively. Immediately after the beginning of the experiment, the film thickness reached almost 240 nm. Then, it started to continuously decrease and was stabilized after approximately 10 seconds between 80 and 100 nm with no significant change until the end of the test. The character of film formation was in a good agreement with that of ball-on-lens configuration presented by Vrbka et al. [50], who were the first who changed the non-conformal ball-on-disc configuration to a configuration with the higher degree of conformity (ball-on-lens). From the particular interferograms of the contact zone, it was apparent that, at the beginning, a strong aggregation of proteins in the central contact zone occurred, while the increasing time led to thinning of the layer, which was uniform over the contact area. The experiment was repeated once more under the same operating conditions, finding that results were almost the same, proving the precision and reproducibility of the employed technique. Moreover, the test was performed with PAO oil of a viscosity $\eta = 0.0255$ Pa·s as a representative of simple Newtonian fluid. Completely different character of film formation could be observed in that case. If the rubbing surfaces were not protected by the proteins contained in BS, breakdown of the lubricating film could be observed in less than 5 seconds leading to a rapid wear of chromium layer on the contact surface of the cup. On the other hand, although a thinner film was detected, in general; the natural swinging of the pendulum lasted longer compared to the test performed with BS (75 s vs. 50 s). This indicates that the shear forces between the proteins cause an increase of friction, as was previously discussed in literature [61].

As the optical interference does not allow to separate the individual constituents of the model fluid, fluorescence optical method had to be developed as one of the main goals of the current dissertation. Following study [II] presents the ability of the technique for the film thickness measurement in both, EHL and i-EHL contacts. Initially, the method was verified comparing the results of film thickness in rigid EHL contact (ceramic vs. glass) with the theoretical prediction. The experiments were realized under pure rolling conditions, considering the range of speeds from 10 to 500 mm/s. Constant load of 12 N was applied for all the rolling speeds. Film thickness continuously increased over a sped range, it varied from 100 nm at 10 mm/s to 1.5 µm at 500 mm/s. The film thickness profiles well corresponded with the EHL

theory, while typical horseshoe-shaped constriction could be observed on the contact images with increasing speed. With the exception of the lowest rolling speeds, the measured central thicknesses were in an excellent agreement with the prediction, proving the validity of the method.

Subsequently, the experimental configuration was changed, substituting the ceramic ball by the ball made from phenol. Modulus of elasticity of phenolic ball was 4 GPa representing compliant contact body. The speed range was the same as in the case of EHL contact; however, three different load levels were investigated. In general, there was no significant effect of load on the lubricant film thickness. What was in discrepancy with i-EHL theory was that the film slightly increased with increasing load, while opposite behaviour was expected. Nevertheless, the same phenomena was observed even by Fowell et al. [41]. For all the tested loads, the film linearly increased with increasing speed, while the measured data were a little bit lower compared to prediction when the load was 12 N, and 26 N, respectively. In the case of the highest load (41 N), a satisfactory agreement of prediction and experimental data could be observed. When focusing on the profiles of lubricant film, it might be concluded that the slope of the central zone increased with increasing speed. However, the slope was not as significant as previously observed [38],[40]. The difference probably comes from the differences in elastic moduli. In the mentioned references, the authors investigated the samples, whose elasticity was just in the range of units of MPa. As the modulus of phenol is 4 GPa, it is estimated that the central region of the contact zone becomes flattened with increasing stiffness of the contact body. This statement is supported by classical EHL theory derived for rigid bodies, were the central plateau region can be observed.

In the literature review, it was presented that the fluorescent method can be applied for several applications. Therefore, we employed the developed technique for the investigation of the lubricant rupture ratio at EHL contact outlet [III]. The experimental configuration consisted of the steel ball and the steel disc in an inverted position compared to the previous study. To check the effect of contact ellipticity, the ball was consequently substituted by the rollers of a various radius of curvature resulting to the ellipticities from 1 to 4. Experiments were realized under various mean speeds and SRRs, while the evaluation was based on the qualitative comparison of the intensities of the central parts of the contact drags on the both components. The effect of lubricant viscosity was also studied. So far, there was no an experimental study investigating the phenomena of lubricant division after passing the contact. Therefore, the data were confronted with those based on numerical simulation [60]. The results showed that the film tend to attach to the faster rotating component while the ratio increased with increasing SRR. Similar behaviour was observed for all the tested speeds and ellipticities. The effect of lubricant viscosity seemed to be not a substantial parameter. Although the trend well correlated with the mentioned numerical analysis, the slope of the curve was not as steep. The difference was attributed to several aspects which could not be considered in the theoretical analysis; such as thermal processes, or shear thinning behaviour of fluid. In addition, the configuration was highly non-conformal, while it might be better to investigate

these phenomenon using a pair of identical rolling elements to avoid the effect of different surface geometry.

In this study, we also checked the reproducibility of the fluorescent method in a greater detail. The contact was lubricated by mineral oil and 20 images of the contact drag were captured with 1 second delay. As the speed was constant, it was expected that the thickness of the layer is also constant. It was found that the maximal deviations against the mean value were from -2.6% to 2.9%.

The main part of the dissertation is focused on the assessment of the lubricant film formation in hip joint replacements in terms of individual proteins. As the film thickness could not be measured by the fluorescent microscopy, all the experiments were initially realized with the use of optical interferometry determining the lubricant film thickness development as a function of time. Three commonly used materials of artificial heads were investigated; CoCrMo alloy [IV], BIOLOX®*forte* (Al_2O_3) and BIOLOX®*delta* (75% Al_2O_3, 24% ZrO_2, Cr_2O_3) [V], respectively. As all of the previous studies dealing with the lubrication of hip replacements, with the exception of our paper [I], were performed utilizing ball-on-disc tribometers, our experiments were conducted in the same setup to be able to confront the results with previously published data. The tests were realized under two mean speeds, three SRRs and constant load. Following the experiment design, ale the tests were repeated three times under the same operating conditions with various lubricants. The content and ratio of albumin and γ-globulin was still the same; however, firstly the both proteins were non-stained (film thickness); secondly, albumin was stained (albumin protein film development); and finally, γ-globulin was stained (γ-globulin protein film development). The curves describing the thickness as well as particular protein film evolution were later compared allowing to define the role of individual constituents in relation to complex film behaviour.

The first paper [IV] dealt with the development of the methodology, while the main attention was paid to metal femoral head. The results showed that the fundamental parameter influencing the protein film formation is the level of slip between the components. Under pure rolling conditions, the lubricant film gradually increased with time for both the tested speeds, while the total film thickness was approximately two times higher at higher speed. When focusing on the role of proteins, the change of fluorescent intensity of γ-globulin was almost negligible; however, the intensity of albumin film well corresponded with the development of film thickness. Therefore, it was concluded that film is formed predominantly due to presence of albumin. Considering the negative sliding (the ball is faster than the disc) led to a completely different character of film formation. At lower speed, the film was very thin just in the range of units of nm over the whole time of the experiment. The protein film intensities were very low as well, indicating that the film could not be fully developed. This fact was attributed to the disruption of the film as a consequence of the fast rotation of the ball. Increasing the sliding speed caused an increase of film thickness during the second half of the test while the film was attributed to γ-globulin. On the images of excited area, it could be observed that γ-globulin layer thickness increased on the bottom of the disc due to gradual protein adsorption onto the surface. When the disc was faster than the ball (positive sliding),

the film increased rapidly up to 120 nm at lower and 40 nm at higher speed. After reaching the maximum, the film started to decrease. The increasing/decreasing tendency could be observed for both speeds while the difference was the time/sliding distance before reaching the maximum. In terms of proteins, albumin intensity was in a good agreement with the global tendency; therefore, it was concluded that the film was formed mainly due to presence of albumin as in the case of pure rolling. However, even the contribution of γ-globulin was remarkable especially at lower sliding speed.

Finally, the developed methodology was applied for the determination of protein film formation considering ceramic femoral heads [V]. The same experimental conditions were investigated in an effort to compare the results with those of metal head. Under pure rolling, the development of film thickness was very similar to metal component – continuous increase was detected independently of sliding speed and the type of ceramic. Again, the effect of albumin was dominant; nevertheless, the thickness of γ-globulin slightly increased with time. The results under negative sliding were not as clear and were strongly affected by both, material and sliding speed. Forte ceramic exhibited combined increasing/decreasing tendency. At lower speed the film was formed by the combination of both proteins, while in the case of higher speed, the contribution of γ-globulin was negligible. Similar behaviour was observed for delta ceramic at low speed regime. At higher speed, the film increased just after the start of the test, as a consequence of an immediate increase of γ-globulin film. Within the first minute, γ-globulin dropped to a very low level, while the further development of protein film was relatively stable between 12 and 20 nm and was attributed to albumin film. In the case of positive sliding, similar character of film formation compared to metal head was obtained for forte ceramic. The role of albumin was crucial; however, the contribution of γ-globulin increased with sliding distance at higher speed. Delta ceramic exhibited a rapid initial increase followed by a slight continuous decrease with the same behaviour of proteins as in the case of forte.

Biotribology 1–2 (2015) 61–65

Contents lists available at ScienceDirect

Biotribology

journal homepage: http://www.elsevier.com/locate/biotri

Visualization of lubricating films between artificial head and cup with respect to real geometry

M. Vrbka [a,*], D. Nečas [a,1], M. Hartl [a,2], I. Křupka [a,3], F. Urban [a,4], J. Gallo [b,5]

[a] Faculty of Mechanical Engineering, Institute of Machine and Industrial Design, Brno University of Technology, Technická 2896/2, 616 69 Brno, Czech Republic
[b] Orthopaedic Clinic, University Hospital Olomouc, I. P. Pavlova 6, 775 20 Olomouc, Czech Republic

ARTICLE INFO

Article history:
Received 7 January 2015
Received in revised form 27 April 2015
Accepted 11 May 2015
Available online 16 May 2015

Keywords:
Artificial hip joint
Pendulum simulator
Protein film formation
Conformity
Bovine serum
Film thickness
Colorimetric interferometry

ABSTRACT

The aim of this study is to propose a novel experimental approach enabling in-situ observation of film formation within hip joint replacements with respect to real geometry (including radial clearance) of rubbing surfaces. A pendulum hip joint simulator in combination with thin film colorimetric interferometry was employed for film thickness evaluation between metal femoral head and glass acetabular cup lubricated by bovine serum solution. Glass acetabulum was developed according to dimensions of artificial cup so the real radial clearance between components was considered. The pendulum, deflected at an initial position, was released and allowed to oscillate freely in the flexion–extension plane; therefore the transient character of motion was considered. Maximum central film thickness of 232 nm was measured at the beginning of the experiment. After a short time it decreased and became quite stable (around 90 nm) until the end of the measurement. The preliminary results shown that novel experimental approach seems to be a very powerful tool for studying lubrication processes within artificial hip joints while considering different loading and kinematic conditions, influence of geometry, clearance and material combination of contact pairs.

1. Introduction

In recent years, an extensive research has been conducted to clarify interfacial lubrication processes within hip joint replacements. Lubricant film thickness between rubbing surfaces influences friction, wear and therefore the service life of artificial joints. However, in vivo measurement is not suitable in this case; the artificial joint is surrounded by human tissues, which disables usage of conventional experimental methods, and also ethical consideration must be taken into account.

In general, two different approaches can be applied while studying lubricant film thickness; numerical simulations and experimental measurements. Several attempts have been made to predict film thickness numerically [1–3]. However, it is well known that a synovial fluid is a non-Newtonian liquid and corresponds to shear thinning behaviour [4,5]. This makes numerical predictions to be extremely complicated. Furthermore, protein adsorption, whose simulation is particularly difficult, significantly affects film thickness [6] and tribochemical layers [7].

In terms of experimental validation, electrical and optical methods represent two groups of routine techniques. The first experimental study about lubricant film within artificial hip joint using electrical resistivity method was given by Dowson et al. [8]. The aim of this study was to detect the gap between metallic head and cup during whole walking cycle. Achieved results were only qualitative in this case. The same method was applied by Smith et al. [9] while studying the surface separation of ceramic components during walking cycle. Since ceramic is non-conducting material, rubbing surfaces were coated with thin titanium nitride layer to allow the application of the resistivity technique. However, electrical methods usually suffer from very high sensitivity and, in addition, do not allow observing lubricant film formation directly, so that any information about physical or chemical processes is missing.

Mavraki and Cann [4,10] employed optical interferometry while studying lubricant film thickness within the model of hip joint replacements. They focused on the influence of mean speed and different model fluids on central film thickness. These articles were followed by Myant and Cann [5]; Myant et al. [11] where the influence of load was also introduced [11]. Although these articles brought a lot of important information about the fundamentals of protein film formation, lubricant film thickness was studied in classical ball-on-disc EHL simulator where the contact of non-conformal bodies occurs.

* Corresponding author. Tel.: +420 5 4114 3237.
E-mail addresses: vrbka.m@fme.vutbr.cz (M. Vrbka), necas@fme.vutbr.cz (D. Nečas), hartl@fme.vutbr.cz (M. Hartl), krupka@fme.vutbr.cz (I. Křupka), urban@fme.vutbr.cz (F. Urban), jiri.gallo@fnol.cz (J. Gallo).
[1] Tel.: +420 5 4114 3227.
[2] Tel.: +420 5 4114 2769.
[3] Tel.: +420 5 4114 2723.
[4] Tel.: +420 5 4114 3238.
[5] Tel.: +420 5 8844 3607.

http://dx.doi.org/10.1016/j.biotri.2015.05.002
2352-5738/

From the literature review it can be assumed that the conformity of rubbing surfaces and therefore the radial clearance can substantially influence film thickness [12–14]. In our previous studies, we have applied two experimental configurations to verify this hypothesis [15,16]. As was shown by Vrbka et al. [16], changing the experimental setup from ball-on-disc to more conformal ball-on-lens configuration led to significant differences in film thickness measurements. But even in this case, the diametral clearance was still quite high (about 3.2 mm), which does not correspond to real situation (0.04–0.2 mm).

The above information indicates that so far there has not been in vitro study about film thickness determination respecting the real geometry of head and cup. The aim of this study is to introduce a novel experimental approach, which enables to evaluate the film thickness inside the contact of artificial joints with respect to real geometry of both parts, including the radial clearance. For this purpose, an optical interferometry measurement method was combined with a pendulum hip joint simulator to enable the evaluation of film thickness and the observation of protein film formation.

2. Materials and methods

An experimental apparatus, employed in the present study, consists of a pendulum hip joint simulator and optical imaging system. The simulator, originally designed by Stanton [17], is composed of two main parts; a base frame with acetabular cup and pendulum with femoral head. The optical imaging system includes the episcopic microscope, halogen illuminator, CMOS digital camera and PC, while the microscope and camera are mounted in an inverted position, as can be seen in Fig. 1. For observation of film formation inside the contact, the acetabular cup was transparent.

If the contact of metal femoral head and glass acetabular cup is illuminated, then colour Newton rings can be observed. Thin film colorimetric interferometry, presented by Hartl et al. [18] was used for film thickness evaluation. Authors focused on ball-on-disc configuration and applied two different approaches [18]. Firstly, the glass disc was coated by chromium layer only. Secondly, the disc was, moreover, coated by silicon dioxide "spacer" layer. It was clearly proved that there is no influence of spacer layer on measured film thickness. In our case, the contact surface of glass cup is coated only with semi-reflective chromium layer to increase the contrast of interference fringes. The evaluation of the film thickness is based on three steps:

1. The calibration curves are obtained from an interferogram of a lightly loaded static contact, which is matched with measured contact profile. Therefore, information about the dependence between the colour and the film thickness is given.
2. Interferograms of fully loaded contact during the swinging motion of pendulum are captured via a high-speed camera.
3. Captured interferograms are matched with calibration curves, so the thickness at arbitrary location of the contact can be determined.

In our study, femoral head Aesculap NK430K (CoCr29Mo, ISO 5832-12) and optical glass (BK7) acetabular cup were investigated. By using the optical scanning method (GOM ATOS Triple Scan) it was found that the actual diameters of head and cup were 27.988 mm and 28.080 mm, respectively. Therefore, the rubbing surfaces have shown the diametral clearance of 92 μm. Initial surface topography of metal head was analysed in greater detail using the optical measurement method based on phase shifting interferometry (Bruker Contour GT X8). Evaluated average surface roughness *Ra* was 3.8 nm. The contact surface of glass cup was considered to be optically smooth.

For the purpose of this study, a human synovial fluid was substituted by a 25% bovine serum (BS) solution (Sigma-Aldrich B9433) in deionized water. Total protein concentration was 22.4 mg/ml and the lubricant was prepared in volumes of 12 ml and immediately stored in a freezer at −22 °C. The solution was taken out from the freezer 2 h before testing to thaw naturally and then supplied to the glass cup; thereby a vicinity of the contact pair was fully bathed. All components, which were in contact with BS, were cleaned in 1% sodium dodecyl sulphate solution, rinsed in distilled water, and then washed in an isopropyl alcohol before assembly.

Test conditions of all experiments were as follows. Applied load, achieved by putting the weights on the pendulum arms, was 532 N, while the resulting maximum contact pressure reached 28.7 MPa (contact zone diameter was approximately 6 mm). As can be seen in Fig. 1, the acetabular cup can be tempered by heating cartridges, so all the measurements were carried out under body temperature of 37 °C. BS solution was also heated just before the test. The pendulum was deflected at an initial offset angle of 16°, released, and allowed to oscillate freely in the flexion–extension plane.

3. Results and discussion

Previously, the majority of authors have applied simplified unidirectional pure sliding or rolling/sliding conditions while studying lubrication processes within artificial hip joints [4,5,10,11,15,16]. Although it was declared that this approach can provide important information about the fundamentals of protein film formation, in real situation kinematic and loading conditions are transient. In hip joints, there are three types of motions; flexion/extension, abduction/adduction and inward/outward rotation, while the flexion/extension is a dominant during the gait cycle.

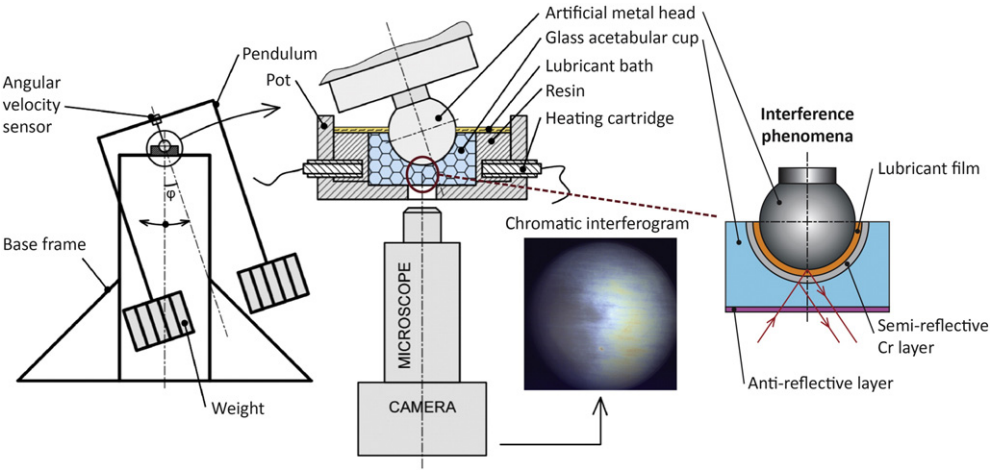

Fig. 1. Observation of lubricant film using optical test device — a pendulum hip joint simulator.

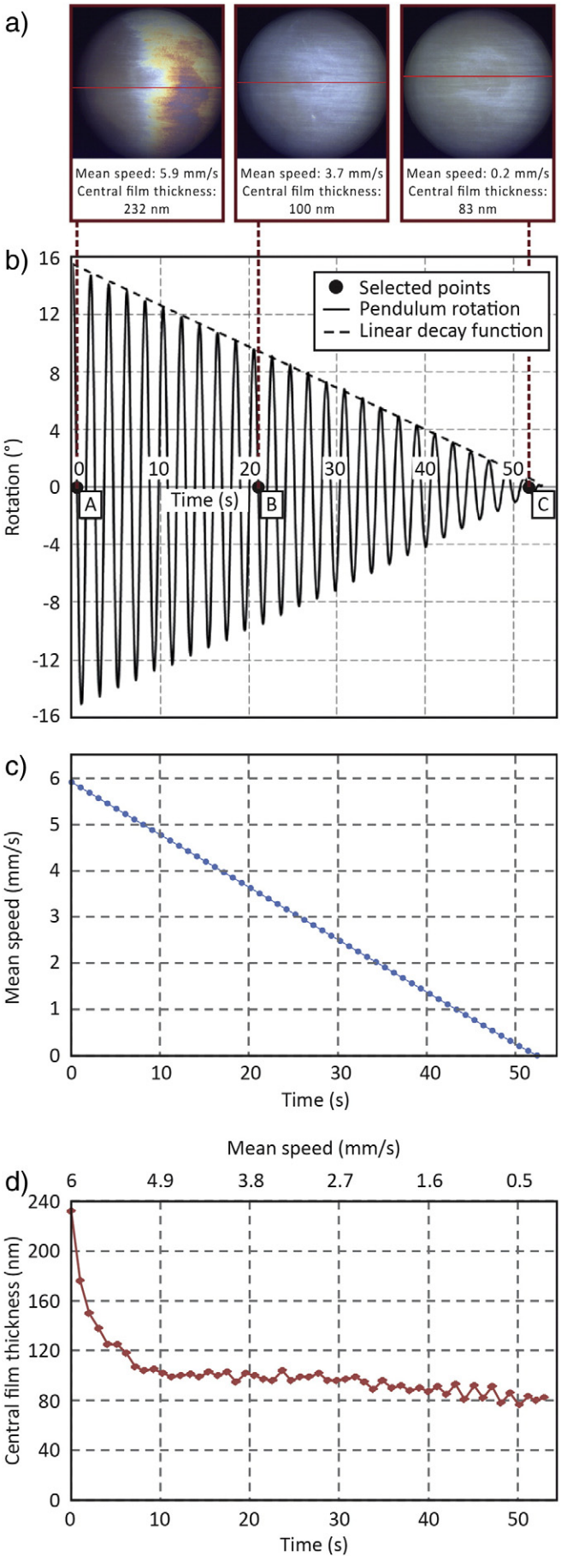

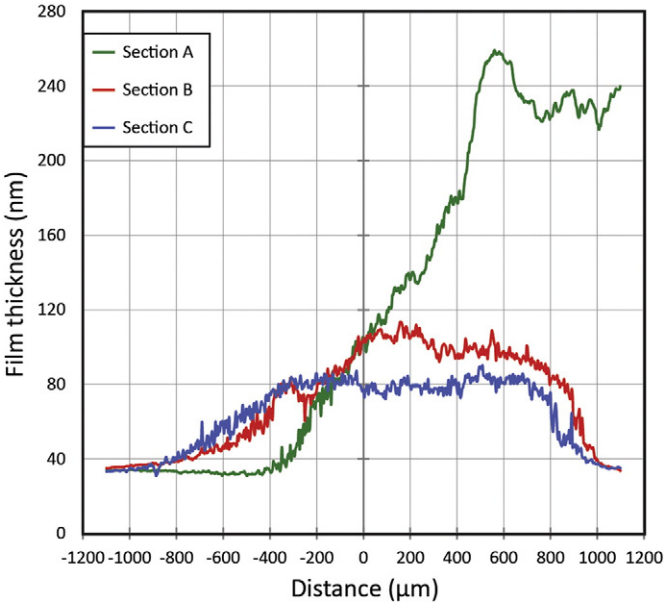

Fig. 3. Distribution of film thickness in the direction of pendulum rotation. Individual sections correspond to the lines displayed on chromatic interferograms, see Fig. 2a. Inlet is on the left.

The hip joint simulator, employed in the present study, allowed investigating lubrication processes during flexion/extension motion in a range of −16 to 16°. The pendulum simulator response represents a damped transient sinusoidal motion. As can be seen in Fig. 2b, in case of metal femoral head sliding against glass acetabular cup, the character of amplitude decay was linear. Therefore both rotation and velocity are linearly damped sinusoidal functions of frequency of 0.5 Hz. For further analyses, three points A, B and C of pendulum equilibrium state have been chosen, see Fig. 2b. According to the character of pendulum response decay, dependence of equilibrium points mean speed on time is also linear (Fig. 2c), while the uniform deceleration is 0.11 mm/s^2.

Chromatic interferograms corresponding to selected points A, B, and C are shown in Fig. 2a. Central film thickness is an averaged value of total number of points belonging to the circle area with the radius equal to 1/20 of the contact zone radius where centres of both the circle and the contact zone are identical. At the beginning of the experiment (point A), a relatively thick lubricant film was formed between the components. Maximum film thickness is around 260 nm at that time. After some time (point B), the lubricant layer is uniform without any significant protein aggregations, while the central film thickness is about 100 nm. At the end of pendulum oscillation (point C), the lubricant film is still uniform and the central film thickness of the layer reaches 80 nm. Distribution of film thickness, evaluated pixel by pixel, in the direction of pendulum swinging for selected points, is shown in Fig. 3. In this figure, a strong protein aggregation (section A), as well as the uniformity of lubricant film (sections B, C) can be clearly seen.

Development of central film thickness as a function of time and mean speed is drawn in Fig. 2d where two separate scales are used simultaneously. As can be seen in this figure, immediately after starting the experiment, central film thickness reached its maximum value 232 nm and after a short time it decreased and became quite stable (around 90 nm) for the rest of the experiment. This tendency does not

Fig. 2. From the top: Chromatic interferograms (inlet is on the left) depicting the behaviour of lubricant film thickness in selected points A ($t_A = 0.6$ s, $u_{mA} = 5.9$ mm/s), B ($t_B = 21.1$ s, $u_{mB} = 3.7$ mm/s) and C ($t_C = 51.8$ s, $u_{mC} = 0.2$ mm/s), which correspond to the equilibrium state position of the pendulum ($\varphi = 0°$, $F_{max} = 532$ N) and are highlighted in the graph b) showing the damping of pendulum oscillation. c) Dependence of mean speed of pendulum equilibrium points on time. d) Development of central film thickness as a function of time and mean speed.

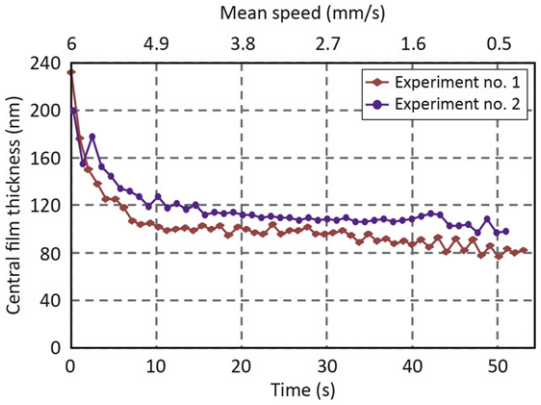

Fig. 4. Repeatability of measurements. The curves depict the development of central film thickness as a function of time and mean speed.

correspond to the ball-on-disc results (non-conformal contact) under unidirectional pure sliding conditions obtained by Vrbka et al. [16] where film thickness gradually increased from 0 to 880 nm and after a few tens of seconds it decreased, and at the end of the measurement the average value was around 50 nm. On the contrary, there is a good agreement with ball-on-lens results [15]. In that case, a very similar character of film formation was observed, however the film thickness values were significantly lower in comparison with the real geometrical configuration. Therefore it can be assumed that the importance of conformity of rubbing surfaces was clearly evidenced.

To be able to better understand the credibility of results, the experiment was repeated under the same operating conditions after some time. The comparison of the results for the first and the second experiment can be seen in Fig. 4. Quite good repeatability was observed as there is no significant difference between the curves representing the film thickness development. Similar character of film formation can be also observed on chromatic interferograms shown in Fig. 5a,b.

Moreover in the meaning of validation of employed experimental technique, the measurement was also conducted with PAO oil of a dynamic viscosity equal to $\eta = 0.0255$ Pa·s as a representative of a simple Newtonian liquid. For better illustration, chromatic interferograms for all the experiments are displayed in Fig. 5. On these interferograms, different characters of film formation can be observed. When lubricated by bovine serum, contact surfaces are protected by protein layer therefore there is no significant wear of rubbing surfaces. However, in case of oil, after just a few seconds (≈ 4.2) breakdown of lubricating film occurs which leads to significant wear of chromium layer, as can be seen on interferograms in the lower right corner in Fig. 5. On the contrary, even if there is a thinner oil film, swinging motion of pendulum lasted longer (75 s) in comparison with bovine serum lubrication (approximately 50 s). This is probably due to shear forces between proteins causing an increase of the coefficient of friction, as was indicated by Brockett et al. [19].

According to the essential effect of surface conformity, introduced by Vrbka et al. [16] in combination with direct evidence of the importance of transient conditions pronounced by Myant and Cann [20], it can be concluded that the described experimental approach seems to be a very suitable tool for further investigation of lubrication processes within hip joint replacements, while considering different loading and

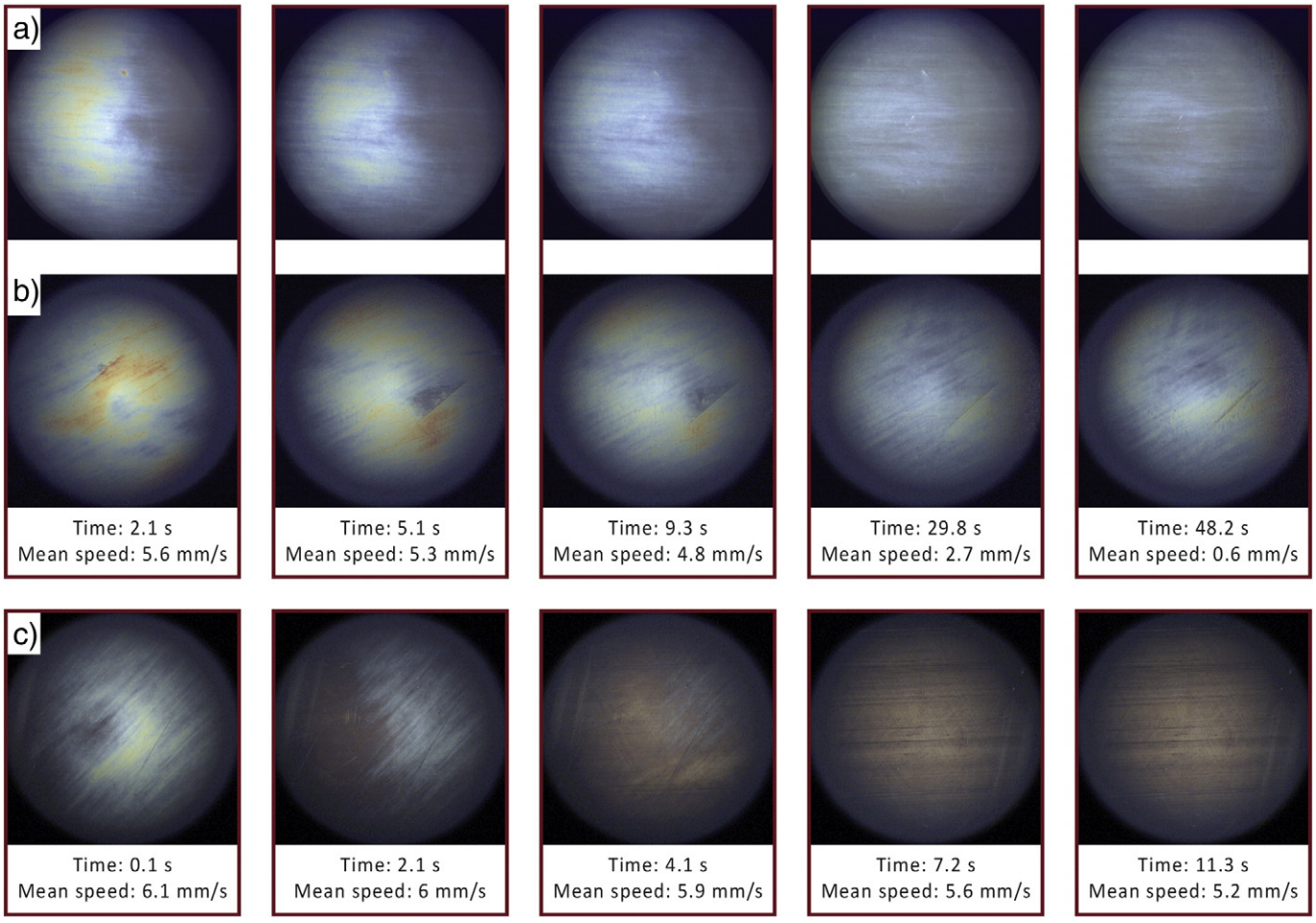

Fig. 5. Chromatic interferograms captured in equilibrium position of the pendulum during the experiments. a) Experiment with bovine serum number 1. b) Experiment with bovine serum number 2. c) Experiment with oil. Inlet is on the left.

kinematic conditions, influence of geometry, radial clearance and material combination of contact pairs.

4. Conclusions

A novel experimental approach enabling in-situ observation of protein film formation with respect to real geometry (including clearance) and transient motion of hip joint replacements was introduced in the present paper. Thin film colorimetric interferometry was implemented into the pendulum hip joint simulator for film thickness determination. This makes the apparatus to be a very powerful tool for studying lubrication processes within artificial hip joints. According to the author's knowledge, the pendulum simulator in combination with optical measurement of film thickness has never been used before.

Funding

This research was carried out under the project NETME CENTRE PLUS (LO1202) with financial support from the Ministry of Education, Youth and Sports under the National Sustainability Programme I. This research was also supported by the project "The influence of joint fluid composition on formation of lubricating film in THA" (NT/14267-3/2013) financed by the Internal Grant Agency of the Ministry of Health of the Czech Republic (NT/14267-3/2013).

Declaration of conflicting interests

The authors declare that there is no conflict of interest.

Acknowledgements

The authors express thanks to D. Paloušek for optical scanning of artificial hip joint pairs.

References

[1] Dowson D. Tribological principles in metal-on-metal hip joint design. Proc IMechE H J Eng Med 2006;220:161–71.
[2] Jalali-Vahid D, Jin ZM, Dowson D. Effect of start-up conditions on elastohydrodynamic lubrication of metal-on-metal hip implants. Proc IMechE J J Eng Tribol 2006;220:143–50.
[3] Dowson D, Jin ZM. Metal-on-metal hip joint tribology. Proc IMechE H J Eng Med 2006;220:107–18.
[4] Mavraki A, Cann PM. Lubricating film thickness measurements with bovine serum. Tribol Int 2011;44:550–6.
[5] Myant C, Cann PM. In contact observation of model synovial fluid lubricating mechanisms. Tribol Int 2013;63:97–104.
[6] Scholes SC, Unsworth A. The effects of proteins on the friction and lubrication of artificial joints. Proc IMechE H J Eng Med 2006;220:687–93.
[7] Wimmer MA, Sprecher C, Hauert R, Täger G, Fischer A. Tribochemical reaction on metal-on-metal hip joint bearings — a comparison between in-vitro and in-vivo results. Wear 2003;255:1007–14.
[8] Dowson D, McNie CM, Goldsmith AAJ. Direct experimental evidence of lubrication in a metal-on-metal total hip replacement tested in a joint simulator. Proc IMechE C J Mech Eng Sci 2000;214:75–86.
[9] Smith SL, Dowson D, Goldsmith AAJ, Valizadeh R, Colligon JS. Direct evidence of lubrication in ceramic-on-ceramic total hip replacements. Proc IMechE C J Mech Eng Sci 2001;215:265–8.
[10] Mavraki A, Cann PM. Friction and lubricant film thickness measurements on simulated synovial fluids. Proc IMechE J J Eng Tribol 2009;223:325–35.
[11] Myant C, Underwood R, Fan J, Cann PM. Lubrication of metal-on-metal hip joints: the effect of protein content and load on film formation and wear. J Mech Behav Biomed Mater 2012;6:30–40.
[12] Jin ZM, Dowson D, Fisher J. Analysis of fluid film lubrication in artificial hip joint replacements with surfaces of high elastic modulus. Proc IMechE H J Eng Med 1997;211:247–56.
[13] Smith SL, Dowson D, Goldsmith AAJ. The effect of diametral clearance, motion and loading cycles upon lubrication of metal-on-metal total hip replacements. Proc IMechE C J Mech Eng Sci 2001;215:1–5.
[14] Brockett CL, Harper P, Williams S, Isaac GH, Dwyer-Joyce RS, Jin Z, Fisher J. The influence of clearance on friction, lubrication and squeaking in large diameter metal-on-metal hip replacements. J Mater Sci Mater Med 2008;19:1575–9.
[15] Vrbka M, Návrat T, Křupka I, Hartl M, Šperka P, Gallo J. Study of film formation in bovine serum lubricated contacts under rolling/sliding conditions. Proc IMechE J J Eng Tribol 2013;227:459–75.
[16] Vrbka M, Křupka I, Hartl M, Návrat T, Gallo J, Galandáková A. In situ measurements of thin films in bovine serum lubricated contacts using optical interferometry. Proc IMechE H J Eng Med 2014;228:149–58.
[17] Stanton TE. Boundary lubrication in engineering practice. Engineer 1923;135:678–80.
[18] Hartl M, Křupka I, Poliščuk R, Liška M, Molimard J, Querry M, Vergne P. Thin film colorimetric interferometry. Tribol Trans 2001;44:270–6.
[19] Brockett C, Williams S, Jin Z, Isaac G, Fisher J. Friction of total hip replacements with different bearings and loading conditions. J Biomed Mater Res B Appl Biomater 2007;81:508–15.
[20] Myant CW, Cann P. The effect of transient conditions on synovial fluid protein aggregation lubrication. J Mech Behav Biomed Mater 2014;34:349–57.

FILM THICKNESS MAPPING IN LUBRICATED CONTACTS USING FLUORESCENCE

DAVID NECAS, PETR SPERKA, MARTIN VRBKA
IVAN KRUPKA, MARTIN HARTL
Brno University of Technology, Faculty of Mechanical Engineering
Institute of Machine and Industrial Design, Brno, Czech Republic

DOI: 10.17973/MMSJ.2015_12_201524

e-mail: necas@fme.vutbr.cz

The present paper presents experimental method for film thickness mapping inside the contact of two bodies. Despite extensive experimental research in the area of contacts of rigid bodies, little is known about the film formation when at least one of the bodies is compliant. This is due to limitations disabling the usage of conventional methods. In present study, mercury lamp induced fluorescence is developed and applied. Evaluation process is verified by comparing theoretical predictions and experimental data for piezoviscous-elastic contact of ceramic ball and glass disc. Consequently, phenolic sample is used as a representative of compliant material. The contact was lubricated by mineral oil and the experiments were carried out under pure rolling conditions. Film thicknesses in a range from 50 nm to 1.2 um were measured for compliant contact. The measured data are little bit lower compared to theory, indicating that thermal effects may influence the lubricant film.

KEYWORDS
isoviscous, elastohydrodynamic, film thickness, fluorescence, compliant

1. INTRODUCTION

Tribological performance of machine elements play an important role nowadays, since it is well known that the friction influences power loss and therefore determines the efficiency of machine components [Reddyhoff 2010]. In an effort to better understand the lubrication processes, evaluation of lubricant film thickness is desirable. In many applications, elastohydrodynamic lubrication (EHL) occurs. EHL is typical for contact of rigid non-conformal bodies like gears, rolling bearings, or cams. Under EHL conditions, contact pressure causes substantial elastic deformation of surfaces and, in addition, leads to an increase of lubricant viscosity [Esfahanian 1991]. The operating lubrication regime of such contacts is known as piezoviscous-elastic (PE). In this case, optical interferometry method [Hartl 2001], as well as the electrical methods based on the change of electrical quantity [Spikes 1999], seem to be an established experimental approaches for film thickness measurement. An optical interference is a physical phenomenon occurring by composing the two light beams which are reflected from nearby interfaces. Due to the principle of the method, analysed bodies have to be reflective. Electrical methods converts the change in electrical quantity into a change of film thickness, therefore it is necessary to ensure sufficient electrical conductivity of the tested materials.

Much more challenging task is to investigate the film thickness when at least one of the contact bodies is compliant. The compliant means that modulus of elasticity of the body is in a range of units of GPa at maximum. Related to lubrication, isoviscous-elastic (IE) lubrication (i-EHL) regime usually occurs. In that case, the surfaces are deformed elastically, however the contact pressure is too low to increase the viscosity of lubricant [Esfahanian 1991]. Examples of compliant contacts can be found in both, technical and biological systems. From the technical point of view, typical applications are windscreen wipers, rubber o-seals, or tyres. In relation to biological systems, synovial joints, contact lenses or tongue-palate contact during food processing can be mentioned [Myant 2010b, Fowell 2014].

In meaning of theoretical predictions, two equations are generally used for film thickness estimation. Hamrock-Dowson derived the formula for film thickness determination as a function of dimensionless speed and load parameter [Hamrock 1978]. Later, the equation based on the dimensionless Moes load and lubricant parameter (M, L) was pronounced by Nijenbanning et al. [Nijenbanning 1994]. In the present study, the Hamrock-Dowson equation was used for comparison with the obtained experimental data.

For experimental investigation of compliant contacts, several methods were previously applied, such as optical interferometry [Roberts 1968, Roberts 1977a, Roberts 1977b], ultrasonic reflection method [Gasni 2011], Raman spectroscopy [Bongaerts 2008], or magnetic resistance method [Poll 1992]. However, each of the above mentioned approaches exhibits some limitations due to the characteristics of i-EHL contacts [Myant 2010a]:

- Film thickness varies in a very wide range – from several nanometers to the hundreds of micrometers.
- Larger contact areas in comparison with PE contacts.
- High roughness of surfaces, limited possibilities of polishing.
- Poor electrical conductivity and insufficient reflectivity of surfaces.
- Complicated coating by the reflective layers. These layers are prone to wear and may influence the surface properties of base material.

According to above mentioned information, usage of common experimental methods is very limited. From the literature [Spikes 1999], it can be assumed that optical method based on fluorescence microscopy seems to be a suitable approach for the investigation of film thickness in compliant contacts. The main difference against the optical interferometry is as follows. While the interferometry provides the direct distance between two surfaces based on the reflected light beams, fluorescence gives the information about the amount of lubricant which is presented inside the contact [Reddyhoff 2010]. The amount of lubricant is expressed by the intensity of lubricating film. It was previously proved that the dependence between the intensity of film and its thickness is linear [Azushima 2006].

First application of fluorescence method in tribology was pronounced in 1970th [Smart 1974, Ford 1978]. In the pilot study [Smart 1974], the authors employed fluorescence induced by a mercury lamp to measure the thickness of oil film on steel rotating cylinder. In the consequent study, the differences in excitation were analysed in a detail [Ford 1978]. A blue laser was used as the source of excitation. It was concluded that using the laser instead of the mercury lamp can bring several advantages such as higher efficiency of fluorescence, better stability of illumination, or less demanding design of the experimental apparatus. On the contrary, laser produces more inhomogeneities, such as speckles, so the calibration process is more complicated. A problem of losing the fluorescence emission was also discussed, as it can significantly influence the measured data.

Sugimura et al. [Sugimura 2000] investigated the lubricant film thickness by fluorescence technique in conventional ball-on-disc apparatus, originally introduced by Gohar and Cameron [Gohar 1963]. The authors could detect films down to 30 nm. A significant problem with calibration connected with the interference phenomena when the contact of steel ball and glass disc was illuminated was mentioned. In this case, the steel ball was substituted by glass lens during calibration. However, it was later pointed out [Myant 2010c] that different reflectivity between the calibration and test specimen can lead to inaccuracies in results.

The usage of fluorescent method for film thickness mapping in compliant contacts was provided by Myant et al. [Myant 2010c]. Laser induced fluorescence was employed to evaluate the film thickness between polydimethylsiloxane (PDMS) pin sliding against the glass disc. The effects of fully flooded conditions, as well as the starved lubricating conditions were investigated. Calibration process was described in a

detail, as it significantly influences measured data. In this case, the calibration curve was obtained by using the same configuration as was used during the test. It was indicated that it is necessary to consider real optical properties of the contact bodies during calibration. In the paper, the authors were able to measure film thickness in a range from 200 nm to 25 um. In comparison with the theoretical predictions, the measured values were usually lower than predicted.

From the above mentioned references it is apparent that the investigation of compliant contacts is still a challenging task in the area of tribology. The aim of this study is to introduce an experimental approach enabling film thickness measurement in lubricated contacts independently on the reflectivity and conductivity of investigated materials. For this purpose, an optical method based on fluorescence microscopy in combination with ball-on-disc apparatus was employed.

2. MATERIALS AND METHODS

The experimental apparatus, employed in the present study, consists of conventional ball-on-disc tribometer [Gohar 1963] and optical imaging system, as can be seen in Fig. 1. Both components, the ball and the disc can be driven independently, so various kinematic conditions can be applied. Optical imaging system includes mercury lamp, episcopic microscope, scientific complementary metal oxide semiconductor (sCMOS) digital camera and PC.

For the film thickness measurement, optical method based on fluorescence microscopy was used. A fluorescence phenomenon was described as a consequence of three following steps [Haugland 1996]:

- Excitation: A photon is supplied by an external light source (lamp, laser) and is absorbed by the fluorophore, creating an excited electronic single state.
- Excited-state lifetime: Lasts usually 1 – 10 ns. During that time, the molecule can undergo some relaxation (energy dissipation) and is left in a state from which it can emit fluorescence.
- Fluorescence emission: A photon of energy is emitted, while the fluorophore returns to its ground state. Due to energy dissipation during the previous phase, the photon has lower energy and therefore the longer wavelength than the excited photon. The difference in wavelengths is known as Stokes shift, which is absolutely fundamental phenomenon since it allows separation of the measured emission from excitation.

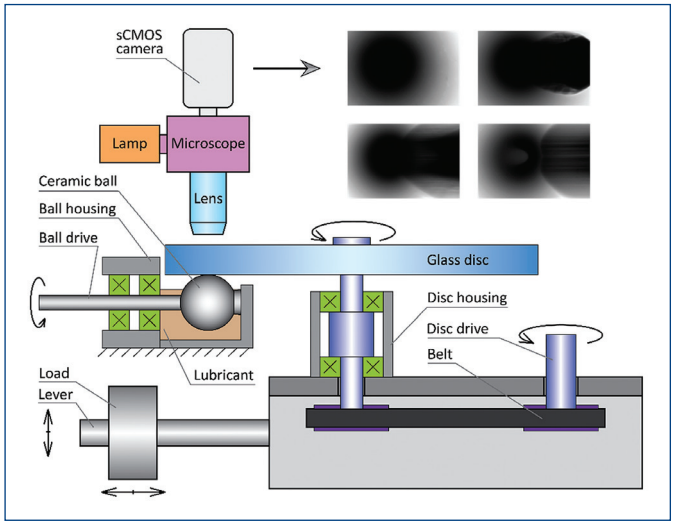

Figure 1. Scheme of the experimental apparatus.

The evaluation of lubricant film is fundamentally affected by the calibration process. The calibration curve is obtained from the knowledge of Hertz theory and the image of lightly loaded static contact. Moreover, to avoid light scattering, background image of lubricant is taken. The calibration curve is then matched with images taken by sCMOS camera, so the film thickness in arbitrary point can be determined.

To validate the measurement method, film thickness of PE contact, created by ceramic ball and glass disc was evaluated and compared with theoretical predictions. Hamrock and Dowson [Hamrock 1977] defined the following formula for dimensionless film thickness estimation in elliptical contact:

$$H_c = 2.69 \cdot U^{0.67} \cdot G^{0.53} \cdot W^{-0.067}(1 - 0.61 \cdot e^{-0.73 \cdot k}) \quad (1)$$

where H_c is defined by h_c/R'. h_c is central film thickness. For point contact, the ellipticity parameter k is reduced to unity. The dimensionless parameters *U, W, G* are:

$$\text{dimensionless speed parameter, } U = \frac{\eta_0 \cdot u}{E' \cdot R'} \quad (2)$$

$$\text{dimensionless load parameter, } W = \frac{F}{E' \cdot R'^2} \quad (3)$$

$$\text{dimensionless material parameter, } G = \alpha \cdot E' \quad (4)$$

where *u* is the rolling speed, η_0 is the dynamic viscosity of lubricant, *F* is the applied load, α is the pressure-viscous coefficient, *R´* is the reduced radius of curvature given by $1/R' = 1/r_x + 1/r_y$ and E´ is the reduced elastic modulus defined as $2/E' = (1 - \mu_1^2)/E_1 + (1 - \mu_2^2)/E_2$, where r_x, r_y denote the radii in the rolling direction, E_1, E_2, μ_1, μ_2 are elastic modulus and Poisson´s ratios of the contacting bodies.

As a representative of compliant bodies, phenolic ball of the elastic modulus equal to 4 GPa was used. For i-EHL contacts, the formula for dimensionless central film thickness is as follows [Hamrock 1978]:

$$H_{c,compliant} = 7.32 \cdot U^{0.64} \cdot W^{-0.22}(1 - 0.72 \cdot e^{-0.28 \cdot k}) \quad (5)$$

Mineral oil of dynamic viscosity $\eta = 0.6444$ Pa·s was applied as a test lubricant since it emits fluorescence naturally when illuminated in UV. Sufficient amount of lubricant was used, therefore the lubricant film could be fully developed. The test conditions were as follows. In case of PE contact (ceramic-on-glass), the applied load was equal to 12 N, resulting in the maximum contact pressure of 401.7 MPa. Because of the repeatability, the experiment was conducted two times. The tests with ceramic ball were realized to validate the evaluation algorithm. After that, the measurements were carried out with the phenolic ball of low elastic modulus. Three different loads were applied, 12 N, 26 N, and 41 N, respectively; leading to Hertzian contact pressures equal to 66.5, 83.8, and 100.2 MPa. Independently on applied materials, the experiments were performed under pure rolling conditions for the rolling speeds in a range from 10 to 500 mm/s. Therefore, the dependence between film thickness and rolling speed was obtained. All the test conditions are summarized in Tab. 1.

	PE contact	IE (compliant) contact
Load [N]	12	12; 26; 41
Maximum contact pressure [MPa]	401.7	66.5; 83.8; 100.2
Slide-to-roll ratio [1]	0	0
Speed range [mm/s]	10 – 500	10 – 500

Table 1: Test conditions applied during the experiments.

3. RESULTS AND DISCUSSION

3.1 Method validation

In case of the PE contact, film thickness varied from 100 nm for 10 mm/s, up to 1.5 um for 500 mm/s. Images taken by sCMOS camera for ceramic-on-glass contact pair under various rolling speeds are displayed in Fig. 2. With increasing the rolling speed, typical horseshoe-shaped constriction is formed. The values of film thickness plotted against rolling speed and compared with theoretical predictions provided by

Hamrock and Dowson [Hamrock 1977] are shown in Fig. 3. As can be seen in this figure, the film thickness gradually increased over the whole range of applied speeds. As there is an excellent agreement between expected and measured data, the relevance of the evaluation process was clearly proved. The profiles of lubricant film along the rolling direction for selected speeds are drawn in Fig. 3.

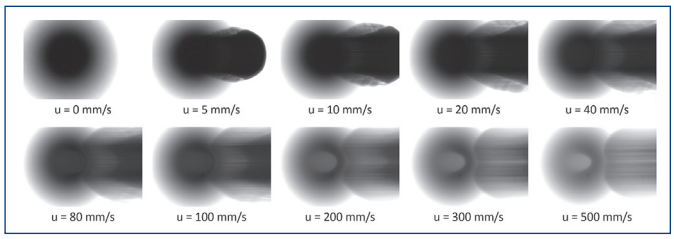

Figure 2. Film thickness maps of the lubricated PE contact. Inlet is on the left of each image.

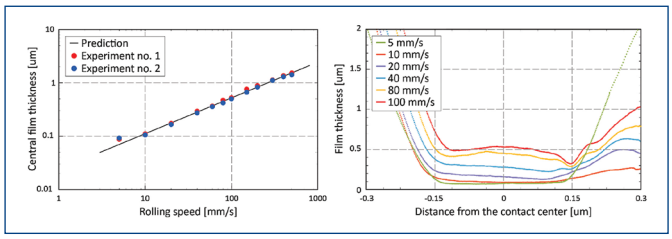

Figure 3. Left: The dependence between film thickness and rolling speed. Right: Film profiles for selected rolling speeds (inlet is on the left).

3.2 Compliant contact

For compliant contact, different loading and kinematic conditions were applied, as was mentioned above. Images of the contact loaded by force equal to 12 N are shown in Fig. 4. Generally, there was no significant effect of load on lubricant film. However, against expectations, increasing load led to an increase of lubricant film. The same phenomena was observed by Fowell et al. [Fowell 2014], where a slight increase of film thickness in contact between PDMS hemisphere and glass disc was detected while the load raised from 11 mN to 23.5 mN. The effect of load on lubricant film will be investigated in a more detail in further study. One of the point is the behaviour of phenolic sample under high pressure conditions. The surface topography can also play an important role. As is shown in Fig. 5, for all the applied loads, the measured film thicknesses were lower than predicted. As was pointed out by Myant et al. [Myant 2010c], in case of low viscosity fluids, there was a very good correlation with theory. On the contrary, when glycerol was used as a lubricant, the authors detected lower films than predicted. This fact is attributed to thermal effects and hygroscopic nature of applied fluid. Although the measurements in the present paper were realized under controlled ambient temperature (22 °C), the results can be also influenced by local thermal effects occurring inside the contact of two bodies. Viscosity of applied mineral oil was analysed in a detail, finding that increasing the temperature for just 3 °C leads to decrease of viscosity from 0.6444 Pa·s to 0.5122 Pa·s. As the viscosity drops, the lubricant film becomes lower. Experimental results are in very good agreement for the load equal to 41 N. Profiles of film thickness in the rolling direction for this load are plotted in the right part of Fig. 5. Previously, the authors were not able to observe such a significant constriction at the contact outlet in case of compliant contacts [Fowell 2014, Myant 2010c]. However it should be noted that in these references, very soft samples, with the modulus of elasticity in a range of units of MPa, were investigated. Another effect associated with relatively higher elastic modulus of the phenolic ball is the slope of the film in the rolling direction. Indications that central plateau region, which is associated with EHL, is absent in case of compliant contacts was confirmed by [Myant 2010a]. The slope of converging edge is supposed to increase with increasing speed [Fowell 2014, Myant 2010a, Myant 2010c]. Although there is an increase of slope with increasing rolling speed (see Fig. 5), the change is not such a rapid than previously observed [Fowell 2014, Myant 2010c]. This indicates that the higher elastic modulus of the compliant body leads to flattening of the central contact zone.

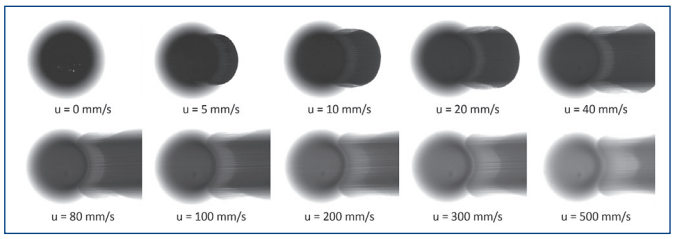

Figure 4. Film thickness maps of the lubricated compliant contact for load equal to 12 N. Inlet is on the left of each image.

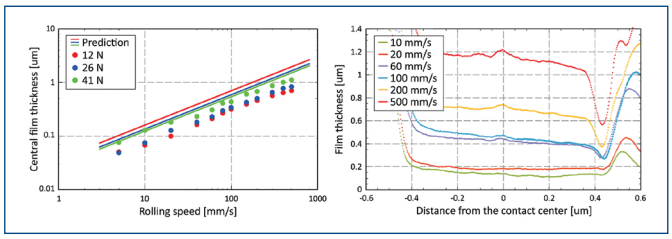

Figure 5. Left: The dependence between film thickness and rolling speed for different loading conditions. Right: Film profiles for selected rolling speeds for load equal to 41 N (inlet is on the left).

4. CONCLUSION

In the present paper, the experimental approach based on the fluorescent microscopy was introduced. The method was validated by conducting the central film thickness measurement for ceramic-on-glass contact, while the data were compared with the theoretical prediction made by Hamrock and Dowson [Hamrock 1977]. As there was a very good agreement with prediction, the relevance of the measured data was clearly proved. The main benefit of the above described technique is that the compliant bodies can be investigated. The phenolic ball was used as a representative of compliant material. Quite good correlation with prediction [Hamrock 1978] was found, however, the values were a little bit lower compared to expectations. This fact is attributed especially to thermal effects, as was previously pointed out by [Myant 2010c]. It can be concluded that the applied experimental approach is suitable for studying the compliant contacts. In the following paper, the effect of material properties, as well as the effect of loading and kinematic conditions, will be investigated.

ACKNOWLEDGEMENTS

The research leading to these results has received funding from the Ministry of Education, Youth and Sports under the National Sustainability Program I (Project LO1202). The authors express thanks to K. Dockal for the film thickness measurements.

REFERENCES

[Azushima 2006] Azushima, A. In situ 3D measurement of lubrication behavior at interface between tool and workpiece by direct fluorescence observation technique. Wear, February 2006, Vol. 260, No. 3, pp. 243-248.

[Bongaerts 2008] Bongaerts, J.H.H., et al. In situ confocal Raman spectroscopy of lubricants in a soft elastohydrodynamic tribological contact. Journal of Applied Physics, July 2008, Vol. 104, No. 1, pp. 014913.

[Esfahanian 1991] Esfahanian, M. and Hamrock, B.J. Fluid-Film Lubrication Regimes Revisited. Tribology Transactions, 1991, Vol. 34, No. 4, pp. 628-632.

[Ford 1978] Ford, R.A.J. and Foord, C.A. Laser-based fluorescence techniques for measuring thin liquid films. Wear, December 1978, Vol. 51, No. 2, pp. 289-297.
[Fowell 2014] Fowell, M.T., et al. A study of lubricant film thickness in compliant contacts of elastomeric seal materials using a laser induced fluorescence technique. Tribology International, December 2014, Vol. 80, pp. 76-89.
[Gasni 2011] Gasni, D., et al. Measurements of lubricant film thickness in the iso-viscous elastohydrodynamic regime. Tribology International, July 2011, Vol. 44, No. 7-8, pp. 933-944.
[Gohar 1963] Gohar, R. and Cameron, A. Optical measurement of oil film thickness under elastohydrodynamic lubrication. Nature, November 1963, Vol. 200, pp. 458-459.
[Hamrock 1977] Hamrock, B.J. and Dowson, D. Isothermal elasto-hydrodynamic lubrication of point contacts: part III—fully flooded results. Journal of Tribology, April 1977, Vol. 99, No. 2, pp. 264-275.
[Hamrock 1978] Hamrock B.J. and Dowson, D. Elastohydrodynamic lubrication of elliptical contacts for materials of low elastic modulus. 1-fully flooded conjunction. Journal of Tribology, April 1978, Vol. 100, No. 2, pp. 236-245.
[Hartl 2001] Hartl, M., et al. Thin Film Colorimetric Interferometry. Tribology Transactions, 2001, Vol. 44, No. 2, pp. 270-276.
[Haugland 1996] Haugland R. P. Handbook of fluorescent probes and research chemicals. Eugene: Molecular Probes, 1996. ISBN 0-9652240-0-7.
[Myant 2010a] Myant C., et al. An investigation of lubricant film thickness in sliding compliant contacts. Tribology Transactions, August 2010, Vol. 53, No. 5, pp. 684-694.
[Myant 2010b] Myant C., et al. Influence of load and elastic properties on the rolling and sliding friction of lubricated compliant contacts. Tribology International, January 2010, Vol. 43, No. 1, pp. 55-63.
[Myant 2010c] Myant, C., et al. Laser-induced fluorescence for film thickness mapping in pure sliding lubricated, compliant, contacts. Tribology International, November 2010, Vol. 43, No. 11, pp. 1960–1969.
[Nijenbanning 1994] Nijenbanning, G., et al. Film thickness in elasto-hydrodynamically lubricated elliptic contacts. Wear, August 1994, Vol. 176, No. 2, pp. 217-229.
[Poll 1992] Poll, G. and Gabelli, A. Formation of Lubricant Film in Rotary Sealing Contacts: Part II-A New Measuring Principle for Lubricant Film Thickness. Journal of Tribology, April 1992, Vol. 114, No. 2, pp. 290-296.
[Roberts 1968] Roberts, A. D. and Tabor, D. Fluid film lubrication of rubber—an interferometric study. Wear, February 1968, Vol. 11, No. 2, pp. 163–166.
[Roberts 1977a] Roberts, A. D. Studies of lubricated rubber friction: Part 1: Coupling optical observations to friction measurements. Tribology International, April 1977, Vol. 10, No. 2, pp. 115–122.
[Roberts 1977b] Roberts, A. D. Studies of lubricated rubber friction: Part 2: Optical techniques applied to practical problems. Tribology International, June 1977, Vol. 10, No 3, pp. 175–183.
[Reddyhoff 2010] Reddyhoff, T., et al. Lubricant Flow in an Elasto-hydrodynamic Contact Using Fluorescence. Tribology Letters, June 2010, Vol. 38, No. 3, pp. 207-215.
[Smart 1974] Smart, A.E. and Ford, R.A.J. Measurement of thin liquid films by a fluorescence technique. Wear, July 1974, Vol. 29, No. 1, pp. 41-47.
[Spikes 1999] Spikes, H.A. Thin films in elastohydrodynamic lubrication: the contribution of experiment. Proceedings of the Institution of Mechanical Engineers, Part J: Journal of Engineering Tribology, May 1999, Vol. 213, No. 5, pp. 335-352.
[Sugimura 2000] Sugimura J., et al. Study of elastohydrodynamic contacts with fluorescence microscope. Tribology Series, 2000, Vol. 38, pp. 609-617.

CONTACTS

Ing. David Necas
Ing. Petr Sperka, Ph.D.
doc. Ing. Martin Vrbka, Ph.D.
prof. Ing. Ivan Krupka, Ph.D.
prof. Ing. Martin Hartl, Ph.D.
Brno University of Technology, Faculty of Mechanical Engineering
Institute of Machine and Industrial Design
Technicka 2896/2, 616 69 Brno, Czech Republic
tel.: +420 541 143 227, e-mail: necas@fme.vutbr.cz
tel.: +420 541 143 238, e-mail: sperka@fme.vutbr.cz
tel.: +420 541 143 237, e-mail: vrbka.m@fme.vutbr.cz
tel.: +420 541 142 723, e-mail: krupka@fme.vutbr.cz
tel.: +420 541 142 769, e-mail: hartl@fme.vutbr.cz

Tribol Lett (2015) 59:39
DOI 10.1007/s11249-015-0565-7

ORIGINAL PAPER

Lubricant Rupture Ratio at Elastohydrodynamically Lubricated Contact Outlet

David Košťál[1] · David Nečas[1] · Petr Šperka[1] · Petr Svoboda[1] · Ivan Křupka[1] · Martin Hartl[1]

Received: 23 January 2015 / Accepted: 1 July 2015 / Published online: 17 July 2015

Abstract Elastohydrodynamically lubricated (EHL) contacts rarely exist as single contacts. Multiple contacts or single contacts subjected to the repeated over-rolling represent more often the case in practical applications. A typical example is the rolling element bearing. A lubricant rupture mechanism at each contact outlet determines the lubricant availability to the succeeding contact. This work presents a quantitative description of the lubricant film thickness rupture in EHL contact outlet with the use of the fluorescent microscopy. A rupture ratio of the film thickness between two diverging surfaces exiting the contact was measured for both pure rolling and rolling–sliding conditions. The influence of variation of several parameters such as lubricant properties, rolling speed or rolling element ellipticity to the lubricant rupture ratio was investigated. Understanding of the physical phenomena of the lubricant rupture extends further possibilities in both experimental and theoretical researches of the starved EHL.

Keywords EHL · Starvation · Lubricant rupture

List of Symbols

Ca	Capillary number; $\frac{\eta_0 U}{\sigma}$
h_c	Central film thickness
$u_{1,2}$	Entrainment speeds of surfaces
subscripts 1;2	Relation to the disc;ball
u_m	Mean speed; $(u_1 + u_2)/2$
SRR	Slide-to-roll ratio; $\frac{2(u_1-u_2)}{(u_1+u_2)}$
k	Ellipticity of the element
σ	Surface tension
η	Viscosity at atmospheric pressure
δ_1	Dimensionless film thickness on the disc
δ_2	Dimensionless film thickness on the ball
Δ	Rupture ratio parameter; $\frac{\delta_1}{\delta_1+\delta_2}$

1 Introduction

Lubricant film thickness generated within EHL non-conformal contacts is one of the most important parameters determining the performance and life of machine parts. Film thickness in the central zone depends on the sum of thickness of the layers supplied to the contact. In case of pure rolling conditions, it is assumed that in the outlet of an EHL contact, the adhering lubricant is equally distributed on rubbing surfaces [1].

However, most of lubricated contacts repeatedly travel over the same spot in the oil film, and the outlet region leaves thin residual shoulders of lubricants downstream of the contact. There is a concern that the lubricant supplied into the inlet region might not provide an adequate supply of the EHL contact as under fully flooded conditions.

Without some degree of external replenishment into the track, the inlet region can become starved which increases the possibility of damage to rubbing surfaces. Lubricant oil entering the inlet region may flow around the contact; therefore, the entire amount of lubricant adhered to contact

This article is part of the Topical Collection on STLE Tribology Frontiers Conference 2014.

✉ David Košťál
kostal@fme.vutbr.cz

[1] Faculty of Mechanical Engineering, Institute of Machine and Industrial Design, Brno University of Technology, Technicka 2896/2, 61669 Brno, Czech Republic

surfaces cannot enter the contact area. Due to the relative motion of contact surfaces, a substantial part of lubricant is pushed out of contact track causing back and side outflow [2]. This behaviour can be clearly seen in rolling bearings.

The occurrence of starvation can result in film breakdown accompanied by interactions of rubbing surfaces. The ability to predict the occurrence of starvation to achieve an optimum bearing performance and component life is obviously desirable. Currently, the film thickness and pressure distribution in EHL contacts can be predicted using theoretical models of starvation occurrence [3]. However, these models use the inlet oil layer thickness as the input parameter; this is generally not known during experiments.

The aim of this work is to experimentally determine how the lubricant is distributed onto the rubbing surfaces and to verify the theoretical model in order to provide a fast and easy prediction of lubricant behaviour. Ratio between lubricant film thicknesses adhering to each of the contact surfaces after passing through EHL contact is called a lubricant rupture ratio.

Surface fluid inlet and outlet layer thickness on a solid surface are found in a large number of practical applications where a thin film of fluid is split onto surfaces. Examples of these applications can be found in lubrication, roll coating, screen printing, paint films and in biological systems and are in greater detail described in the literature [4]. Many theoreticians have been interested in the boundary conditions that should be used within the context of lubrication theory to define the inlet oil layer thickness. Most of the earliest studies were concerned with the understanding cavitation in journal bearings [5]. A correct approach to the formation of thin liquid film was first performed by Ruschak [6] who used matched asymptotic expansions in the context of roll coating. This approach is a time-consuming and must be adapted according to the exact geometry. However, this method may be adapted for any film-forming flow. This work was followed by Taroni [7] and extended for a finite contact angle.

The formation of inlet layer film is a problem of great interest among researchers as the flow in the vicinity of the meniscus determines the fluid flux downstream which is crucial in many applications. Coyne and Elrod [8, 9] studied the film separation between two parallel surfaces, with one moving surface, theoretically. This study showed that these conditions are not strictly applicable to lightly loaded journal bearings. Approximate boundary conditions such as those by Reynolds [10], Coyne and Elrod [8, 9] and Hewson [11, 12] are thus likely to remain popular as they often give sufficiently accurate results.

In theoretical and experimental studies, it has been shown that the film thickness inside the contact is very sensitive to the shape and thickness of inlet oil layer [13, 14]. In such a contact, the shape and thickness of the inlet layer of oil, supplied to the contact on the running track, are of crucial importance to the film formation and contact performance [15]. Most recently, theoretical works were extended taking into account the sliding effect. In this work, a prediction of the remaining liquid quantity on each moving surface is solved for general cases. It determines how much lubricant will remain available for the following contact [16].

2 Material and Methods

For the purpose of present study, a ball-on-disc tribometer in combination with optical evaluation system was employed. To be able to observe the lubricant track separately on both components, the ball was placed on the top of the disc, as shown in Fig. 1. The optical imaging system included mercury lamp, epifluorescent microscope, sCMOS digital camera and PC.

As the evaluation method, fluorescence induced by mercury lamp was used. This technique was originally introduced by Smart and Ford [17], who observed the thickness of lubricant film on rotating cylinder. Later, it was pointed out that the use of mercury-lamp-induced fluorescence allows detecting lubricant films down to 30 nm [18]. The principle of the method is based on the intensity of fluorescent emission. A fluorescence phenomenon can be described as a sequence of three following phases [19]:

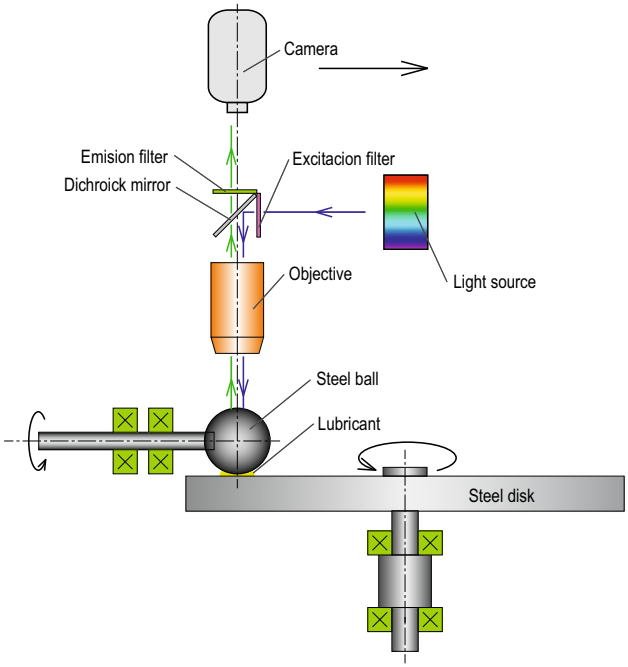

Fig. 1 Illustration of the method

1. Excitation: a photon is supplied by an external light source such as lamp or laser and is absorbed by the fluorophore, creating an excited electronic single state.
2. Excited-state lifetime: it lasts usually 1–10 ns; during this time, the molecule undergoes relaxation (dissipation of energy occurs) and is left in a state from which the fluorescence can be emitted.
3. Fluorescence emission: a photon is emitted returning the fluorophore to its ground state. Because of the energy dissipation during excited-state lifetime, this photon has a lower energy and therefore the longer wavelength than the excitation photon. The difference in wavelengths, also known as Stokes shift, is absolutely fundamental since it allows a separation of emission and excitation.

The evaluation of lubricant rupture in the contact outlet was based on qualitative comparison of the intensities of pixels in contact tracks on both rubbing surfaces as illustrated in Fig. 2. It was proved by Azushima [20] that in case of thin films there is a linear dependence between the intensity of emission and thickness of the lubricant layer, so that the intensity can be considered as the non-calibrated film thickness. Measured thickness is labelled as δ_1 and δ_2 in the results. Thickness was not calibrated to the specific one because only a ratio between two values is considered in this study.

Examples of the fluorescence technique output are presented in Fig. 3. Darker areas can be interpreted as areas with thinner lubricant film. Output image is 16-bit bitmap which provides 65536 intensity levels. Therefore, even areas, which seem to be almost black, provide still measurable intensity. To avoid the influence of optical properties of contact elements, both components were made from the same bearing-grade steel and polished. The diameter of steel ball and disc was 25.4 and 150 mm, respectively. To investigate the effect of ellipticity, a steel ball was substituted by a steel spherical roller with the diameter of 25.4 mm in rolling direction and 66 mm in perpendicular direction in experiments labelled as influence of geometry with ellipticity $k = 1.8$. Prior to measurements, the initial surface topography of components was analysed in a greater detail using the phase shifting

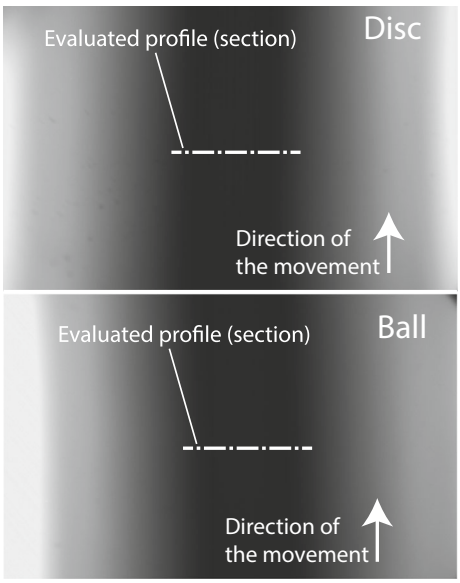

Fig. 3 Fluorescent images for SRR = 0

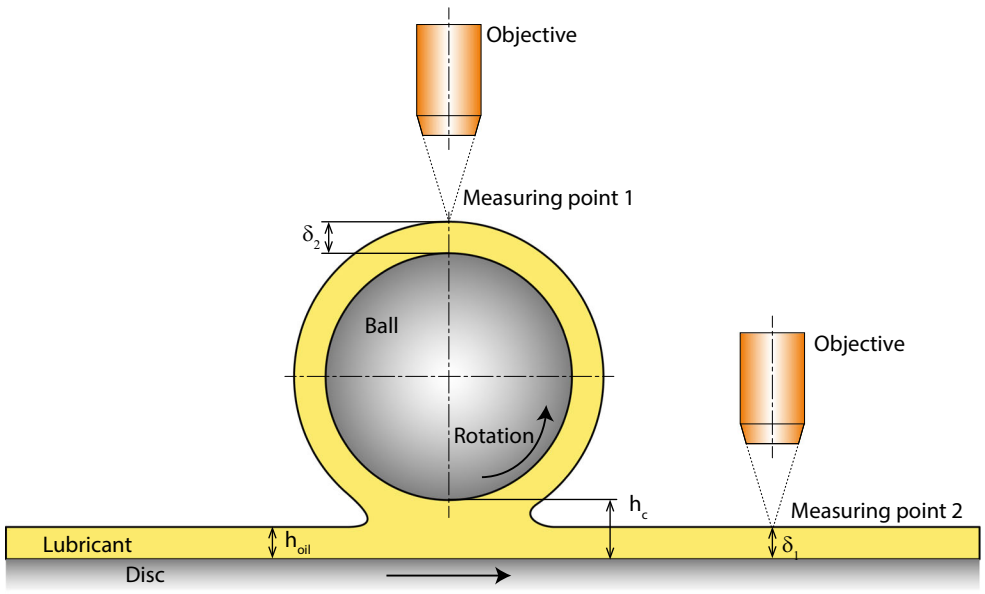

Fig. 2 Illustration of the measured spots on the apparatus

interferometry profilometer. Evaluated surface roughness for the ball (1), the roller (2) and the disc (3) was as follows: $Ra_1 = 10$ nm, $Ra_2 = 10$ nm, $Ra_3 = 20$ nm. As test lubricants, several mineral oils were used since they emit fluorescence naturally when illuminated in UV. Mineral oils also exhibit a very good durability of fluorescence emission. Even if the illumination lasts several minutes, there is an absolutely negligible loss of fluorescence. Four different lubricants R834/80, R533/73, R560/88 and SN650 were used with the dynamic viscosities 0.19, 0.64, 1.4 and 0.45 Pa s, respectively. At the beginning of each test, a sufficient amount of lubricant was added into a contact track to achieve fully flooded conditions. Each point in the test was measured twice in the sequence of ball-disc-ball-disc, and deviation was quantified around 2.5 % for all measurements. This proves stability of the fluorescence and other conditions. Therefore, each data point in this article is the averaged value of two measurements. Plotting both values for each condition would make the plot difficult to read due to higher number of lines and points. In Fig. 4 are both lines plotted as example for mean speed of 220 mm/s from Fig. 7 where both are plotted as average.

The contact was loaded by an external force equal to 30 N which corresponds to maximum Hertzian pressure of 0.8 GPa. It should be noted that both components could be driven independently by their own servomotors; therefore, different kinematic conditions could be applied. Measurements were conducted for the range of slide-to-roll ratio from -1.5 to 1.5. A pure sliding experiment is not necessary because one of the components is stationary in this case, so it can be assumed that whole lubricant layer remains on the moving surface.

Reproducibility of the method was tested by evaluation of 20 images captured with one second delay, which corresponds roughly to 0.5 revolutions of the disc and 2.8 revolutions of the ball. Lubrication conditions were fully flooded and speeds of both surfaces were kept constant. Therefore, the film thickness should be almost the same for all images. The film profile from each image was evaluated, and central values were averaged into one value. These values are plotted together with the mean value in Fig. 5. Maximal deviations from mean values were from -2.6 to 2.9 %.

3 Results and Discussion

This chapter is divided to the two main sub-chapters. First presents the study of lubricant rupture at contact outlet for pure rolling conditions. Second chapter presents study of the influence of the various parameters to the rupture ratio as function of the different slide-to-roll ratios (SRRs). SRR is calculated by Eq. 1

$$\mathrm{SRR} = \frac{2(u_1 - u_2)}{(u_1 + u_2)}[-] \tag{1}$$

3.1 Pure Rolling

The lubricant rupture ratio under pure rolling conditions should be almost equal according to the literature [16]. This case was therefore measured as first. Obtained results can be seen in Fig. 6. These profiles were evaluated from the example images in Fig. 3. Concerning only the central part of the profile (track bed), almost the same profiles for the disc and the ball can be seen; this confirms the above-mentioned predictions. Profiles slightly differ in the outer regions, which can be explained by either differences in the geometry or a different direction of the inertial forces. However, it was not the subject of this study, so it was not investigated any further and only the central part passing through the contact was considered.

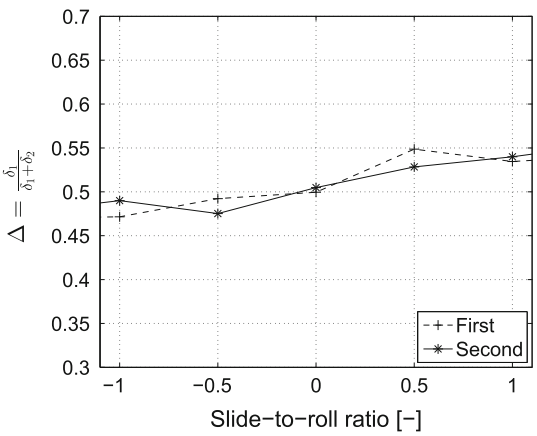

Fig. 4 Two measurements of the same conditions example

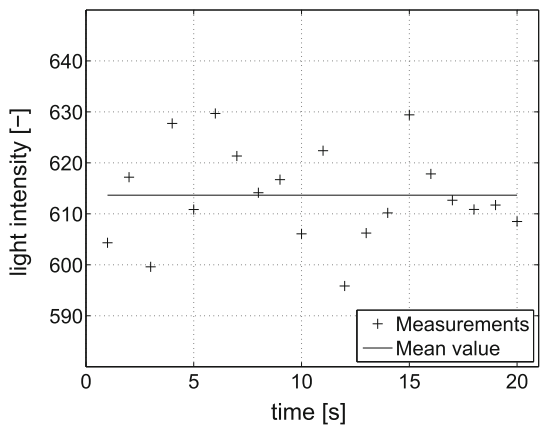

Fig. 5 Reproducibility evaluation

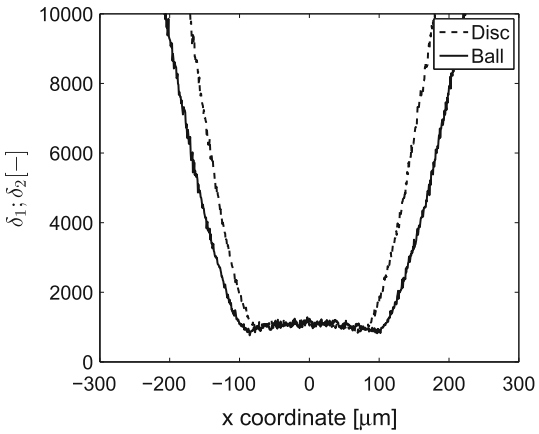

Fig. 6 Outlet film thickness profile for pure rolling conditions

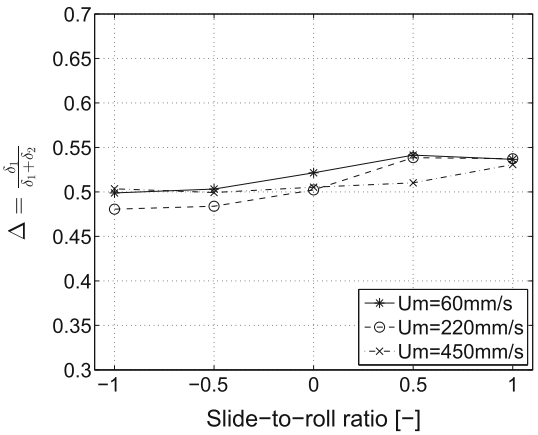

Fig. 7 Outlet film thickness rupture ratio Δ as function of SRR for three different mean speeds

3.2 Rolling–Sliding

This chapter presents the influence of various operating conditions under different slide-to-roll ratios to the lubricant rupture ratios. The assumed behaviour according to the literature is that a slower surface should contain a thinner lubricant film than a faster surface. Cases of pure sliding (SRR = 2) and slide-to-roll ratios close to this state were not investigated. There is no film lubricant when the surface is stopped because the lubricant cannot be carried from the contact to the place where is measured. Cases of high SRR were also excluded because the lubricant film is subjected to changes due to gravity and capillary and inertial forces for a long time before the measurements. This can cause a change in the lubricant profile due to a reflow of lubricant pushed out of the track, which would influence the results. The time between exiting of the contact and measuring was kept less than two seconds for all presented cases, so there is no change due to the mentioned aspects. For times shorter than 2 s, no significant reflow of lubricant was observed.

3.2.1 Influence of the Mean Speed

Three cases of mean speeds were measured ($u_m = 60, 220$ and 450 mm/s). Speed for each surface was calculated from the mean speed u_m. The same lubricant was used for all cases (R834/80). A central film thickness prediction for given conditions according to Hamrock and Dowson's formula is $h_c = 121,289$ and 467 nm, respectively. Therefore, it is the EHL contact having a lubricant film which can be sufficiently measured by the fluorescence imaging technique.

A change in the rupture ratio is presented in Fig. 7. There can be seen a slight dependency on SRR which seems to be independent of the mean speed because the observed tendency is almost the same for all three cases. However, the same behaviour as in the literature [16] can be observed. This means that the slower surface contains a thinner lubricant film than the faster surface. The expected result for the SRR = 0 is $\Delta = 0.5$. However, this is not observed for the slower mean speed. Moreover, the Δ values for the highest mean speed are above 0.5 for negative SRR, while they are expected to be smaller than 0.5. These deviations in trends can be explained by other processes which do not have such influence under different conditions, e.g. cavitation for the low mean speed and difference in inertial forces directions for the high mean speed.

Cavitation causes a scattered distribution of outlet film thickness in the lubricant track by creating spikes as shown in Fig. 8. This figure illustrates a 3D representation of the track in the lubricant layer behind the contact outlet which is plotted from Fig. 9. The image was captured immediately after stopping the test rig drives. This is the only way how to see the cavitation, but there is a delay between stopping and capturing; therefore, there can be expected lubricant reflow influence. Other images used for all measurements were captured during the movement, so there is no reflow, but there is motion blur as shown in Fig. 3. Exposure time for most of the results was 0.1 s. This means even for the lowest mean speed of 60 mm/s blur in the length of 6 mm, which is roughly 20 times more than contact pressure zone which was captured.

Scattering increases with increasing lubricant viscosity. Cavitated areas make the evaluation problematic due to the motion blur of the images because the cavitated lubricant layer is still considered as two-dimensional constant which is not entirely correct. Moreover, the cavitated profile is subjected to the time-dependent changes caused by inertial forces and surface tension, which can also influence the evaluated results.

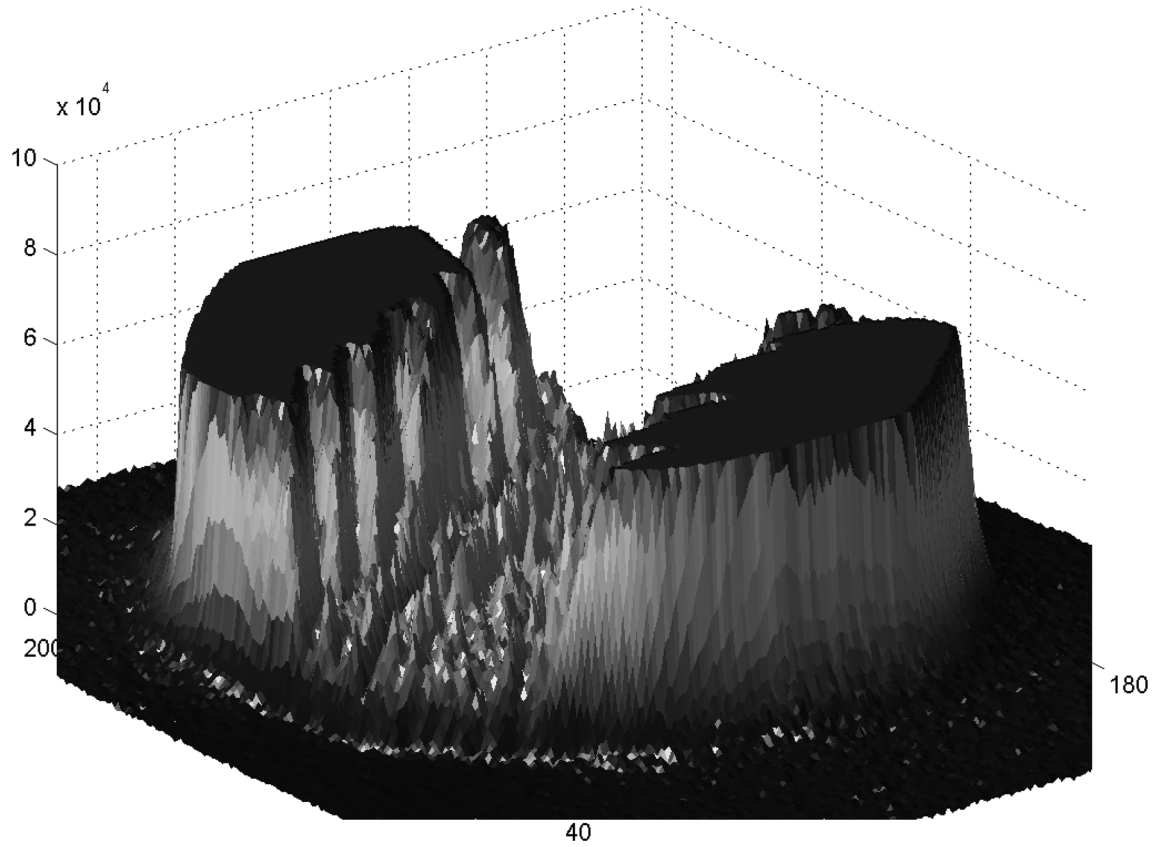

Fig. 8 3D dimensionless representation of track in the lubricant profile behind contact outlet

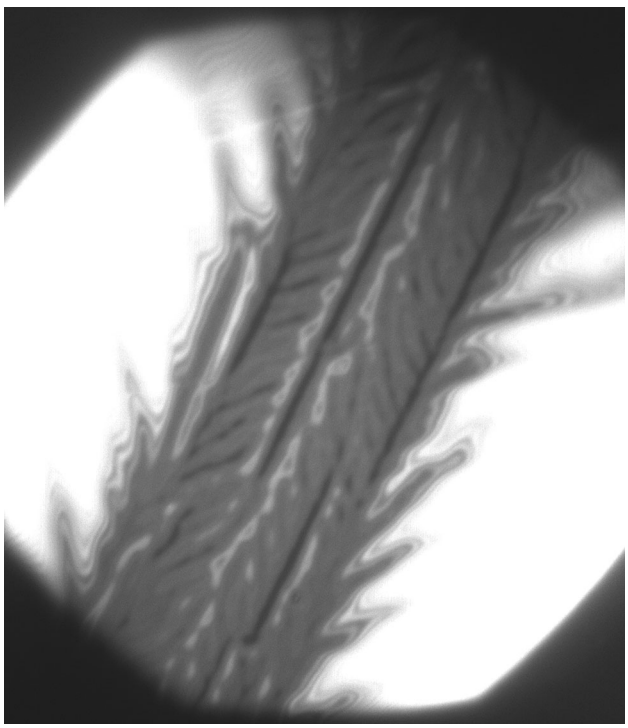

Fig. 9 Captured image of track in the lubricant profile behind the contact outlet

3.2.2 *Influence of the Contact Geometry*

Four cases were studied. The same steel disc was used in both cases but with a different counterpart. The first case is measured with the steel ball ($k = 1$) and the other cases are measured with spherical rollers ($k = 1.5; 2.5; 4$). A spherical roller under the same conditions (mean speed, lubricant, load) provides a different contact pressure, contact shape and film thickness. However, one of the most important differences is a significantly wider contact. It could be assumed that wider contact will change the lubricant flow patterns, and thus, it could change the behaviour at the contact outlet. Lubricant was the same (R560/88) for all four cases. Mean speed was constant for all cases: $u_m = 220\,\mathrm{mm/s}$.

Results of the rupture ratios for different geometries can be seen in Fig. 10. However, a different geometry caused only a small difference. Even for the cases of SRR $= 1.5; -1.5$ the difference between results for different rolling elements is under 6 %. Given the fact that measurement reproducibility is roughly of the same value, it can be assumed that there is no obvious influence of the geometry–ellipticity.

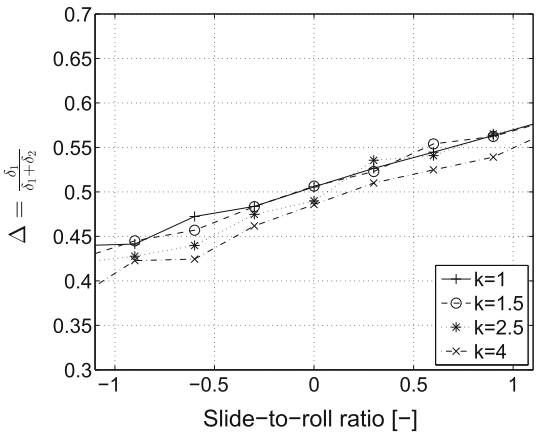

Fig. 10 Outlet film thickness rupture ratio Δ as function of SRR for four different ellipticities

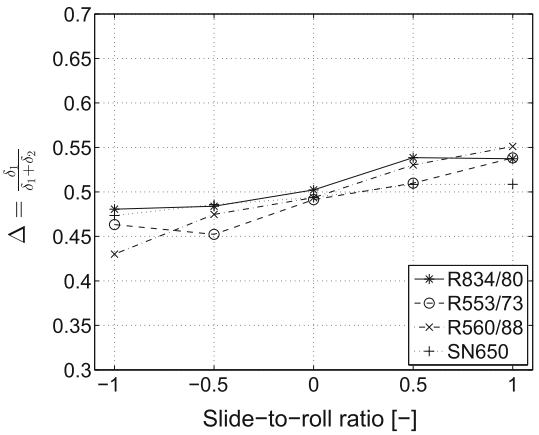

Fig. 11 Outlet film thickness rupture ratio Δ as function of SRR for four different lubricants

3.2.3 *Influence of Lubricant Properties*

The influence of four different lubricants was studied. Two main parameters influencing the behaviour of lubricant flow are viscosity and surface tension. Both of these parameters were measured for each lubricant, and the values can be seen in Table 1. Rupture ratios measured with these lubricants for different SRRs are plotted in Fig. 11. Mean speed of $u_m = 220\,\mathrm{mm/s}$ was used in all cases.

Most significant differences can be seen in this chapter compared with the previous chapters. A minimum change of rupture ratio for extreme values of SRR (1; −1) can be seen for SN650 oil where Δ varies from 0.47 to 0.51. However, this oil does not have a maximum or minimum value of surface tension, viscosity or the capillary number. Maximal difference of Δ can be seen for R560/88 oil where values vary from 0.43 to 0.55. This oil is extremely viscous compared with the other oils used during the experiment. Dynamic viscosity of this oil is 1.4 Pa s. This could suggest that viscosity is the driving parameter. However, this was not confirmed during experiments with remaining oils because no obvious dependency was found.

Table 1 Capillary number values

Lubricant (−)	η (Pa s)	u_m ($\mathrm{m\,s^{-1}}$)	σ ($\mathrm{N\,mm^{-1}}$)	Ca (−)
R834/80	0.2	0.22	6.6	6.6
R834/80	0.2	0.06	6.6	1.8
R834/80	0.2	0.45	6.6	13.6
R533/73	0.64	0.22	41.6	3.4
R560/88	1.4	0.22	28.5	10.8
SN650	0.45	0.22	31	3.2

3.2.4 *Influence of the Capillary Number and a Comparison with Theory*

It is mentioned in theory that the influence of viscosity, surface tension and rolling speed studied separately in the previous chapters can be governed by a single parameter called capillary number (Ca). This parameter can be calculated with the use of Eq. 2, and it has been shown that Ca can have effect to a lubricant flow and shape of the outlet meniscus. Therefore, in this chapter, six cases from previous chapters are plotted together in one figure and they are labelled with calculated Ca, so this can be taken as a different approach to the previous results and summary.

$$Ca = \frac{\eta_0 U}{\sigma} \tag{2}$$

Capillary numbers for all the cases are listed in Table 1. Results for these cases are plotted in Fig. 12. In this plot as well as in the previous cases, the same tendency can be seen. The layer of lubricant is thicker on the faster moving surface and thinner on the slower surface. The ratio between these two thicknesses is marked as Δ in the plot.

Experimental results are scattered from 0.43 to 0.5 for SRR = −1 and from 0.51 to 0.55 for SRR = 1. There can be seen the highest difference of 0.12 for capillary number 10.8 when the difference between Δ values for SRR 1 and −1 is compared. However, even higher $Ca = 13.6$ showed the difference of only 0.03. Low Ca numbers 1.8, 3.2 and 3.4 showed differences 0.04, 0.04 and 0.0, respectively; there is no observable trend. These data confirm the conclusion from literature [16] that the capillary number cannot be a driving parameter of this behaviour.

A relationship between SRR and Δ presented by Bruyere [16] and mentioned in the introduction can be seen as a solid line in Fig. 12. The vertical axis of this plot is extended to 0–1 range with regard to the previous results to provide a better visual comparison between theory and

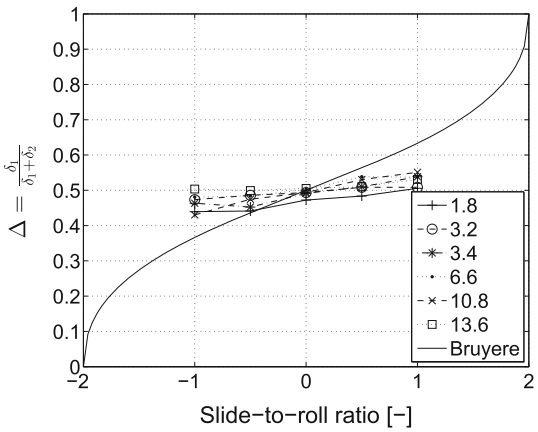

Fig. 12 Outlet film thickness rupture ratio Δ as function of SRR for six different capillary numbers

experiments. In case of SRR = 0 is theory matching with experiments very well as well as in the previous cases, which could be expected.

However, it is clear that the experimentally observed dependency is smaller in comparison with the theory for SRR $< >$ 0. The averaged experimental result for SRR = −1 is 0.48, while the result calculated from theory is only 0.37. The experimental value of Δ for SRR = 1 is 0.53, while the theoretical result is 0.63. Based on these numbers, it can be concluded that trend is smaller than the one described theoretically. There could be another influence connected to sliding which was not considered in this work, such as thermal processes, shear thinning or a change in the flow profile, which causes restriction of the SRR influence described theoretically. Governing of these aspects should be the next step in this research area. Another explanation could include geometry limitation. All experiments were conducted on a ball-on-disc experimental rig. Therefore, geometry of surfaces is not symmetric, which could have some influence. Suggestions for future study are to conduct experiments on the modified experimental rig equipped with a pair of identical rolling elements (rollers, spherical rollers or balls).

4 Conclusions

This paper presents the study of the lubricant rupture ratio in the EHL contact outlet with the use of fluorescence imaging technique. The ratio is 0.5 (see SRR = 0 in Fig. 12) for pure rolling conditions, which means that a half of lubricant thickness measured in the contact remains on each contact surface. Lubricant thickness tends to increase on the faster moving surface when sliding (SRR $< >$ 0) is introduced and to decrease on the slower surface. A scale of this influence does not seem to be dependent on the mean speed, lubricant properties or the contact geometry. All of these aspects were studied without any apparent dependency. The experiments showed that values of Δ vary from 0.43 to 0.55 for SRR = −1 and SRR = 1, respectively. The influence of SRR is almost negligible for the lower values of SRR, and the experimental results have confirmed the predicted behaviour for SRR $< >$ 0, but the trend is much smaller.

Acknowledgments This work is an output of cooperation between Czech Science Foundation under Project No.: 13-30879P and NETME Centre, regional R&D centre built with the financial support from the Operational Programme Research and Development for Innovations within the project NETME Centre (New Technologies for Mechanical Engineering), Reg. No. CZ.1.05/2.1.00/01.0002 and, in the follow-up sustainability stage, supported through NETME CENTRE PLUS (LO1202) by financial means from the Ministry of Education, Youth and Sports under the 'National Sustainability Programme I'.

References

1. Svoboda, P., Kostal, D., Krupka, I., Hartl, M.: Experimental study of starved EHL contacts based on thickness of oil layer in the contact inlet. Tribol. Int. **67**, 140–145 (2013)
2. Lugt, P.M., Morales-Espejel, G.E.: A review of elasto-hydrodynamic lubrication theory. Tribol. Trans. **54**(3), 470–496 (2011)
3. van Zoelen, M.T., Venner, C.H., Lugt, P.M.: The prediction of contact pressure-induced film thickness decay in starved lubricated rolling bearings. Tribol. Trans. **53**(6), 831–841 (2010)
4. Weinstein, S.J., Ruschak, K.J.: Coating rows. Ann. Rev. Fluid Mech. **36**, 29–53 (2004)
5. Savage, M.D.: Cavitation in lubrication—1. On boundary conditions and cavity-fluid interfaces. J. Fluid Mech. **80**(pt 4), 743–755 (1977)
6. Ruschak, K.J.: Boundary conditions at a liquid/air interface in lubrication flow. J. Fluid Mech. **119**, 107–120 (1982)
7. Taroni, M., Breward, C.J.W., Howell, P.D., Oliver, J.M.: Boundary conditions for free surface inlet and outlet problems. J. Fluid Mech. **708**, 100–110 (2012)
8. Coyne, J.C., Elrod JR, H.: Conditions for the rupture of a lubricating film - 1. ASME- Paper 69-Lub-3 (1969)
9. Coyne, J.C., Elrod Jr, H.: Conditions for the rupture of a lubricating film—2. J. Lubric. Technol. Trans. ASME **93 Ser F**(1), 156–167 (1971)
10. Reynolds, O.: On the theory of lubrication and its application to Mr. Beauchamp Tower's experiments, including an experimental determination of the viscosity of olive oil. Proc. R. Soc. Lond. **40**, 191–203 (1886)
11. Hewson, R.W.: Free surface model derived from the analytical solution of stokes flow in a wedge. J. Fluids Eng. Trans. ASME **131**(4), 0412051–0412055 (2009)
12. Hewson, R.W., Kapur, N., Gaskell, P.H.: A model for film-forming with Newtonian and shear-thinning fluids. J. Nonnewton. Fluid Mech. **162**(1–3), 21–28 (2009)
13. Lee-Prudhoe, I., Venner, C.H., Cann, P.M., Spikes, H.: Experimental and theoretical approaches to thin film lubrication problems. Solid Mech. Appl. **134**, 241–255 (2006)
14. Chevalier, F., Lubrecht, A.A., Cann, P.M.E., Colin, F., Dalmaz, G.: Starvation phenomena in E.H.L. point contacts. Tribol. Ser. **31**, 213–223 (1996)
15. van Zoelen, M.T., Venner, C.H., Lugt, P.M.: Free surface thin layer flow on bearing raceways. J. Tribol. **130**(2), 1–10 (2008)

16. Bruyere, V., Fillot, N., Morales-Espejel, G.E., Vergne, P.: A two-phase flow approach for the outlet of lubricated line contacts. J. Tribol. **134**(4), (2012). doi: 10.1115/1.4006277
17. Smart, A.E., Ford, R.A.J.: Measurement of thin liquid films by a fluorescence technique. Wear **29**(1), (1974)
18. Sugimura, J., Hashimoto, M., Yamamoto, Y.: Study of elasto-hydrodynamic contacts with fluorescence microscope. Tribol. Ser. **38**, 609–617 (2000)
19. Lyon, H.O., Prento, P.: Haugland rp. handbook of fluorescent probes and research chemicals, 6th ed. Ugeskrift for laeger **159**(27), 4285–4286 (1997)
20. Azushima, A.: In lubro 3d measurement of oil film thickness at the interface between tool and workpiece in sheet drawing using a fluorescence microscope. Tribol. Int. **38**(2), 105–112 (2005)

JOURNAL OF THE MECHANICAL BEHAVIOR OF BIOMEDICAL MATERIALS 55 (2016) 295–307

Available online at www.sciencedirect.com

ScienceDirect

www.elsevier.com/locate/jmbbm

Research Paper

The effect of lubricant constituents on lubrication mechanisms in hip joint replacements

*David Nečas**, *Martin Vrbka*, *Filip Urban*, *Ivan Křupka*, *Martin Hartl*

Faculty of Mechanical Engineering, Brno University of Technology, Czech Republic

ARTICLE INFO

Article history:
Received 29 June 2015
Received in revised form
2 November 2015
Accepted 9 November 2015
Available online 19 November 2015

Keywords:
Hip replacement
Fluorescent microscopy
Colorimetric interferometry
Albumin
γ-globulin
Lubricant film thickness

ABSTRACT

The aim of the present paper is to provide a novel experimental approach enabling to assess the thickness of lubricant film within hip prostheses in meaning of the contribution of particular proteins. Thin film colorimetric interferometry was combined with fluorescent microscopy finding that a combination of optical methods can help to better understand the interfacial lubrication processes in hip replacements. The contact of metal femoral head against a glass disc was investigated under various operating conditions. As a test lubricant, the saline solution containing the albumin and γ-globulin in a concentration 2:1 was employed. Two different mean speeds were applied, 5.7 and 22 mm/s, respectively. The measurements were carried out under pure rolling, partial negative and partial positive sliding conditions showing that kinematic conditions substantially affects the formation of protein film. Under pure rolling conditions, an increasing tendency of lubricant film independently on rolling speed was detected, while the total thickness of lubricant film can be attributed mainly to albumin. When the ball was faster than the disc (negative sliding), a very thin lubricant film was observed for lower speed with no significant effect of particular proteins. The increase in sliding speed led to the increase of film thickness mainly caused due to the presence of γ-globulin. On the contrary, when the disc was faster than the ball (positive sliding), the film formation was very complex and time dependent while both of the studied proteins have shown any qualitative change during the test, however the effect of albumin seems to be much more important. Since a very good agreement of the results was obtained, it can be concluded that the approach consisting of two optical methods can provide the fundamental information about the lubricant film formation in meaning of particular proteins while the simultaneous presence of other constituents in model synovial fluid.

*Corresponding author. Tel.: +420 541 143 227.
E-mail address: necas@fme.vutbr.cz (D. Nečas).

http://dx.doi.org/10.1016/j.jmbbm.2015.11.006
1751-6161/

1. Introduction

A total hip replacement is one of the most successful surgical treatments of modern medicine. In OECD countries, 160 operations per 100,000 inhabitants were conducted in 2011 as is reported in Health and Glance 2013: OECD indicators. Although there was a rapid improvement of applied materials during the last tens of years (Pramanik et al., 2005), artificial hip joints still suffer from limited longevity. The need of re-operations as the consequence of implant failure leads to deterioration of daily life, especially in case of younger patients (Adelani et al., 2013). The most common cause of this failure is aseptic loosening accompanied by osteolysis due to wear of rubbing surfaces (Joshi et al., 1993). Several authors focused on investigation of wear of rubbing surfaces under various operating conditions (Goldsmith et al., 2000; Smith et al., 2001a; Wang et al., 2004). However, little is yet known about interfacial lubrication processes in hip replacements, even though such a knowledge can help to reduce wear and therefore can eventually extend the implant longevity. The tribological performance of contact pair is substantially influenced by prevailing lubrication regime and material properties of the components. To ensure minimisation of wear, a complete separation of rubbing surfaces by fluid film is necessary. However, in case of hip implants, a boundary or mixed lubrication regime usually occur (Jin et al., 2006).

In relation to lubrication mechanisms, determination of lubricant film thickness seems to be a crucial task. A mathematical model for film thickness estimation in metal-on-metal joints was pronounced several times (Dowson, 2006; Dowson and Jin, 2006; Jalali-Vahid et al., 2006). The analysis usually comes from the classical elastohydrodynamic lubrication (EHL) theory assuming that the lubricant film is affected by elastic deformation of contact surfaces in combination with fluid entrainment. It should be considered that both natural and artificial joints are not lubricated by simple Newtonian fluids. Human synovial fluid (SF), as well as bovine serum (BS), which is often used as its model (Essner et al., 2005), exhibit non-Newtonian and shear thinning behaviour (Mavraki and Cann, 2011). Moreover, it was proved that protein adsorption on rubbing surfaces significantly influences the lubricant film (Parkes et al., 2014; Scholes and Unsworth, 2006) and tribochemical layers (Wimmer et al., 2003). Because of the above information, numerical predictions in biological systems are particularly complicated. An experimental approach for film thickness evaluation based on the change of electrical resistivity was introduced by Dowson et al. (2000). The authors focused on the qualitative analysis of the gap between metallic components of artificial joint during the walking cycle. This study was followed by Smith et al. (2001b) who applied the same method on a ceramic pair. Although the electrical method can provide the information about the qualitative change of lubricant film between articulating surfaces, it does not allow observing the contact in situ; therefore it is quite demanding to describe the changes in terms of lubricant film formation.

In recent years, extensive research has been conducted into lubricating film formation within hip joints replacements. The pilot study was provided by Mavraki and Cann (2009), who focused on the fundamentals associated with SF lubrication. Different protein solutions were employed to model healthy and periprosthetic SF. In addition, the experiments were also carried out with BS. Friction measurements were realized on the commercial Mini Tractione Machine (MTM) apparatus finding that at low speeds (<20 mm/s) a boundary lubrication regime is typical for all applied lubricants reducing the friction. Film thickness was evaluated by using a ball-on-disc tribometer in combination with optical interferometry method. The experiments were performed under pure rolling conditions, constant load equal to 5 N, and room temperature. For BS, film thickness gradually increased with increasing rolling speed. During a subsequent decrease of speed back to initial value, the film was time independent with just a little tendency to increase (up to 28 nm at 5 mm/s). At the end of the experiment, the residual film thinner than 20 nm was detected suggesting the importance of adsorbed protein layer. The authors concluded that both friction and film thickness measurements were time dependent.

The following reference, given by the same authors (Mavraki and Cann, 2011), extended the previous study by investigating the influence of various loading and kinematic conditions on film thickness in the contact lubricated by BS. The effect of high (ball-on-disc) and low (lens-on-disc) contact pressure as well as the influence of BS concentration was examined. In a ball-on-disc configuration, the experiments were realized under pure rolling and pure sliding conditions. Under pure rolling, the film thickness increased with increasing speed from 5 to 50 nm with no significant effect of subsequent speed sweep. At the end of the experiment, a thin lubricant film in a range from 9 to 19 nm attributed to protein adsorption was detected. Under pure sliding, a substantial drop (around 70%) in lubricant film was observed. Low contact pressure generally led to a thicker film (60–80 nm), especially at lower speeds. A significant scatter in results was explained by inherent nature of applied fluid.

The effect of proteins in model fluid on film formation was analysed by Fan et al. (2011) who firstly employed a real metal femoral component. The CoCrMo ball was stationary while the glass disc was sliding as a counterface. Film thickness was evaluated in a range of speeds from 2 to 60 mm/s for simple protein solutions and compared with BS results. It was concluded that protein containing solutions form a thicker film than BS and show a complex time-dependent behaviour. The thicknesses of adsorbed film after a few minutes of sliding were in a good agreement with previous papers (Mavraki and Cann, 2009; Mavraki and Cann, 2011). The thickness of the layer was augmented by hydrodynamic effect especially at low speeds. Deposited films of 20–50 nm were measured at the end of the test. In author's opinion, this was due to molecule aggregations in the inlet zone creating a reservoir of high-viscosity material periodically passing through the contact and forming a much thicker film.

Myant et al. (2012) evaluated the film thickness between the glass disc sliding against the CoCrMo ball as a function of time and mean speed. The effect of variable load was also investigated. A series of BS and simple saline protein solutions were used as test lubricants. Static test under zero speed was conducted to provide the influence of test fluid on

adsorbed protein layer. Globulin solutions formed a much thicker film, around 30 nm at the end of the experiment, compared to albumin solutions (around 1–3 nm). BS was somewhere between the values while the thickness of deposited film was equal to approximately 10 nm. The time test was realized for speed of 10 mm/s showing the increasing tendency for all tested fluids with time/sliding distance, respectively. Again, the thickest film was measured for globulin solution, particularly more than 200 nm. Increasing the load from 5 to 20 N led to a substantial decrease of film thickness. The results of film thickness as a function of mean speed (0–50 mm/s) exhibit a large scatter preventing drawing the clear conclusions; however, the influence of protein content on film formation is obvious.

The observation of contact zone was enhanced later (Myant and Cann, 2013), giving a detailed description of the protein aggregation, so called "inlet phase", in front of the contact. The authors found a satisfactory agreement between the length of the inlet phase and the central film thickness. The results confirmed the previously observed mechanisms (Fan et al., 2011), the combination of adsorbed boundary layer supported by high-viscosity film as a consequence of hydrodynamic effect. The high-viscosity film is caused by aggregated proteins forming a gel-like layer which entrains the contact in time intervals, mainly at low speeds. The increasing speed causes shear thinning of the layer, thus leading to the reduction of film thickness. As the measured thicknesses were significantly higher in relation to predictions derived for classical EHL, it can be concluded that protein containing solutions do not correspond to the EHL mechanism. The aspects of protein lubrication were summarised by Myant and Cann (2014a), who explained in a greater detail the protein aggregation lubrication (PAL) mechanisms in metal-on-metal hip replacements. Several implications of PAL for the implant tribology were highlighted. Particularly, a reduction of contact pressure has a positive effect on the PAL. On the contrary, the effect of increase in sliding speed is negative; nevertheless the concentration of proteins should be taken into account.

The study focused on film formation for metal and ceramic components was given by Vrbka et al. (2013). As in the previous references, ball-on-disc simulator was employed and the film thickness as a function of time was evaluated using the thin film colorimetric interferometry. Different slide-to-roll ratios (SRR) were applied to investigate the influence of rolling/sliding conditions. The applied load of 5 N resulted in maximum contact pressure 180 MPa in the case of metal/glass and 190 MPa for ceramic/glass contact. The contact was lubricated by BS. Under pure rolling conditions, the increasing time-dependent tendency of lubricant film on rolling speed was observed for both materials. Film thickness was always higher in the case of metal component independently of rolling speed; it reached around 100 nm for 20 mm/s. A maximum value for ceramic was only 15–20 nm for the same speed. Under rolling/sliding conditions, film formation was strongly dependent on the faster component. Under positive sliding, where the disc was faster than the ball, film thickness rapidly increased at the beginning of the experiment, independently of ball material. After reaching its maximum value in the range of hundreds of nm, it started to drop and was only around just a few nm at the end of the test. For metal, the influence of speed under these conditions was observed, not in case of ceramic component. An absolutely different character of film formation was detected when the ball was faster than the disc. In this case, the lubricant film was very thin for both materials. Local protein aggregations formed in just a small area of the contact zone reached 20–25 nm for the metal ball and around 5 nm for the ceramic one. This study confirmed a substantial effect of kinematic conditions, especially positive/negative SRR on the protein film formation. In this reference it was pointed out that other factors should be included, such as oxidation of BS, transient loading and kinematic conditions, or conformity of rubbing surfaces.

The significance of transient kinematic conditions was declared by Myant and Cann (2014b). The main attention of this study was paid to different types of motions and their effect on the protein film formation. The authors conducted pure sliding experiments for three different motion types; firstly, the constant speed (20 mm/s) with constant sliding direction; secondly, sinusoidal speed (0–20 mm/s) with constant sliding direction; and finally the sinusoidal velocity (-20 to 20 mm/s) with reversing sliding direction over each cycle. For all applied motions, film thickness gradually increased for around 300 of cycles and then it became quite stable until the end of the experiment. Not significant differences were observed for the constant and sinusoidal speed conditions, where the film thickness reached around 100 (± 20) nm. However, a much lower film was measured for sinusoidal velocity, just approximately 30 nm. In addition, the protein aggregation in the inlet zone (Fan et al., 2011) was not observed under sinusoidal velocity, as the inlet is heavily disrupted in every cycle inhibiting the build-up of protein gel-like phase.

Following the implications from the previous paper (Vrbka et al., 2013), Vrbka et al. (2014) studied the influence of geometry on the lubricant film. The real joints, as well as hip prosthesis, are representatives of bodies with very high degree of conformity. In the effort to approach the real conformity of rubbing surfaces, an experimental configuration was changed from the previously used ball-on-disc one to a more conformal ball-on-lens configuration. A non-conformal ball-on-disc setup leads to a very high contact pressures and small contact areas. Compared to that, higher conformity ensured by ball-on-lens arrangement helps to reduce the contact pressure as a consequence of larger contact zone. The results confirmed the suggestions about the significance of surface geometry. As was already published (Vrbka et al., 2013), negative partial sliding when the ball was faster than the disc (SRR $= -150\%$) led to a very thin lubricant layer. According to this, an extremely thin lubricant film could be expected under pure negative sliding conditions (the glass lens was a stationary component). However, the change of surface conformity caused a considerably different character of film formation. Immediately after the beginning of the experiment, the film reached around 95 nm, independently of sliding speed. After a short time, it slightly decreased to approximately 40 nm for 40 mm/s and 20–25 nm for 10 mm/s with no significant effect of increasing time or sliding distance until the rest of the experiment. The

influence of surface wettability was also investigated. It was shown that the chromium layer on glass disc or glass lens has hydrophobic nature supporting the protein adsorption and therefore a thicker lubricant film. On the contrary, a silica layer, which is naturally hydrophilic, exhibited almost zero film thickness.

The effect of conformity of rubbing surfaces was clearly proved in our previous study (Vrbka et al., 2015), where the film thickness was evaluated between the head and the cup of real dimensions by using the combination of hip joint simulator and thin film colorimetric interferometry. The character of film formation was similar to ball-on-lens results (Vrbka et al., 2014). The film thickness was relatively high (around 240 nm) immediately after the beginning of the test while it was decreasing during the first 10 s and then it was stabilized to approximately 90 nm.

From the literature review (Fan et al., 2011; Mavraki and Cann, 2009, 2011, Myant and Cann, 2013, 2014a, 2014b; Myant et al., 2012; Vrbka et al., 2013, 2014, 2015), it is clear that the proteins contained in model fluids play an important role in relation to thickness of the lubricant film. For film thickness mapping, a combination of ball-on-disc simulators with optical interferometry method seems to be a well-established experimental approach. It was proved that this optical method enables to evaluate the film thickness, as well as to observe the contact of components in situ; therefore the phenomena such as inlet protein aggregation (Fan et al., 2011; Myant and Cann, 2013) or PAL (Myant and Cann, 2014a) can be identified. Although several papers described the influence of different lubricant composition on film thickness, little has been yet known about the role of particular constituents while the simultaneous presence of other components. However, the explanation of protein film formation in terms of contribution of individual parts of model fluid could help to better understand the lubricating mechanisms within artificial hip joints. Therefore, the aim of this study is to introduce an experimental approach enabling the in situ observation of lubricant film in an effort to assess the effect of presence of albumin and γ-globulin on the development of lubricant film thickness. For this purpose, an optical method based on fluorescent microscopy was employed since it enables to observe each constituent stained by fluorescent markers, independently of the other fluid components.

2. Materials and methods

Lubricant film thickness was evaluated using a conventional ball-on-disc tribometer (Gohar and Cameron, 1963) where the circular contact between the ball and the disc is realized. Both components can be driven independently by their own servomotors, so different kinematic conditions and SRR can be applied. The contact was observed by optical imaging system which consists of mercury lamp for illumination, microscope, digital camera, and PC. The scheme of an experimental approach is displayed in Fig. 1.

Two optical methods were employed to determine the protein film formation. Initially, the film thickness was measured by thin film colorimetric interferometry (Hartl et al., 2001), as it was proved that this method is sufficiently precise to measure the thickness of lubricant layer with the resolution equal to 1 nm. In this case, the contact was observed by complementary metal-oxide semiconductor (CMOS) high speed camera (Phantom V710). Thin film colorimetric interferometry is based on matching the captured interferograms with a calibration curve, which is obtained

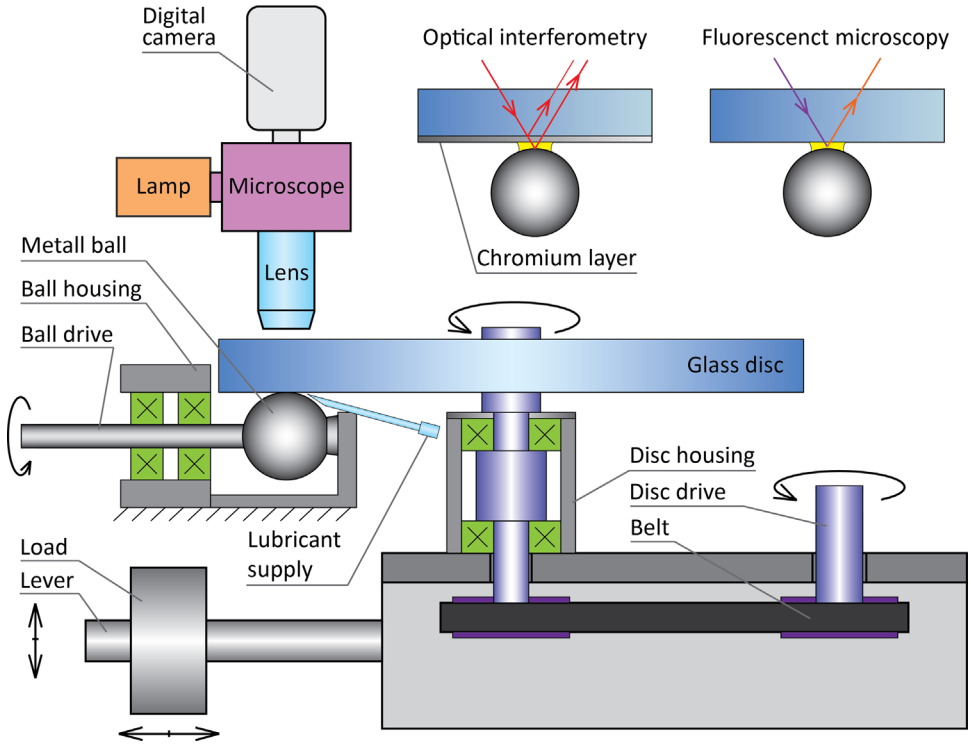

Fig. 1 – : Scheme of the applied experimental approach.

from the image of lightly loaded static contact giving the information about the dependence between the particular colour and the film thickness.

The experiments were then repeated under the same operating conditions by using an optical imaging method based on fluorescent microscopy (Smart and Ford, 1974). This approach allows to observe the fluorescently stained constituents of lubricant film while the simultaneous presence of other parts. It was declared that the dependence between the fluorescence intensity and the film thickness is linear (Azushima, 2006); therefore, in this paper, the fluorescence intensity is considered as dimensionless film thickness. The difference between the above described methods is that the optical interferometry determines the size of the gap between the components based directly on light interference. The fluorescent microscopy studies the amount of fluorescent dye added to the base lubricant, giving the information about the volume of fluid inside the contact (Reddyhoff et al., 2010). The main purpose of the combination of these methods is that the experimental configuration disabled the film thickness evaluation directly by fluorescent method. This is due to the following undesirable phenomena.

1. Interference of light beams arising at the interface of bottom surface of the disc and lubricant and the interface of lubricant and the ball. The problem of light interference was mentioned previously in literature (Sugimura et al., 2000). Although the optical interferometry desires the light interference as contrast as possible, in the case of fluorescent microscopy, this is a huge limitation. Sugimura et al. (2000) solved this effect by using different material of sample during the calibration process. Although this seems to be quite a simple way how to avoid interference, it was later mentioned by Myant et al. (2010) that the different optical properties of calibration sample can lead to irregularities in results.
2. Quenching effect as a consequence of chromium presence in tested materials. The quenching phenomena was mentioned several times (Jie et al., 1998; Varnes et al., 1972; Zhang et al., 2009). Since the loss of fluorescence is not dependent just on the chromium content but also on the type of applied fluorescent marker, it is very complicated to assess the effect of chromium on layer thickness. However, it should be noted that the applied approach is based on matching the film thickness obtained by optical interferometry with the protein film development given by fluorescent microscopy. Even if the results are influenced by the quenching effect, the measurement error is constant in the course of the entire experiments; therefore the general knowledge about the film formation is applicable.

A contact pair was realized by the metal (CoCrMo) femoral head (Zimmer) of a nominal diameter of 28 mm and the glass disc (BK7) coated with a thin chromium layer to enhance the interference in the case of film thickness measurement. It was pointed out previously that the protein film can be influenced by the nature of contact surfaces. However, it should be noted that the authors (Vrbka et al., 2014) compared two variants of coating layers; strongly hydrophilic and strongly hydrophobic. In the present study we performed several experiments with coated and uncoated disc finding that there is no significant effect of layer on protein film formation because the difference of pure and coated disc wettability is not so substantial. On the contrary, the chromium layer caused more quenching of fluorescence leading to an increase of scatter in results; therefore it was decided to use an uncoated disc for experiments conducted with fluorescently stained lubricants.

The initial surface topography of femoral component was analysed in a greater detail by the optical method based on phase shifting interferometry (Bruker Contour GT X8). Five reference points were selected; one on the canopy of the head and four in the contact drag. The measured data for particular points were as follows; $Ra_1=7.41$ nm, $Ra_2=8.19$ nm, $Ra_3=6.90$ nm, $Ra_4=7.87$ nm, $Ra_5=8.67$ nm, respectively, therefore the average value of surface roughness was equal to $Ra=7.81$ nm. The contact surface of glass disc was considered as optically smooth.

Table 1 – Summary of the performed experiments.

Experimental method	SRR	Disc speed (mm/s)	Ball speed (mm/s)	Mean speed (mm/s)	Model fluid
Optical interferometry	0	5.7	5.7	5.7	A:G=2:1
Optical interferometry	0	22	22	22	A:G=2:1
Optical interferometry	−1.5	1.425	9.975	5.7	A:G=2:1
Optical interferometry	−1.5	5.5	38.5	22	A:G=2:1
Optical interferometry	1.5	9.975	1.425	5.7	A:G=2:1
Optical interferometry	1.5	38.5	5.5	22	A:G=2:1
Fluorescent microscopy	0	5.7	5.7	5.7	Labelled A: Non-labelled G=2:1
Fluorescent microscopy	0	5.7	5.7	5.7	Non-labelled A: Labelled G=2:1
Fluorescent microscopy	0	22	22	22	Labelled A: Non-labelled G=2:1
Fluorescent microscopy	0	22	22	22	Non-labelled A: Labelled G=2:1
Fluorescent microscopy	−1.5	1.425	9.975	5.7	Labelled A: Non-labelled G=2:1
Fluorescent microscopy	−1.5	1.425	9.975	5.7	Non-labelled A: Labelled G=2:1
Fluorescent microscopy	−1.5	5.5	38.5	22	Labelled A: Non-labelled G=2:1
Fluorescent microscopy	−1.5	5.5	38.5	22	Non-labelled A: Labelled G=2:1
Fluorescent microscopy	1.5	9.975	1.425	5.7	Labelled A: Non-labelled G=2:1
Fluorescent microscopy	1.5	9.975	1.425	5.7	Non-labelled A: Labelled G=2:1
Fluorescent microscopy	1.5	38.5	5.5	22	Labelled A: Non-labelled G=2:1
Fluorescent microscopy	1.5	38.5	5.5	22	Non-labelled A: Labelled G=2:1

As a test lubricant, a protein solution in phosphate-buffered saline (PBS) was used. BS albumin (Sigma-Aldrich A7030) was doped by Rhodamine-B-isothiocyanate (Sigma-Aldrich 283924). The protein concentration in stained suspension was 455.7 mg/ml. γ-Globulin from bovine blood (Sigma Aldrich-G5009) was stained by Fluorescein-5-isothiocyanate (Sigma-Aldrich F7250) resulting in protein concentration of 198.5 mg/ml. The ratio of albumin (A) and γ-Globulin (G) was set as A:G=2:1, the total concentration of A and G in model fluid was 7 mg/ml and 3.5 mg/ml, respectively. The same samples were prepared also with no-stained proteins, as the combination of stained and no-stained protein is necessary to distinguish the constituents in model fluid during the experiment. The test samples were divided into the tubes and deeply frozen to −22 °C. The solution was taken out from the freezer 120 min prior to testing to thaw naturally without any temperature shock. The lubricant was continuously supplied to the inlet zone by a syringe pump for three minutes. The total amount of fluid for each experiment was 10.5 ml. Before the experiment, all components were cleaned in 1% sodium dodecyl sulphate solution, rinsed by distilled water, and then dried by pressed air and washed in an isopropyl alcohol.

The load equal to 5 N was applied by lever system resulting in the maximum contact pressure equal to 180 MPa. The film thickness was observed under two various speeds 5.7 mm/s and 22 mm/s. The experiments were carried out under pure rolling (SRR=0%), partial negative sliding (SRR=−150%), and partial positive sliding (SRR=150%). The time of each experiment was set to 300 s. All the measurements were conducted under ambient temperature (T=22 °C), since it was published previously that the change of temperature from ambient to body temperature does not influence the results significantly (Mavraki and Cann, 2011). To have a better idea about the measurements, the particular experiments are summarised in Table 1.

3. Results

3.1. Pure rolling conditions

First experiments were conducted under pure rolling conditions. Two different speeds were applied, as was mentioned previously. Film thickness as a function of time was evaluated by using a colorimetric interferometry method. The value of film thickness corresponds to the average value inside the circle of the diameter equal to 1/5 of contact zone diameter. It can be seen in Fig. 2 that, independently of rolling speed, the film thickness gradually increased in the course of the entire experiment. At lower rolling speed, the tendency of increase is linear with a small drop after approximately 130 s. The maximum measured thickness at the end of the test was around 15 nm. For 22 mm/s, the film thickness increased linearly for around 200 s without any significant scatter. Then, the slope of increase changed; however the film continued to increase up to almost 40 nm. After the film thickness measurement, two more experiments were conducted for each speed; while the only difference was in the observed lubricant constituent. As in the case of interferometry, the intensity value is the average value from the central zone of the contact. For 5.7 mm/s, it is evident that there is almost no change of thickness of γ-globulin. On the contrary, the intensity of images increased gradually when albumin was observed. This indicates that the protein film formation is mainly due to increase of albumin. A very similar behaviour was observed for higher speed. Again, only one of the proteins showed a significant qualitative change. Even if there was some intensity of γ-globulin film detected, as can be seen in Fig. 3, the level of intensity was considerably lower compared to images of albumin. It should be noted that the scale of axis, giving the information about the fluorescence intensity, was adjusted to correspond to the film thickness for each particular experiment. Therefore, it is not possible to state that the intensity level directly corresponds to film thickness; only the tendency of curves can be compared. The fluorescent images of contact zone for both experiments can be seen in Fig. 3.

3.2. Partial negative sliding

Under partial negative sliding, when the ball was faster than the disc, the film formation seems to be strongly dependent on the applied mean speed. This indicates that the sliding distance can play an important role. When the speed was 5.7 mm/s, the film thickness was very thin, only in the range from 1 to 3 nm. It can be clearly seen from Fig. 4a that none of the proteins showed a qualitative change over the time. In this case, the intensity of fluorescence is very low, in the range from 0 to 100. Increase of mean speed to 22 mm/s led to a substantial change of protein film formation. In this case, there was a very thin film, less than 3 nm, at the beginning of the experiment, which is very similar to a lower speed. However, against expectations, after approximately 100 s the film thickness started to gradually increase while the value of lubricant layer at the end of the test was around 15 nm. Unlike under pure rolling conditions, when the labelled albumin was detected by fluorescent microscopy, any development of intensity could not be observed. It is evident from Fig. 4b that the increase in lubricant film thickness is caused by γ-globulin. The phenomena of increasing γ-globulin intensity can be clearly seen in the lower part of Fig. 5.

3.3. Partial positive sliding

The last set of experiments was conducted while the disc was faster than the ball; therefore positive sliding conditions were applied. As in the previous case, the protein film formation seems to be very complex and time/sliding distance dependent. At lower speed, the film increased continuously without any significant scatter in results. When the lubricant supply stopped, the layer reached its maximum value around 120 nm and started to decrease while the value at the end of the test was somewhere between 50 and 70 nm. As is shown in Fig. 6a, the development of film thickness is in a good agreement with the intensity of albumin protein film. Under pure rolling and partial negative sliding, there was no effect of γ-globulin film observed at the mean speed of 5.7 mm/s. However, under positive sliding conditions the intensity of γ-globulin varies in the range from 0 to 3500 indicating that even γ-globulin contributes to the protein film thickness. Nevertheless, when comparing the above mentioned values with the intensity of

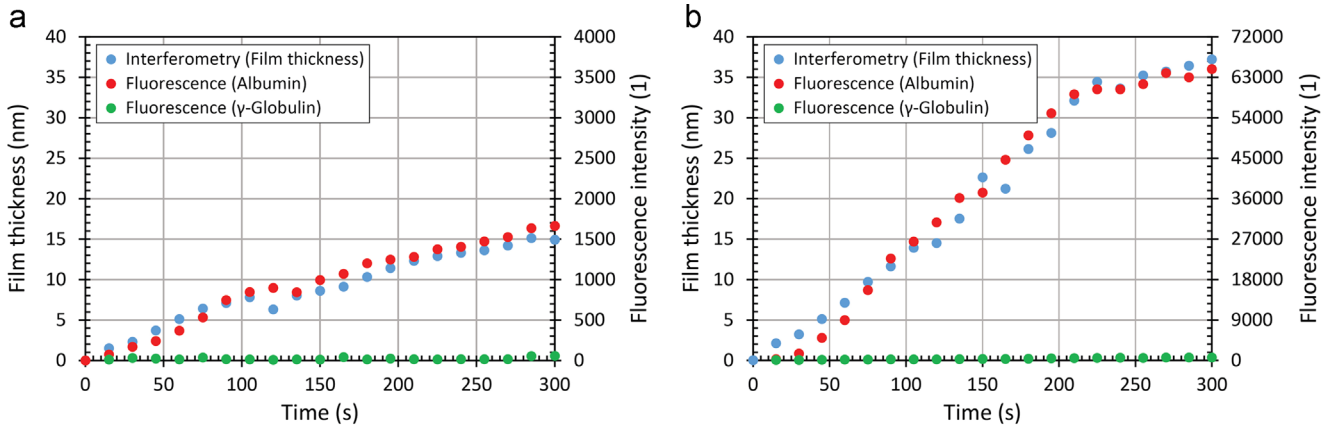

Fig. 2 – Development of film thickness and fluorescence intensity of labelled proteins as a function of time under pure rolling conditions for different mean speeds; a) 5.7 mm/s; b) 22 mm/s.

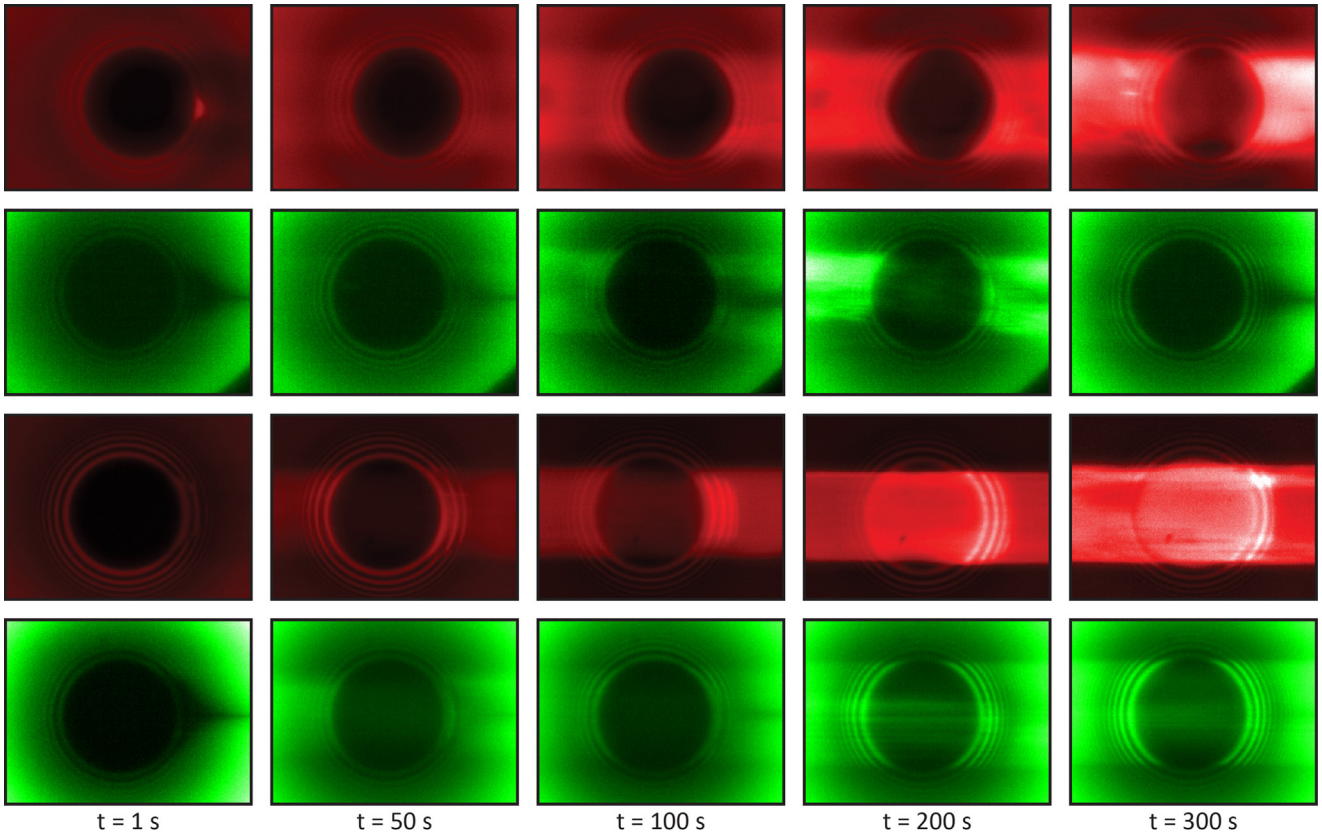

Fig. 3 – Images of the contact zone captured during the experiment under pure rolling conditions. From the top: albumin (5.7 mm/s), γ-globulin (5.7 mm/s), albumin (22 mm/s), γ-globulin (22 mm/s). The inlet is on the left of each image.

albumin, which is around 33,000 at maximum, it is clear that, in this case, albumin plays a key role. The qualitative change of γ-globulin can correspond to the change of film thickness in a range of units of nm. An increase of mean speed led to a different character of film formation, although some very similar phenomena can be determined for both speeds. In the case of 22 mm/s the film thickness increased very quickly up to 40 nm in the first few tens of seconds. After that it started to decrease steeply to almost a zero level. It became constant without any quantitative change until the end of the experiment. From Fig. 6a, it can be assumed that the slope of the increasing and decreasing tendency of the film thickness is almost the same. If the experiment lasted longer, it could be expected that the film thickness would drop to very low values.

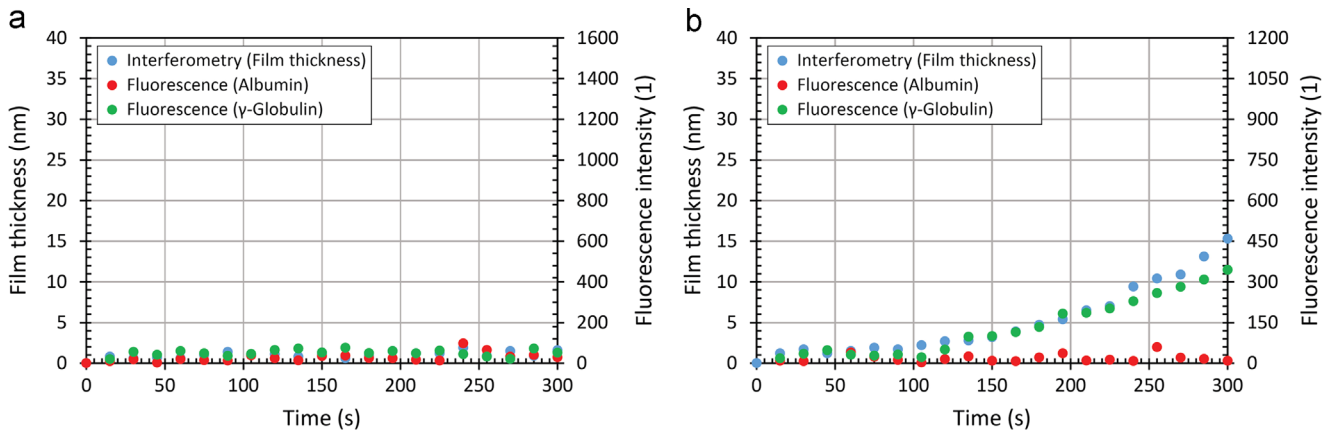

Fig. 4 – Development of film thickness and fluorescence intensity of labelled proteins as a function of time under partial negative sliding (ball is faster than disc) for different mean speeds; a) 5.7 mm/s; b) 22 mm/s.

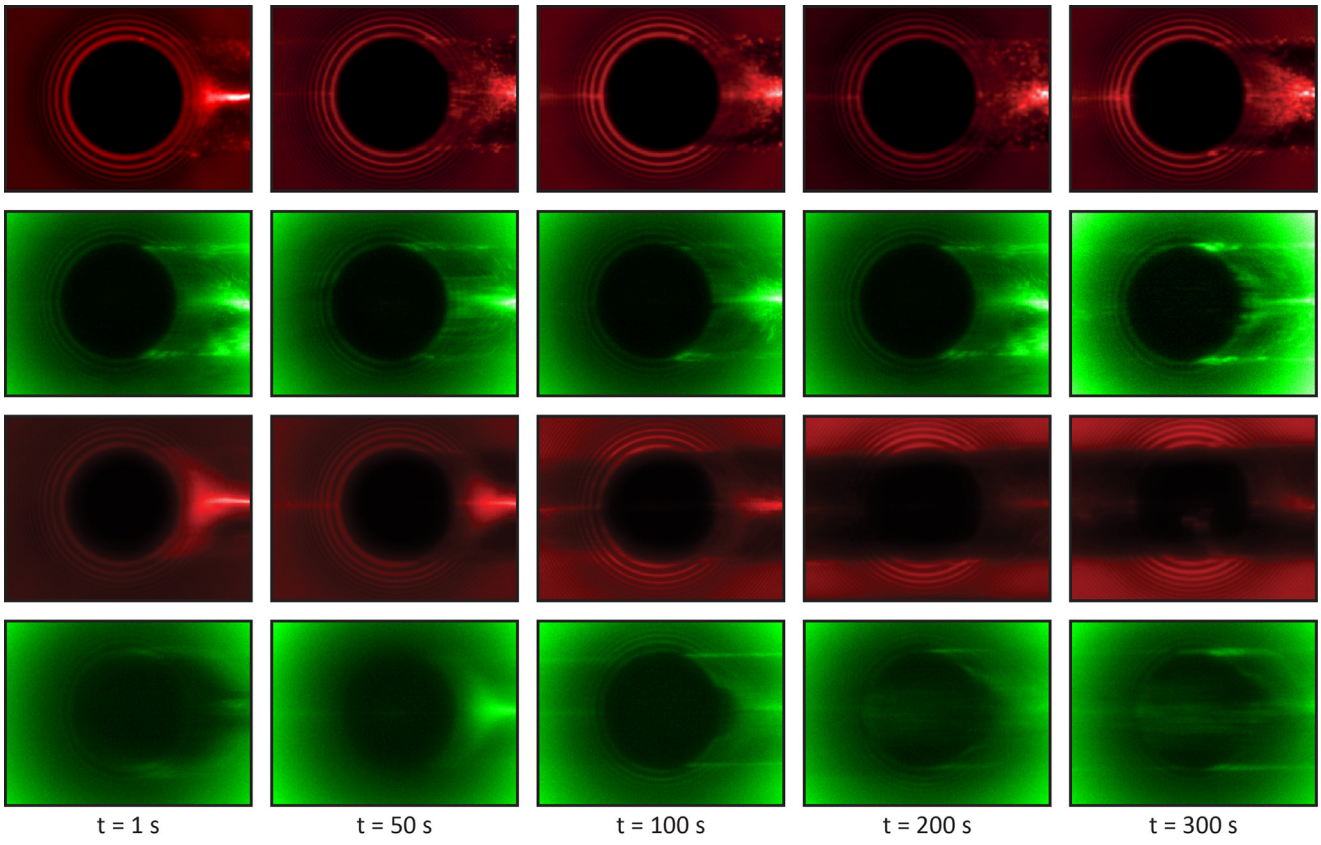

Fig. 5 – : Images of the contact zone captured during the experiment under partial negative sliding (ball is faster than disc). From the top: albumin (5.7 mm/s), γ-globulin (5.7 mm/s), albumin (22 mm/s), γ-globulin (22 mm/s). The inlet is on the left of each image.

The same behaviour can be detected even in case of higher speed, as is displayed in Fig. 6b. The role of proteins also seems to be quite similar. The albumin layer increased steeply in the first 50 s, and then it dropped to nearly a zero level without any subsequent change. The layer of γ-globulin is much thinner, independently of time. However, from the images of the contact zone, see Fig. 7, it would appear that even γ-globulin contributes substantially to layer thickness. In this case, it is necessary to consider that the white colour in the contact zone means that the area is overexposed, indicating that the layer thickness is substantially higher. Although the effect of γ-globulin seems to be more considerable than in most of the previous cases, in author's opinion, the more important protein influencing the layer thickness is albumin.

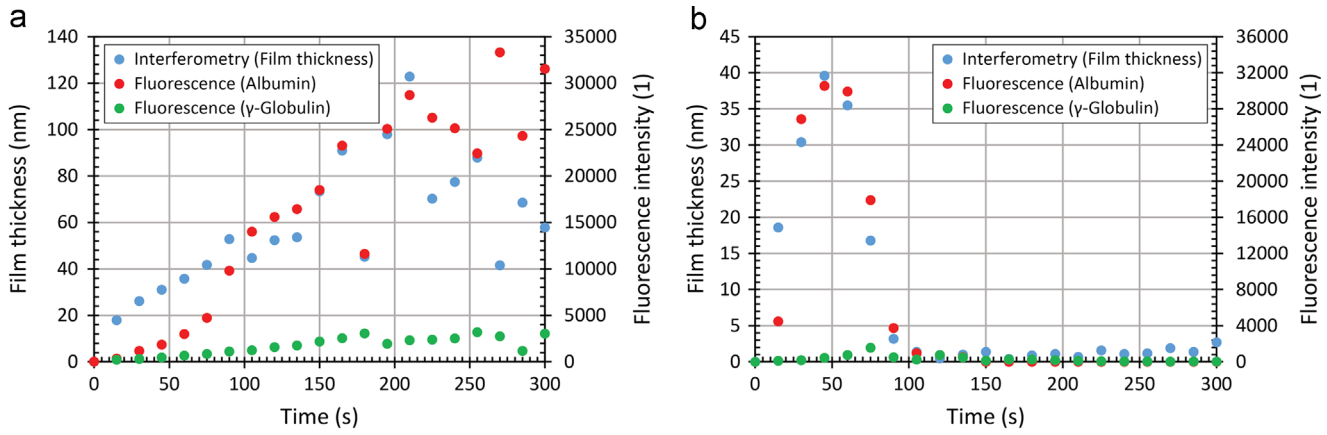

Fig. 6 – Development of film thickness and fluorescence intensity of labelled proteins as a function of time under partial positive sliding (disc is faster than ball) for different mean speeds; a) 5.7 mm/s; b) 22 mm/s.

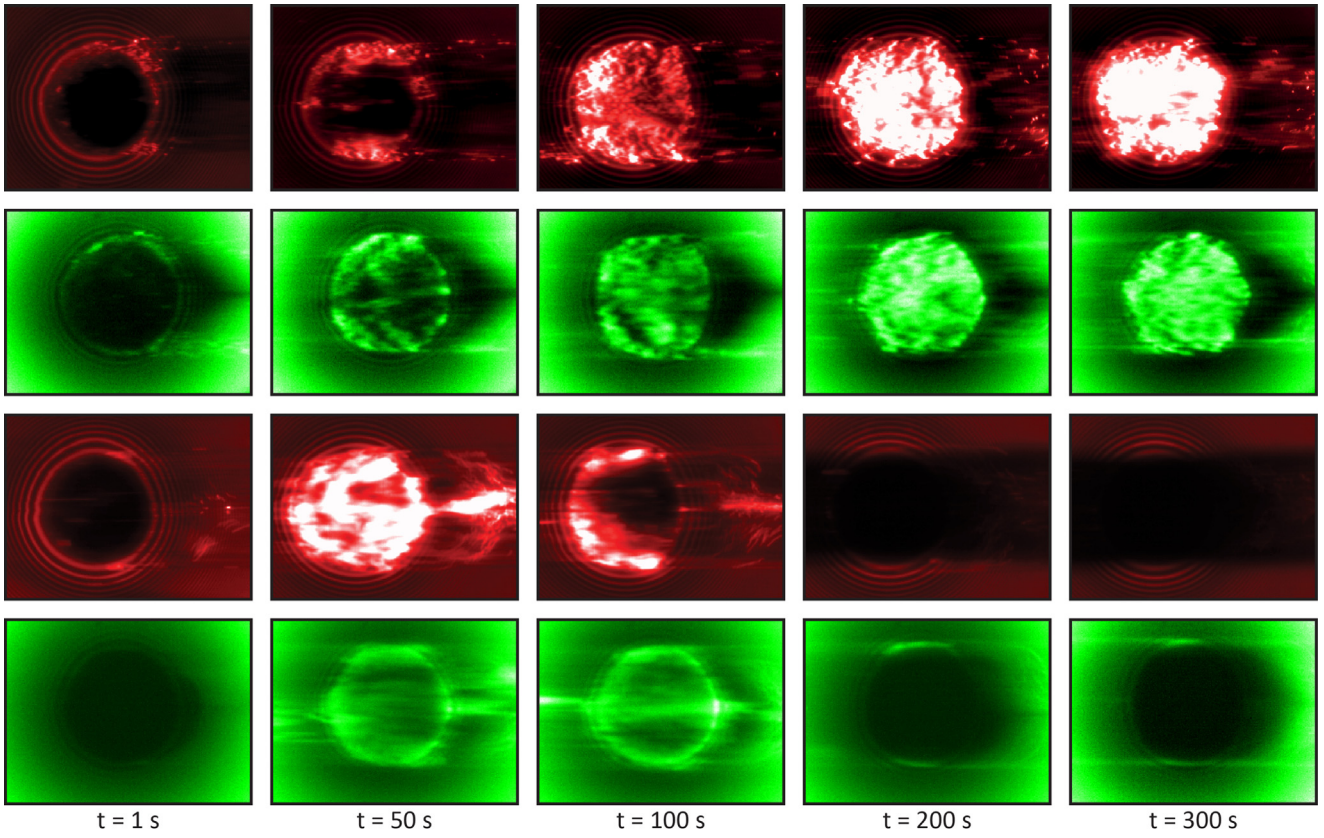

Fig. 7 – Images of the contact zone captured during the experiment under partial positive sliding (disc is faster than ball). From the top: albumin (5.7 mm/s), γ-globulin (5.7 mm/s), albumin (22 mm/s), γ-globulin (22 mm/s). The inlet is on the left of each image.

3.4. Summary of results

As can be seen in Fig. 8, the protein film formation is complex and time/distance dependent. Under pure rolling conditions, the film gradually increases during the test, while there is no substantial scatter in results. Under partial negative sliding, where the ball is faster than the disc, the film thickness is generally very thin. Even at higher speeds, it lasts approximately 100 s before some relevant film can be detected. The most scattered results were obtained when the disc was faster than the ball (positive sliding conditions). In this case, film thickness increases quite rapidly for some time and then it starts to decrease to almost a negligible level. In most cases, the increase in mean speed led to the increase of film thickness. However, under positive sliding the effect of speed was opposite. While the maximum value for 5.7 mm/s

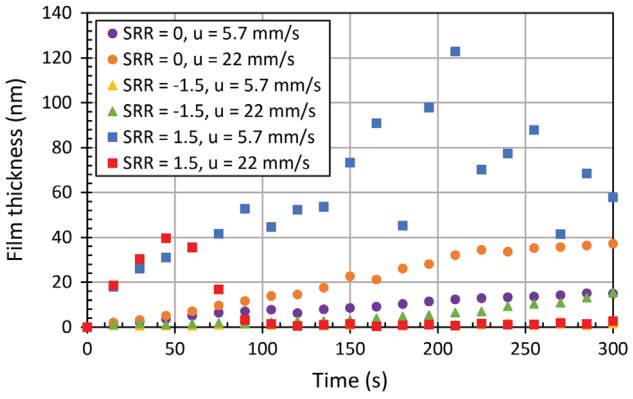

Fig. 8 – Comparison of film thickness measurements by thin film colorimetric interferometry for various operating conditions.

was more than 120 nm, under higher speed, it was only around 40 nm. The graph comparing the fluorescence intensity of labelled proteins for particular experiments is not provided, since the scale is very different for each measurement, depending on the effects caused by excitation intensity, setup of optical chain, or exposure time. However, from the particular images, see Figs. 2–7, independently of kinematic conditions, the film thickness can be well explained in terms of particular protein contribution.

4. Discussion

Several authors focused on mapping of film thickness in the contact lubricated by BS or simple protein solutions in the effort to describe lubrication processes within hip joint replacements (Fan et al., 2011; Mavraki and Cann, 2009, 2011, Myant and Cann, 2013, 2014a, 2014b; Myant et al., 2012; Vrbka et al., 2013, 2014, 2015). Although it is evident that optical interferometry enables to measure film thickness under various operating conditions, according to the author's knowledge, the study, examining the role of particular protein while the simultaneous presence of another protein, has not been published yet. As can be seen in Fig. 2, film thickness increases with time independently of a mean speed under pure rolling conditions. It is apparent that the film thickness is time/rolling distance dependent. The same behaviour was observed by Vrbka et al. (2013); in their research the film thickness was studied for the metal femoral component at different rolling speeds. In the present study, the film is thinner compared to the above mentioned reference. However, the authors, according to Vrbka et al. (2013), applied BS as a test lubricant with the protein concentration equal to 22.4 mg/ml, while the information about the protein ratio was not provided. In our case, the content of proteins was 10.5 mg/ml, indicating that the protein concentration significantly influences the lubricating film. In meaning of particular proteins, there was no qualitative change in the fluorescence intensity corresponding to the behaviour of γ-globulin, see Figs. 2 and 3. Therefore it is clear that the increase of lubricant film can be attributed exclusively to the increase of albumin. Probably, a very thin layer of γ-globulin is firstly adsorbed onto rubbing surfaces, enabling the albumin to adsorb on it and to create a layer structure. It was already described by Nakashima et al. (2007a) that γ-globulin shows a stronger adsorption compared to albumin. This might be an explanation of lubricant film formation under pure rolling. Our results do not correspond to the previously published results provided by Myant et al. (2012), who investigated the effect of protein content on film formation of metal-on-metal joints, finding that simple protein solutions containing γ-globulin form a much thicker layer compared to those with albumin. The present study clearly confirms that the film thickness evaluation using simple protein solutions can result in some inaccuracies because only one particular protein is considered.

When a slippage was taken into account, the protein film formation was completely changed. When the ball was faster than the disc, the film thickness was extremely thin during the whole time of experiment at low speed equal to 5.7 mm/s. Absolutely the same behaviour was observed previously (Vrbka et al., 2014). Even if both proteins were investigated separately, there was no film formed between the rubbing surfaces showing that under these severe conditions the protein film cannot be fully developed. It should be emphasised that under negative sliding, the revolutions of the ball are higher compared to those of the disc. Therefore, the disc rotates for only around 360° during the experiment; so the replenishment of protein film in the contact drag of the disc cannot occur. According to this, no protein adsorption on the disc can be considered. On the contrary, the rotations of ball are relatively high. One rotation lasts around 9 s while the continual passage of the protein layer through the contact can lead to disruption of proteins. This effect can be observed on the top part of Fig. 5, showing the albumin formation over a time range, where a strongly inhomogeneous protein formation can be seen in the outlet zone. The theory about the importance of layer adsorbed at the bottom of the glass disc is supported by the results at higher speed of 22 mm/s. In this case, film thickness started to gradually increase after approximately 100 s. It is evident from Fig. 4b that the film is formed predominantly due to the presence of γ-globulin. It is estimated that this protein film can be attributed to protein adsorption on glass disc. The applied coating layer is naturally hydrophobic. It was pointed out (Malmsten, 1998) that both albumin and γ-globulin can adsorb rather onto hydrophobic surfaces. Although the femoral head is made from CoCrMo alloy indicating its hydrophobic nature, the idea about adsorption on disc is supported by the images of contact zone. At the bottom part of Fig. 5, it can be clearly seen that the γ-globulin cluster is continuous and can be observed even in front of the contact (200 s, 300 s), confirming the presence of γ-globulin in the contact drag of the disc. It was also pointed out by Myant et al. (2012) that γ-globulin forms a thicker layer than albumin in terms of adsorption, which supports our previous assumption.

Under pure rolling and partial negative sliding, there were no significant fluctuations in results. It is clear that film thickness increases gradually with time and rolling distance. Under partial negative sliding, the constant protein film thinner than 5 nm was observed for 5.7 mm/s. An increase of sliding speed led to a slight increase of lubricant film caused mainly by adsorption effect. A totally different behaviour was observed when the disc was faster than the ball. At lower speed, the film

thickness was increasing quite steeply for the first 200 s. The maximum value was more than 120 nm, while a substantial scatter in results was recorded. After reaching the maximum value, the lubricant film started to decrease while the slope of the tendency was nearly the same compared to that of the initial increase. When the speed was 22 mm/s, a very rapid increase of film thickness was observed within the first tens of seconds, followed by rapid decrease to almost a zero level. After that there was no substantial lubricant film. It can be seen in Fig. 6 that the behaviour is almost the same for both speeds; the only difference is the time (sliding distance) before the maximum value of film thickness is reached and, of course, the total film thickness. As in the case of negative sliding, these results can be explained in terms of kinematic conditions. This time, the speed of the ball is not so high, so the protein film is not significantly influenced by a continuous passage through the contact. The higher lubricant film is caused especially due to protein aggregations inside the contact, while the film is disrupted rather by the layer on the disc, which moves very quickly and passes through the contact zone. What is in discrepancy with all previous results is that film thickness is thinner at higher speed. The maximum film thickness at 22 mm/s is less than 40 nm. Again, this is probably due to rotations of the disc disabling a full development of the aggregated film. The same character of film formation under partial positive sliding was observed previously (Vrbka et al., 2013). The positive sliding conditions were also investigated by Mavraki and Cann (2011). It was shown that film thickness was much thinner compared to pure rolling conditions; however an experimental setup allowed to fully bath the contact (Mavraki and Cann, 2011). When trying to detect the importance of particular proteins under positive sliding, Figs. 6 and 7 show that the main contribution is due to the presence of albumin. Nevertheless, even for γ-globulin, some tendency to the increase can be found, especially at lower speed.

In the images of contact zone (Figs. 3, 5 and 7), it can be seen that there is no protein build up in the contact inlet, as was described by Myant and Cann (2013). The accumulation of the proteins before they pass through the contact is probably connected with the conditions of lubrication. The authors (Myant and Cann, 2013) applied fully bathed conditions as was already mentioned; however, in our study, the lubricant is supplied by a syringe pump which can naturally lead to some differences in film formation. Even in previous studies (Vrbka et al., 2013, 2014) no inlet phase was observed independently of operating conditions.

It is very complicated to assess the adsorption processes. From the results, it is expected that usually a very thin γ-globulin film is formed on rubbing surfaces allowing the albumin to form a layer structure leading to an increase in total lubricant film thickness. The phenomena of adsorption of particular proteins while the simultaneous presence of both, albumin and γ-globulin were investigated extensively (Nakashima et al., 2005, 2007a, 2007b, 2007; Yarimitsu et al., 2009). It was concluded that γ-globulin shows a stronger adsorption connected with higher shear strength. On the contrary, the albumin layer is usually bonded by relatively low forces which can be accompanied by lower friction between the rubbing surfaces.

Obviously, the authors realise some limitations of the performed study. First of all, ball-on-disc configuration does not correspond to real hip joint arrangement, where the contact of conformal bodies occurs. Therefore, some differences in protein film formation can be expected, especially due to higher contact pressure. The importance of surface conformity was proved in our previous paper. (Vrbka et al., 2015). However, it should be emphasised that several authors employed ball-on-disc experimental setup to investigate the fundamentals of protein lubrication previously. As the main goal of the present paper is to introduce and validate the novel methodological approach, ball-on-disc configuration seems to be appropriate solution, since the results can be compared with previously published data. Considering the real conformity, there is only one study published yet, therefore it would be particularly complicated to discuss the results.

As the second point, the difference between the properties of the glass disc and materials of acetabular cups should be highlighted. To be able to observe the contact in situ, at least one of the components has to be transparent. The Young's modulus of the optical glass is approximately 85 GPa. Even if it is almost three times lower compared to ceramics or metal alloys, it is still very hard material. Therefore the results obtained for the combination of metal ball with glass disc relate rather to hard-on-hard bearing couples, as was indicated elsewhere (Myant and Cann, 2014a). In an effort to describe similar lubrication mechanisms also in hard-on-soft contacts, the counterparts of the ball have to be fabricated from much more compliant material, with the modulus of elasticity around 2–3 GPa.

Finally, as was mentioned above, it was proved by Myant and Cann (2014b) that the character of motion significantly affects the protein film thickness. It is quite evident that unidirectional test does not correspond to real conditions in hip joint. Moreover, the applied load is constant over the whole time of experiment. Nevertheless, as was already told, this approach seems to be well-established in an effort to understand the fundamentals of protein lubrication mechanisms. Concluding the above mentioned points, the combination of the effect of conformity and motion character together with the effect of material seems to be the essential motivation for the following study.

5. Conclusion

The present study is focused on the influence of proteins contained in model fluid on lubrication of hip joints replacements. Thin film colorimetric interferometry method was used for film thickness evaluation and was combined with the optical method based on fluorescent microscopy. Various model fluids were applied enabling us to determine the contribution of particular proteins to the thickness of lubricant film while the simultaneous presence of another protein. The results can be summarised in the following points:

- The combination of two applied optical methods can provide the information about the role of particular proteins on lubricant film independently of lubricant composition.

- When studying lubrication mechanisms of protein solutions, it is necessary to consider all the constituents contained in the test lubricant. A simple protein solution containing only one constituent cannot provide the information about the complex fluid behaviour.
- Under pure rolling and positive sliding conditions, the film thickness is formed predominantly due to the presence of albumin.
- Under negative sliding, the film thickness is strongly dependent on time (sliding distance). An increase of lubricant film at higher speeds is mainly caused by γ-globulin.
- In author's opinion, γ-globulin forms a very thin protein layer on the base material allowing the albumin to adsorb onto the layer and therefore, to increase the total film thickness in most cases.

The future study should focus on the influence of protein concentration on the lubricant film as well as on the effect of materials and conformity of rubbing surfaces of hip joint components. The effect of transient kinematic conditions should be also investigated. As the synovial fluid is very complex, other constituents such as hyaluronic acid or lipids (Sawae et al., 2008), should also be considered.

Acknowledgement

This research was carried out under the project NETME CENTRE PLUS (LO1202) with financial support from the Ministry of Education, Youth and Sports under the National Sustainability Programme I. The authors express thanks to A. Galandáková for her help with the preparation of model fluids.

REFERENCES

Adelani, M.A., Keeney, J.A., Palisch, A., et al., 2013. Has total hip arthroplasty in patients 30 years or younger improved? A systematic review. Clin. Orthop. Relat. Res. 471 (8), 2595–2601.

Azushima, A., 2006. In situ 3D measurement of lubrication behavior at interface between tool and workpiece by direct fluorescence observation technique. Wear 260 (3), 243–248.

Dowson, D., 2006. Tribological principles in metal-on-metal hip joint design. Proc. Inst. Mech. Eng., Part H.: J. Eng. Med. 220 (2), 161–171.

Dowson, D., Jin, Z.M., 2006. Metal-on-metal hip joint tribology. Proc. Inst. Mech. Eng. Part H: J. Eng. Med. 220 (2), 107–118.

Dowson, D., McNie, C.M., Goldsmith, A.A.J., 2000. Direct experimental evidence of lubrication in a metal-on-metal total hip replacement tested in a joint simulator. Proc. Inst. Mech. Eng. Part C: J. Mech. Eng. Sci. 214 (1), 75–86.

Essner, A., Schmidig, G., Wang, A., 2005. The clinical relevance of hip joint simulator testing: in vitro and in vivo comparisons. Wear 259 (7), 882–886.

Fan, J., Myant, C.W., Underwood, R., et al., 2011. Inlet protein aggregation: a new mechanism for lubricating film formation with model synovial fluids. Proc. Inst. Mech. Eng. Part H: J. Eng. Med. 225 (7), 696–709.

Gohar, R., Cameron, A., 1963. Optical measurement of oil film thickness under elasto-hydrodynamic lubrication Nature 200, 458-459 .

Goldsmith, A.A.J., Dowson, D., Isaac, G.H., et al., 2000. A comparative joint simulator study of the wear of metal-on-metal and alternative material combinations in hip replacements. Proc. Inst. Mech. Eng. Part H: J. Eng. Med. 214 (1), 39–47.

Hartl, M., Křupka, I., Poliščuk, R., et al., 2001. Thin film colorimetric interferometry. Tribol. Trans. 44 (2), 270–276.

Jalali-Vahid, D., Jin, Z.M., Dowson, D., 2006. Effect of start-up conditions on elastohydrodynamic lubrication of metal-on-metal hip implants. Proc. Inst. Mech. Eng. Part J: J. Eng. Tribol. 220 (3), 143–150.

Jie, N., Zhang, Q., Yang, J., et al., 1998. Determination of chromium in waste-water and cast iron samples by fluorescence quenching of rhodamine 6G. Talanta 46 (1), 215–219.

Jin, Z.M., Stone, M., Ingham, E., et al., 2006. (v) Biotribology. Curr. Orthop. 20 (1), 32–40.

Joshi, A.B., Porter, M.L., Trail, I.A., et al., 1993. Long-term results of Charnley low-friction arthroplasty in young patients. J. Bone Jt. Surg. Br. Vol. 75 (4), 616–623.

Malmsten, M., 1998. Formation of adsorbed protein layers. J. Colloid Interface Sci. 207 (2), 186–199.

Mavraki, A., Cann, P.M., 2009. Friction and lubricant film thickness measurements on simulated synovial fluids. Proc. Inst. Mech. Eng. Part J: J. Eng. Tribol. 223 (3), 325–335.

Mavraki, A., Cann, P.M., 2011. Lubricating film thickness measurements with bovine serum. Tribol. Int. 44 (5), 550–556.

Myant, C., Cann, P., 2013. In contact observation of model synovial fluid lubricating mechanisms. Tribol. Int. 63, 97–104.

Myant, C., Cann, P., 2014a. On the matter of synovial fluid lubrication: Implications for Metal-on-Metal hip tribology. J. Mech. Behav. Biomed. Mater. 34, 338–348.

Myant, C., Cann, P., 2014b. The effect of transient conditions on synovial fluid protein aggregation lubrication. J. Mech. Behav. Biomed. Mater. 34, 349–357.

Myant, C., Reddyhoff, T., Spikes, H.A., 2010. Laser-induced fluorescence for film thickness mapping in pure sliding lubricated, compliant, contacts. Tribol. Int. 43 (11), 1960–1969.

Myant, C., Underwood, R., Fan, J., et al., 2012. Lubrication of metal-on-metal hip joints: the effect of protein content and load on film formation and wear. J. Mech. Behav. Biomed. Mater. 6, 30–40.

Nakashima, K., Sawae, Y., Murakami, T., 2005. Study on wear reduction mechanisms of artificial cartilage by synergistic protein boundary film formation. JSME Int. J. Ser. C. Mech. Syst. Mach. Elem. Manuf. 48 (4), 555–561.

Nakashima, K., Sawae, Y., Murakami, T., 2007a. Effect of conformational changes and differences of proteins on frictional properties of poly (vinyl alcohol) hydrogel. Tribol. Int. 40 (10), 1423–1427.

Nakashima, K., Sawae, Y., Murakami, T., 2007b. Influence of protein conformation on frictional properties of poly (vinyl alcohol) hydrogel for artificial cartilage. Tribol. Lett. 26 (2), 145–151.

Parkes, M., Myant, C., Cann, P.M., et al., 2014. The effect of buffer solution choice on protein adsorption and lubrication. Tribol. Int. 72, 108–117.

Pramanik, S., Agarwal, A.K., Rai, K.N., 2005. Chronology of total hip joint replacement and materials development. Trends Biomater. Artif. Organs 19 (1), 15–26.

Reddyhoff, T., Choo, J.H., Spikes, H.A., et al., 2010. Lubricant flow in an elastohydrodynamic contact using fluorescence. Tribol. Lett. 38 (3), 207–215.

Sawae, Y., Yamamoto, A., Murakami, T., 2008. Influence of protein and lipid concentration of the test lubricant on the wear of ultra high molecular weight polyethylene. Tribol. Int. 41 (7), 648–656.

Scholes, S.C., Unsworth, A., 2006. The effects of proteins on the friction and lubrication of artificial joints. Proc. Inst. Mech. Eng. Part H: J. Eng. Med. 220 (6), 687–693.

Smart, A.E., Ford, R.A.J., 1974. Measurement of thin liquid films by a fluorescence technique. Wear 29 (1), 41–47.
Smith, S.L., Dowson, D., Goldsmith, A.A.J., 2001a. The effect of femoral head diameter upon lubrication and wear of metal-on-metal total hip replacements. Proc. Inst. Mech. Eng. Part H: J. Eng. Med. 215 (2), 161–170.
Smith, S.L., Dowson, D., Goldsmith, A.A.J., et al., 2001b. Direct evidence of lubrication in ceramic-on-ceramic total hip replacements. Proc. Inst. Mech. Eng. Part C: J. Mech. Eng. Sci. 215 (3), 265–268.
Sugimura, J., Hashimoto, M., Yamamoto, Y., 2000. Study of elastohydrodynamic contacts with fluorescence microscope. Tribol. Ser. 38, 609–617.
Varnes, A.W., Dodson, R.B., Wehry, E.L., 1972. Interactions of transition-metal ions with photoexcited states of flavines. Fluorescence quenching studies. J. Am. Chem. Soc. 94 (3), 946–950.
Vrbka, M., Návrat, T., Křupka, I., et al., 2013. Study of film formation in bovine serum lubricated contacts under rolling/sliding conditions. Proc. Inst. Mech. Eng. Part J: J. Eng. Tribol. 227 (5), 459–475.
Vrbka, M., Křupka, I., Hartl, M., et al., 2014. In situ measurements of thin films in bovine serum lubricated contacts using optical interferometry. Proc. Inst. Mech. Eng. Part H: J. Eng. Med. 228 (2), 149–158.
Vrbka, M., Nečas, D., Hartl, M., et al., 2015. Visualization of lubricating films between artificial head and cup with respect to real geometry. Biotribology 1–2, 61–65.
Wang, A., Essner, A., Schmidig, G., 2004. The effects of lubricant composition on in vitro wear testing of polymeric acetabular components. J. Biomed. Mater. Res. Part B: Appl. Biomater. 68 (1), 45–52.
Wimmer, M.A., Sprecher, C., Hauert, R., et al., 2003. Tribochemical reaction on metal-on-metal hip joint bearings: a comparison between in-vitro and in-vivo results. Wear 255 (7), 1007–1014.
Yarimitsu, S., Nakashima, K., Sawae, Y., et al., 2007. Study on the mechanisms of wear reduction of artificial cartilage through in situ observation on forming protein boundary film. Tribol. Online 2 (4), 114–119.
Yarimitsu, S., Nakashima, K., Sawae, Y., et al., 2009. Influences of lubricant composition on forming boundary film composed of synovia constituents. Tribol. Int. 42 (11), 1615–1623.
Zhang, L., Xu, C., Li, B., 2009. Simple and sensitive detection method for chromium (VI) in water using glutathione—capped CdTe quantum dots as fluorescent probes. Microchim. Acta 166 (1–2), 61–68.

Available online at www.sciencedirect.com

ScienceDirect

www.elsevier.com/locate/jmbbm

Research Paper

Lubrication within hip replacements – Implication for ceramic-on-hard bearing couples

D. Nečas[a,*], M. Vrbka[a,b], I. Křupka[a,b], M. Hartl[a], A. Galandáková[c]

[a]Faculty of Mechanical Engineering, Brno University of Technology, Czech Republic
[b]CEITEC - Central European Institute of Technology, Brno University of Technology, Czech Republic
[c]Faculty of Medicine and Dentistry, Palacký University Olomouc, Czech Republic

ARTICLE INFO

Article history:
Received 28 January 2016
Received in revised form
30 March 2016
Accepted 1 April 2016
Available online 8 April 2016

Keywords:
Hip replacement
Ceramic
Protein film
Albumin
γ-globulin

ABSTRACT

The objective of the present study is to clarify the lubrication processes within artificial joints considering the ceramic femoral heads focusing on the role of particular proteins. Two optical methods were employed; colorimetric interferometry and fluorescent microscopy. The experiments were conducted in ball-on-disc configuration, where the ball is made from ceramic (Sulox™, BIOLOX®*delta*) and the disc from optical glass. The measurements were realized under pure rolling, partial negative and partial positive sliding, to get a complex information about the protein film behaviour under various conditions. Moreover, two different speeds were investigated; 5.7 and 22 mm/s, respectively. The contact was lubricated by saline solutions containing albumin and γ-globulin in a ratio 2:1, while the total protein concentration was 10.5 mg/ml. Under pure rolling conditions, the film thickness gradually increases with time/rolling distance independently of material and rolling speed, while the dominant fluid constituent is albumin. In the case of negative sliding, the film formation is time/distance/speed dependent. At lower speed, both proteins contribute to film thickness; at higher speed, the effect of γ-globulin is not substantial. When the disc is faster, the character of film formation is similar to the metal component in the case of Sulox ceramic. Biolox ceramic shows a different behaviour, while for both materials, the contribution of γ-globulin increases with increasing speed. As most of the results can be well explained in terms of specific proteins, it can be concluded that the experimental approach is suitable for the investigation of protein film formation considering the ceramic materials.

1. Introduction

Biotribology of hip replacements became of a great importance during the last few decades; since it is well known that the longevity of implants is still limited. Especially in the case of young patients, the risk of failure and consequently the need for revising operation lead to worsening of life quality. As the most common cause of implant failure is osteolysis

*Corresponding author. Tel.: +420 541 143 227.
E-mail address: necas@fme.vutbr.cz (D. Nečas).

http://dx.doi.org/10.1016/j.jmbbm.2016.04.003
1751-6161/

leading to aseptic loosening (Joshi et al., 1993), the main attention of researchers was paid to minimisation of the number of wear particles previously. Several papers focused on in vitro testing of artificial hip joints by using different types of simulators (Goldsmith et al., 2000; Smith et al., 2001; Wang et al., 2004). It is evident that one of the key factors influencing wear is the material of replacement. Nowadays, the materials of implants can be basically divided into two groups; hard materials such as CoCrMo alloys, or ceramic with very high modulus of elasticity in a range of hundreds of GPa, and soft materials represented by polymers with the modulus of elasticity approximately hundred times lower (Pramanik et al., 2005). Generally, in terms of wear it can be assumed that the ceramic-on-ceramic contact pairs exhibit the lowest wear rate (Heisel et al., 2003). Although wear tests can provide important information about the components articulation, so far a little was examined about the protein lubrication mechanisms.

In an effort to better understand the lubrication mechanisms within hip joint replacements, lubricant film thickness is a desired parameter. Though there were some efforts to predict the film thickness numerically (Dowson, 2006; Dowson and Jin, 2006), it must be considered that human synovial fluid (SF) and its models, such as bovine serum (BS) or protein solutions exhibit non-Newtonian and shear thinning behaviour (Mavraki and Cann, 2011). Moreover, protein adsorption, the simulation of which is extremely complicated, substantially influences the protein lubricant film (Scholes and Unsworth, 2006; Parkes et al., 2014). Some of the mechanisms connected with SF lubrication which are not in an agreement with classical elastohydrodynamic lubrication were highlighted by Myant and Cann (2014a), who introduced protein aggregation lubrication (PAL) mechanisms. From the above mentioned, it is evident that numerical simulations cannot fully incorporate all the mechanisms connected with SF lubrication; therefore, the importance of experimental investigation should be emphasised.

In order to explain the lubrication mechanisms, optical interferometry in combination with ball-on-disc experimental apparatus was successfully established for the film thickness measurement. The initial study given by Mavraki and Cann (2009) focused on the film thickness evaluation as a function of mean speed for various model fluids. The following paper extended this knowledge considering the effect of load and rolling/sliding conditions on the film thickness in the contact lubricated by BS (Mavraki and Cann, 2011). Under pure rolling, the protein film increased, while subsequent speed sweep did not influence the protein film substantially. The lubricant film was rapidly reduced when the experiments were realized under pure sliding. As expected, the lowering of contact pressure led to a thicker film.

Fan et al. (2011) focused on the role of proteins contained in model fluid, while using simple solutions of albumin, γ-globulin and BS. The real femoral CoCrMo head was used as a stationary component sliding against a glass disc. The effect of sliding speed was observed; showing that, in general, the simple protein solutions formed a thicker film compared to BS. The data were in a good agreement with the previously published results (Mavraki and Cann, 2009, 2011). Especially at a lower sliding sped the film thickness increased due to hydrodynamic effect. The knowledge about the contribution of the particular proteins was later extended by Myant et al. (2012) who employed the same experimental configuration (CoCrMo head vs. glass disc). Firstly, the static test was performed to find the relation between the type of protein and the adsorbed film concluding that γ-globulin formed a thicker film than BS and the thinnest film was formed by albumin solution, while there was no significant effect of the protein concentration.

The theory about protein lubrication was enhanced by Myant and Cann (2013), who focused on the aggregation of proteins in front of the contact zone. This substance, influencing the lubricant film, was called “inlet phase”, while a good agreement between the length of the inlet phase and central film thickness was found. The lubrication mechanisms confirmed the conclusions given previously by Fan et al. (2011). It was proved that the lubricant film is affected by the adsorbed protein layer supported by high-viscosity film due to the hydrodynamic effect. At low speeds, the aggregated proteins pass through the contact thus increasing the lubricant film. When the speed increases, the layer exhibits a shear thinning behaviour; therefore, the film thickness is reduced. Since the measured data were substantially higher compared to theoretical predictions, it can be concluded that protein lubrication does not correspond to classical elastohydrodynamic lubrication (EHL) mechanisms.

Vrbka et al. (2013) conducted the study with both, metal and ceramic heads to clarify the effect of material on protein film thickness. The experiments were realized under different speeds and slide-to-roll ratios (SRR), and the film thickness was investigated as a function of time; rolling/sliding distance. The contact was lubricated by BS. Independently of kinematic conditions, the film thickness was always higher in the case of metal component. As it was demonstrated that the kinematic conditions substantially affect the protein film and considering some implications, such as the effect of surface conformity, in the following paper, the authors changed the experimental configuration from a non-conformal ball-on-disc to a more conformal ball-on-lens (Vrbka et al., 2014). The purpose of the change of experimental setup was to approach the condition in the real joint where the contact is highly conformal. The higher conformity leads to a lower contact pressure, which can positively affect the protein film. The measurements were realized under pure negative sliding (glass lens was kept stationary). It was shown that the character of film formation is different compared to the ball-on-disc configuration. Immediately after starting the test, the protein film increased. After a short time, it started to slightly decrease and was stabilized dependently on the sliding speed. In the reference, it was also pointed out that the lubricant film can be influenced by the surface wettability. The authors showed that the hydrophobic nature of surface supports the protein adsorption. On the other hand, if the surface is naturally hydrophilic, the thick protein film cannot be formed. As it was clearly shown that the surface conformity had a substantial effect on the protein film; in the follow-up study, we developed a new hip joint simulator based on the principle of pendulum where the real conformity of rubbing surfaces is ensured (Vrbka et al., 2015b). The central film thickness was measured between the metal femoral head and the glass acetabular cup fabricated

according to the dimensions of real cups. The character of protein film was similar to that of the ball-on-lens results obtained in the previous study. The lubricant film was relatively thick at the beginning of the experiment. After a few seconds, it started to gradually decrease and was stabilized, while there was no significant change until the end of the test.

Myant and Cann (2014b) investigated the effect of the motion character on protein lubricant film. Although Vrbka et al. (2015b) were able to apply swinging (flexion–extension) motion on the pendulum simulator, most of the previous papers considered just unidirectional motion which does not correlate with the motion of real joints. However, it was presented that the motion character can substantially influence the protein film, especially when the reversing motion is taken into account (Myant and Cann, 2014b). In that case, the film was reduced to approximately one third compared to unidirectional motion. Moreover, there was no inlet gel-like phase of proteins in front of the contact, observed in previous studies (Fan et al., 2011; Myant and Cann, 2013).

In the previous papers, the authors sufficiently described the effect of various parameters on protein film formation. However, there was no study enabling the assessment of the role of particular proteins while the simultaneous presence of another protein. All the implications about the role of proteins were derived from the results of experiments performed with simple protein solutions. The initial study discussing the role of proteins in complex fluid was introduced by Necas et al. (2015a). For this purpose, the film thickness measurements by optical interferometry were supported by the fluorescent microscopy which enabled us to focus on one particular constituent independently of the other parts of model fluid. Although it was pointed out that the conformity, as well as the motion character, influences the protein film, the experiments were realized on ball-on-disc apparatus, since one of the main goals was to establish a novel experimental approach. For this purpose, the comparison of the results with previously published data was necessary. The authors focused on the metal femoral head and the measurements were realized under various speeds and SRR. It was observed that under pure rolling and positive sliding conditions, the film was formed predominantly due to the presence of albumin. This was in discrepancy with the data published elsewhere (Myant et al., 2012). However, as mentioned above, Myant et al. (2012) employed simple protein solutions while in our study the mixture of proteins was considered. This indicates that the complexity of model fluid must be taken into account when investigating the protein lubrication mechanisms.

From the literature review, it can be assumed that the ball-on-disc experimental setup in combination with optical methods can help to better understand the lubrication mechanisms within hip replacements. The optical interferometry is a suitable method for precise film thickness measurement. Supplementing the experimental programmes with the method based on the fluorescent microscopy enables to assess the role of particular constituents of model fluids independently of its composition. Most of the researchers focused on the description of protein film formation in the contact between the metal femoral head and the glass counterface. However, little is yet known about film formation while considering the ceramic materials. Vrbka et al. (2013, 2014) conducted some experiments with ceramic head; however, so far there is no study about the role of proteins while investigating ceramic material. Therefore, the aim of the present paper is to employ the experimental approach introduced in our previous paper (Necas et al., 2015a) and describe the role of albumin and γ-globulin on the lubricant film formation between ceramic femoral head and glass disc.

2. Materials and methods

Protein film measurements were realized on the previously introduced ball-on-disc tribometer (Necas et al., 2015a). The ball and the disc have its own servomotors; therefore, both components can be driven independently and various speeds and SRR can be applied. The circular contact between the test samples is observed using a microscope. A mercury lamp was used for illumination and the tests were recorded by high speed cameras. The scheme of the applied experimental approach is shown in Fig. 1a.

To be able to determine the role of particular proteins, two optical methods were applied. Initially, the film thickness was measured by thin film colorimetric interferometry (Hartl et al., 2001), since it was shown that this method allows to measure the film thickness with very high accuracy and resolution down to 1 nm. For recording the experiment, a complementary metal-oxide semiconductor (CMOS) high speed camera (Phantom V710) was used. The evaluation is based on matching the captured interferograms with calibration curve obtained for the lightly loaded static contact. The calibration provides the information about the dependence between the colour and the corresponding film thickness. Then, the thickness in arbitrary pixel of interferograms can be determined. Since the interference of light should be as contrasting as possible, the glass disc is covered with an additional, very thin chromium layer. When considering the principle of this method, it provides the information about the size of the gap between two surfaces based on the interference of light. Therefore, it is not possible to distinguish the constituents of the lubricant. For this purpose, fluorescent microscopy is used. This method gives the information about the amount of fluid inside the contact (Reddyhoff et al., 2010). As there is a linear dependence between the fluorescent intensity and film thickness (Azushima, 2006), the intensity can be considered as a dimensionless film thickness. Therefore, when the suitable fluorescent marker is used for staining the proteins, the particular proteins can be observed along with the other proteins that can be contained in the fluid at the same time. The principle of the fluorescent method is shown in Fig. 1b. In this case, a scientific complementary metal-oxide semiconductor (sCMOS) camera (Andor NEO) was employed. As was mentioned in the previous study (Necas et al., 2015a), the glass disc is not coated with a chromium layer when fluorescent microscopy is used. This is due to the quenching effect of the chromium layer which significantly reduces the intensity of fluorescence and the results become more scattered. Several experiments were conducted with coated glass disc revealing that the tendency of curves representing the

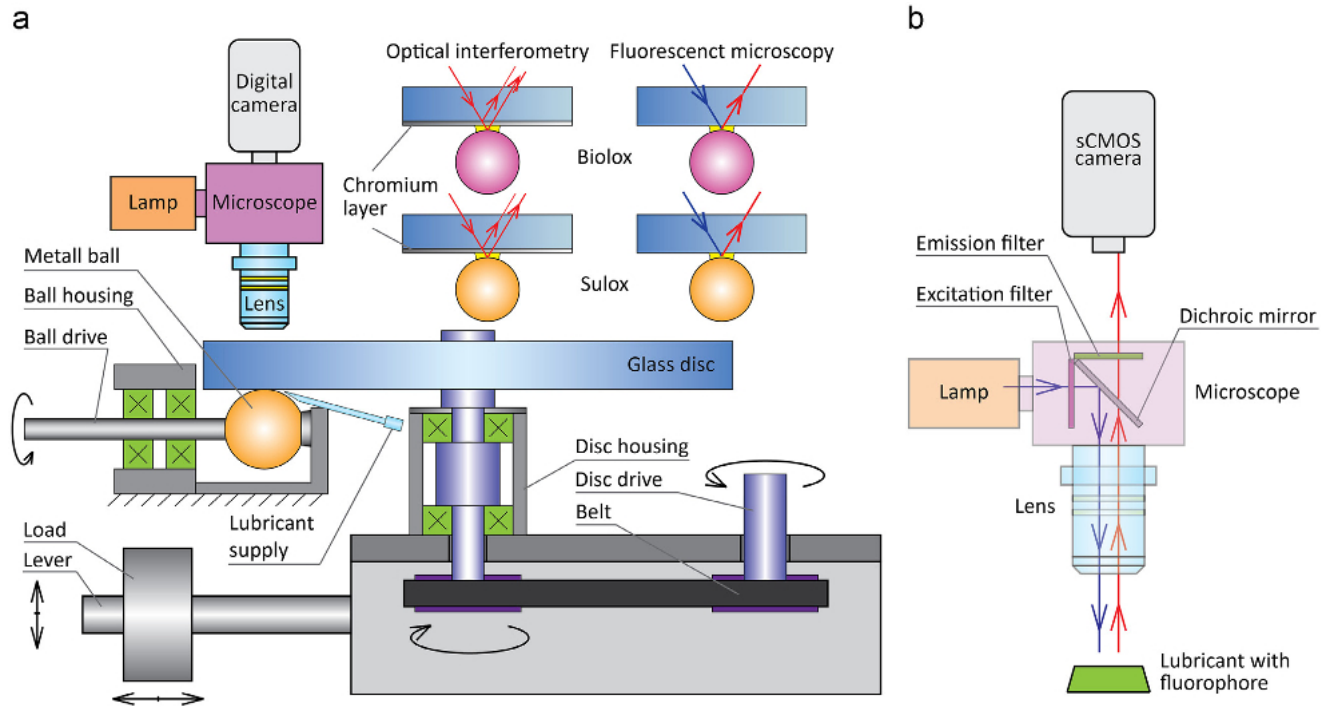

Fig. 1 – a) Scheme of the applied experimental approach. b) Principle of the fluorescent microscopy.

fluorescent intensity is very similar; therefore, the coating layer does not influence the protein film formation.

To be able to provide complex information about the protein film formation, two different ceramic materials were investigated; Sulox^{TM} (Al_2O_3) and BIOLOX$^{®}$*delta* (75% Al_2O_3, 24% ZrO_2, Cr_2O_3), respectively. In the following text, the materials are assigned as Sulox and Biolox only. Both materials are produced by Zimmer, Inc. As a counterface, a transparent disc made from optical glass BK7 was employed. Prior to experiments, the topography of the surface was measured using the optical method based on phase shifting interferometry (Bruker Contour GT X8). Five different points were analysed, one on the canopy of the head and the other four close to the expected contact drag. The results of the roughness measurement are as follows:

Sulox: $Ra_{can}=8.95$ nm, $Ra_1=10.52$ nm, $Ra_2=10.84$ nm, $Ra_3=9.43$ nm, $Ra_4=12.06$ nm.

Biolox: $Ra_{can}=16.70$ nm, $Ra_1=15.24$ nm, $Ra_2=15.20$ nm, $Ra_3=15.47$ nm, $Ra_4=14.78$ nm.

As a model of SF, solution of proteins in phosphate-buffered saline (PBS) was used. Each of the proteins (albumin; γ-globulin) was doped by an appropriate fluorescent marker. Although the different markers can exhibit different efficiency of fluorescence, it should be emphasised that in the present study, the conditions, such as excitation intensity and exposure time, are set to obtain the same intensity at the beginning of the experiment. The results represent just the comparison of the two curves corresponding to the development of albumin and γ-globulin protein film. According to experience from the previous study, albumin was stained by rhodamine-B-isothiocyanate (Sigma-Aldrich 283924) and γ-globulin was marked by fluorescein-5-isothiocyanate (Sigma-Aldrich F7250). The ratio A:G was equal to 2:1, while the protein concentration was 7 mg/ml, and 3.5 mg/ml, respectively. Therefore, the total protein concentration was 10.5 mg/ml. To be able to distinguish the proteins, solutions of non-stained proteins of the same concentration were also prepared. After preparation, all the samples were deeply frozen to −22 °C and were removed from the freezer 2 h prior to testing to avoid any temperature shock during a thawing process. Lubricant was supplied in front of the contact with the speed of 3.5 ml/min for 3 min; duration of each entire test was 5 min. The cleaning process before the test consists of cleaning all the components in 1% sodium dodecyl sulphate solution, rinsing in distilled water, drying by pressed air and washing in an isopropyl alcohol.

It is evident that the contact pressure in ball-on-disc configuration is considerably higher compared to ball-on-cup setup. Therefore, the applied load should be as low as applicable to approach contact pressures presented in the real joints. To ensure sufficient stability of the test device, the minimum applicable load was 5 N, resulting to maximum contact pressure equal to 280 MPa. Human joints operate in the wide range of speeds and loads over the gait cycle. To be able to determine the effect of speed on lubricant film, the protein film formation was investigated under two different speeds, $u_1=5.7$ mm/s, $u_2=22$ mm/s, respectively. As the ball and the disc, can be driven independently, the measurements were conducted under pure rolling (SRR=0), partial negative sliding (SRR=−1.5) and partial positive sliding (SRR=1.5). All the tests were realized under the ambient temperature $T=22$ °C. In relation to human body, it is desirable to consider the temperature. However, as previously published, the increase of temperature to 37 °C did not substantially influence the results (Mavraki and Cann, 2011). A summary of all the performed experiments is provided in Table 1.

Table 1 – Summary of the experiments (OI=optical interferometry, FM=fluorescent microscopy).

Optical method	Ball material	SRR	Disc speed (mm/s)	Ball speed (mm/s)	Mean speed (mm/s)	Model fluid
OI	Sulox; Biolox	0	5.7	5.7	5.7	A:G=2:1
OI	Sulox; Biolox	0	22	22	22	A:G=2:1
OI	Sulox; Biolox	−1.5	1.425	9.975	5.7	A:G=2:1
OI	Sulox; Biolox	−1.5	5.5	38.5	22	A:G=2:1
OI	Sulox; Biolox	1.5	9.975	1.425	5.7	A:G=2:1
OI	Sulox; Biolox	1.5	38.5	5.5	22	A:G=2:1
FM	Sulox; Biolox	0	5.7	5.7	5.7	Labelled A: Non-labelled G=2:1
FM	Sulox; Biolox	0	5.7	5.7	5.7	Non-labelled A: Labelled G=2:1
FM	Sulox; Biolox	0	22	22	22	Labelled A: Non-labelled G=2:1
FM	Sulox; Biolox	0	22	22	22	Non-labelled A: Labelled G=2:1
FM	Sulox; Biolox	−1.5	1.425	9.975	5.7	Labelled A: Non-labelled G=2:1
FM	Sulox; Biolox	−1.5	1.425	9.975	5.7	Non-labelled A: Labelled G=2:1
FM	Sulox; Biolox	−1.5	5.5	38.5	22	Labelled A: Non-labelled G=2:1
FM	Sulox; Biolox	−1.5	5.5	38.5	22	Non-labelled A: Labelled G=2:1
FM	Sulox; Biolox	1.5	9.975	1.425	5.7	Labelled A: Non-labelled G=2:1
FM	Sulox; Biolox	1.5	9.975	1.425	5.7	Non-labelled A: Labelled G=2:1
FM	Sulox; Biolox	1.5	38.5	5.5	22	Labelled A: Non-labelled G=2:1
FM	Sulox; Biolox	1.5	38.5	5.5	22	Non-labelled A: Labelled G=2:1

3. Results

3.1. *Pure rolling conditions*

The initial experiments were realized under pure rolling conditions. It can be seen in Figs. 2 and 3 that the film thickness gradually increases independently of ceramic type. Sulox ceramic shows almost a linear increase of the lubricant layer at lower speed, see Fig. 2a. The film reaches only around 14 nm at maximum. A higher speed leads to a steeper increase of the film thickness during the first 50 s of the experiment. The total film thickness is higher, in particular around 21 nm. In relation to fluid constituents, it is clear from the images of the contact zone (Fig. 2) that mainly albumin contributes to the increase of layer thickness for both speeds. However, even the γ-globulin film is considerable, especially during the last third of the experiment, where the albumin layer does not increase as quickly as the film thickness.

In the case of Biolox ceramic, the following character of film formation was observed (Fig. 3). Initial increase of film thickness lasted approximately 150 s at lower and 200 s at higher speed.

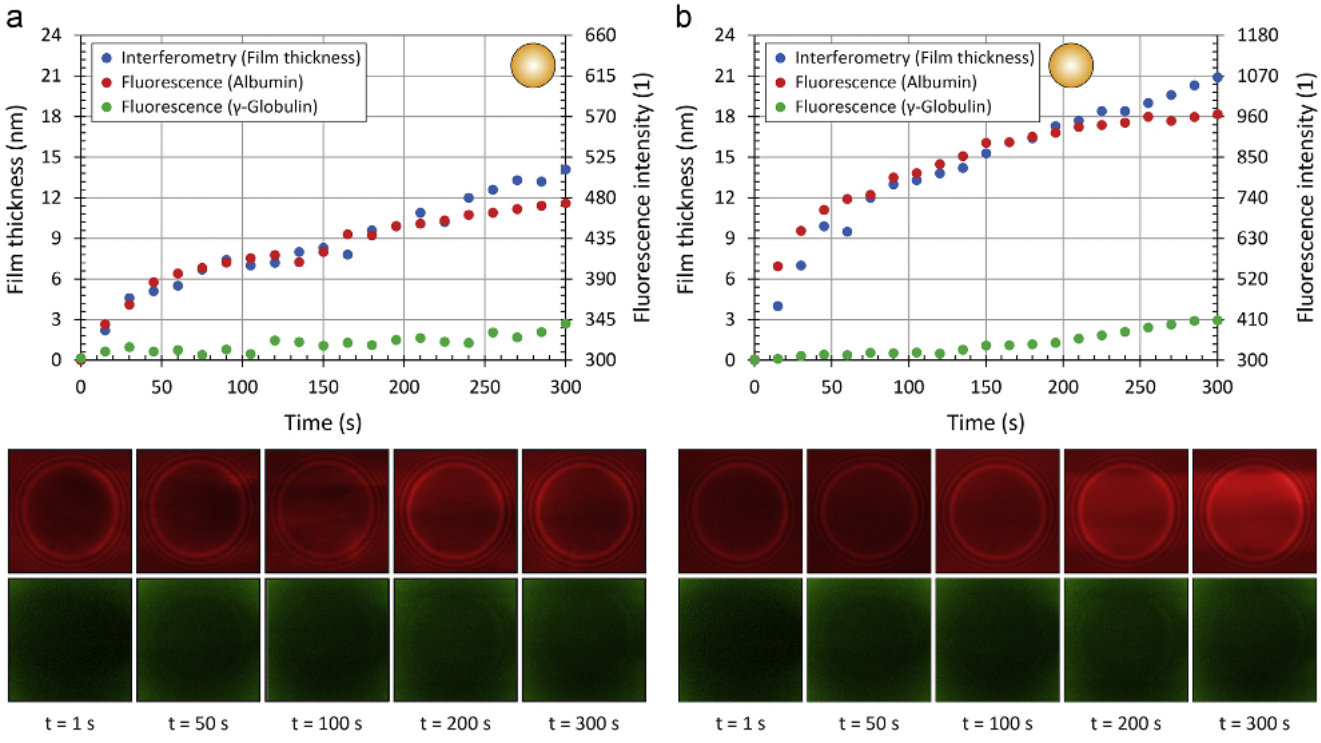

Fig. 2 – Sulox – development of film thickness and fluorescence intensity of labelled proteins as a function of time; fluorescent images of protein film in the contact zone (top – albumin, bottom – γ-globulin) under pure rolling conditions for different mean speeds; a) 5.7 mm/s; b) 22 mm/s.

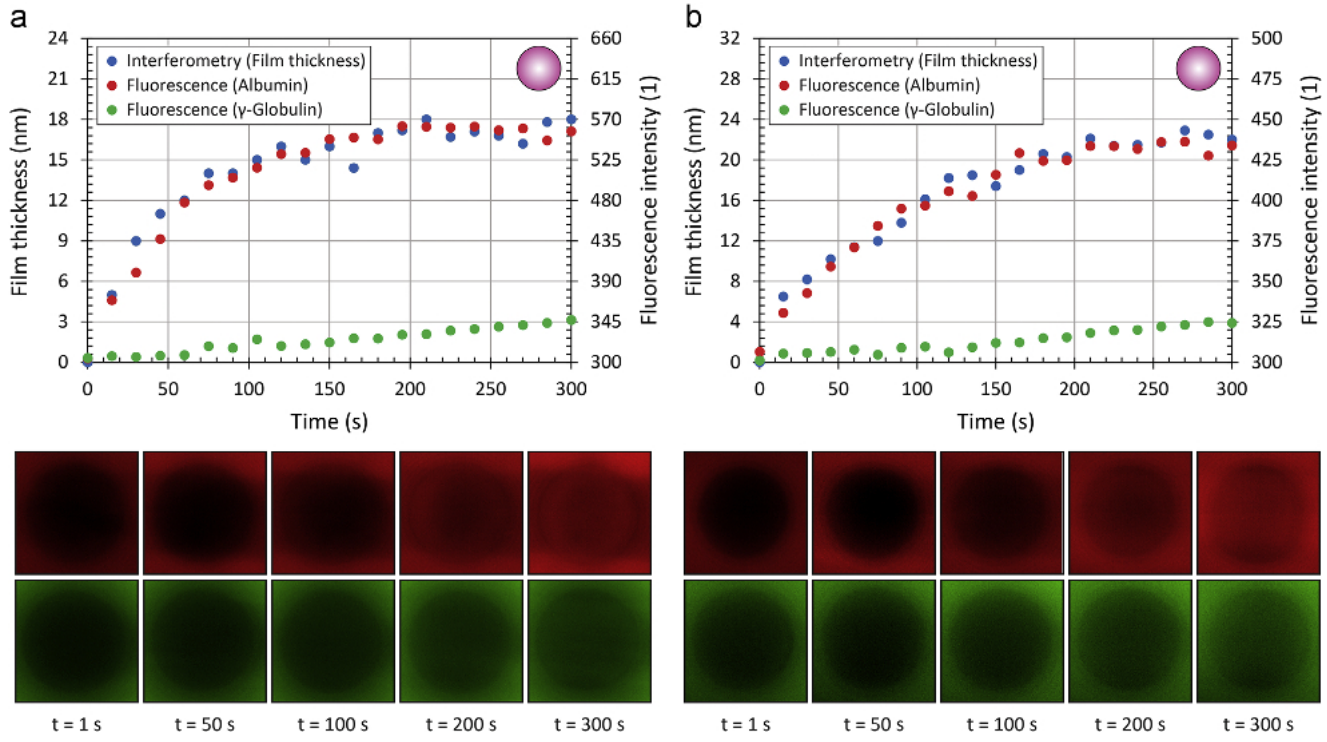

Fig. 3 – Biolox – development of film thickness and fluorescence intensity of labelled proteins as a function of time; fluorescent images of protein film in the contact zone (top – albumin, bottom – γ-globulin) under pure rolling conditions for different mean speeds; a) 5.7 mm/s; b) 22 mm/s.

After that, the film was relatively stable; 17 nm for 5.7 mm/s and around 22 nm for 22 mm/s. Protein development corresponds to the behaviour observed in the case of Sulox ceramic. Again, albumin is a dominant constituent. It must be highlighted that it is not possible to assign the fluorescence intensity directly to the layer thickness. The intensity axis is set to correspond to the curves of film thickness. Actually, the fluorescence intensity is influenced by the surface of the ball, as discussed below, i.e. a different type of ceramic can have a different effect on the intensity of fluorescence emission. Nevertheless, the most important information is the tendency of the curves describing the fluorescence intensity. When the intensity of albumin layer increases considerably against the initial value compared to the intensity of γ-globulin, it is considered that it corresponds to the development of the protein layer due to the principle of linearity (Azushima, 2006).

3.2. *Partial negative sliding*

It is evident that pure rolling conditions do not correspond to the physiological state. In the human body, the acetabular cup is a stationary component and the femoral head performs a multi-directional rotating motion. Therefore, the interaction between the components can be considered as pure negative sliding. Pure sliding in the case of ball-on-disc configuration is very severe and leads to substantial damage of tested components. Therefore, in the conducted experiments, only partial negative sliding (SRR= −1.5) was applied. In contrast to pure rolling, the development of film thickness is very complex and differs according to the used material. The results for Sulox ceramic are shown in Fig. 4. Independently of sliding speed, the tendency is similar – the lubricant film increases during the first half of the test. When the speed was 5.7 mm/s, the maximum measured film thickness was around 18 nm. After reaching the maximum, the film steeply decreases between 150 and 200 s and then becomes stabilized around 8 nm. Very interesting is the behaviour of proteins in this case. As is clear from the intensity curves, the film is formed by a combination of albumin and γ-globulin, while γ-globulin is the dominant constituent for the most of the time. Increasing the sliding speed led to a change of film formation during the second half of the test. In this case, the film started to gradually decrease after reaching a maximum thickness of 45 nm (Fig. 4b). In terms of proteins, γ-globulin film is very thin and stable; however, the albumin tendency is very close to the film thickness development.

In the case of Biolox ceramic, film thickness and albumin formation is comparable to Sulox results; however, the γ-globulin tendency is opposite at lower sped. As can be seen in Fig. 5a, film thickness is kept between 6 and 12 nm. Although the change of the fluorescence intensity is almost negligible, it is apparent that albumin is the dominant protein (Fig. 5a). At higher speed (Fig. 5b), a rapid increase of γ-globulin can be observed at the beginning of the test causing an immediate increase of film thickness to approximately 12 nm during the first few seconds. Then γ-globulin starts to decrease, while the albumin intensity increases. In general, the role of proteins is similar to that of Sulox. Again, the albumin is mainly responsible for the total thickness, which is around 20 nm at maximum.

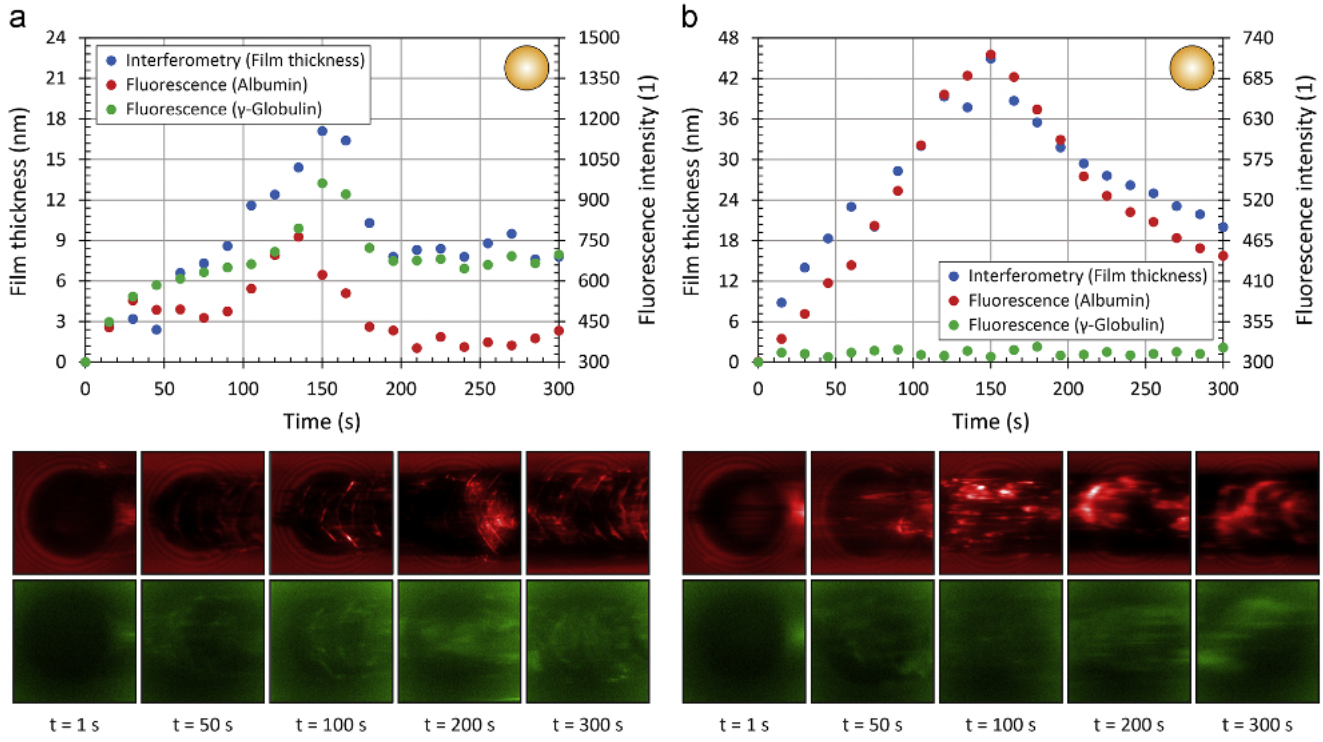

Fig. 4 – Sulox – development of film thickness and fluorescence intensity of labelled proteins as a function of time; fluorescent images of protein film in the contact zone (top – albumin, bottom – γ-globulin) under partial negative sliding for different mean speeds; a) 5.7 mm/s; b) 22 mm/s.

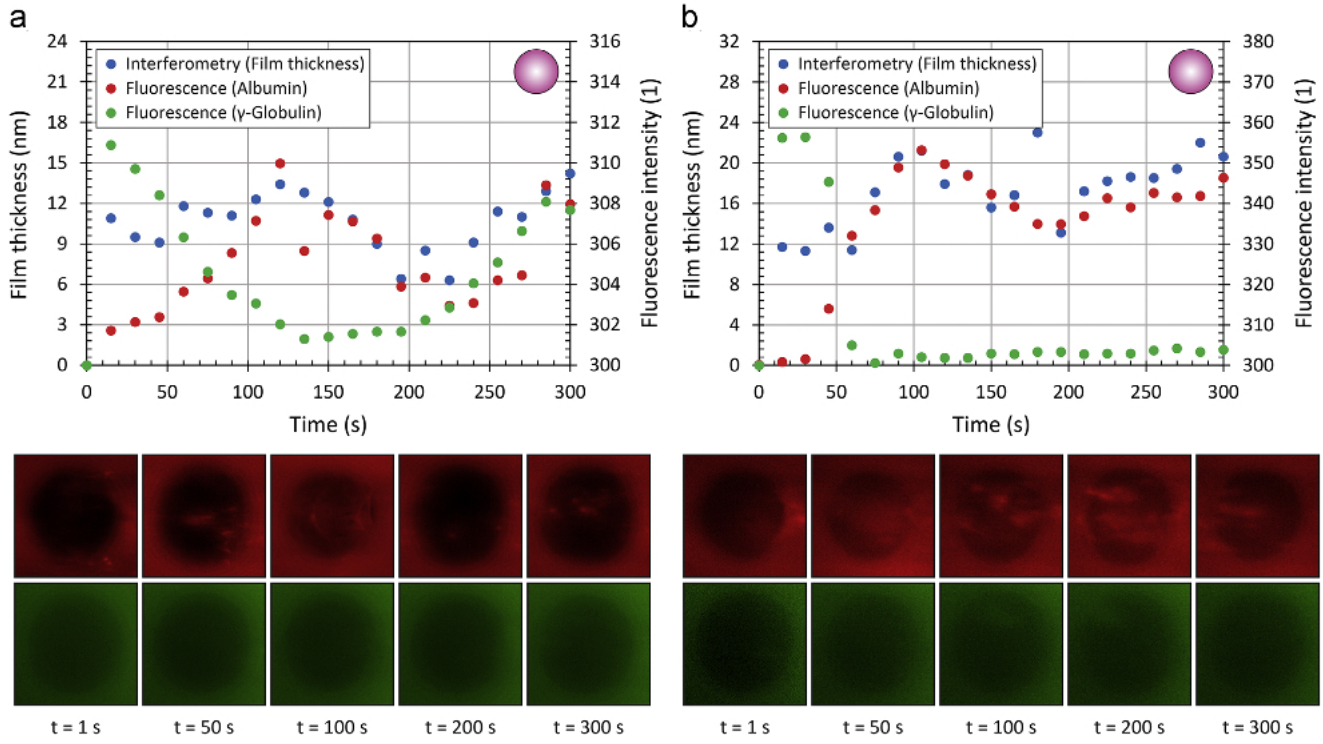

Fig. 5 – Biolox – development of film thickness and fluorescence intensity of labelled proteins as a function of time; fluorescent images of protein film in the contact zone (top – albumin, bottom – γ-globulin) under partial negative sliding for different mean speeds; a) 5.7 mm/s; b) 22 mm/s.

3.3. *Partial positive sliding*

To get a better idea about the behaviour of protein film, considering some slippage between the surfaces, the measurements were also conducted under partial positive sliding (SRR=1.5). In the previous cases, the film thickness was not higher than 25 nm. In this case, for Sulox ceramic, the lubricant film reached more than 150 nm after approximately 150 s at the speed of 5.7 mm/s, see Fig. 6a. It was followed by a gradual decrease of lubricant film to 100 nm at the end of the test. It is

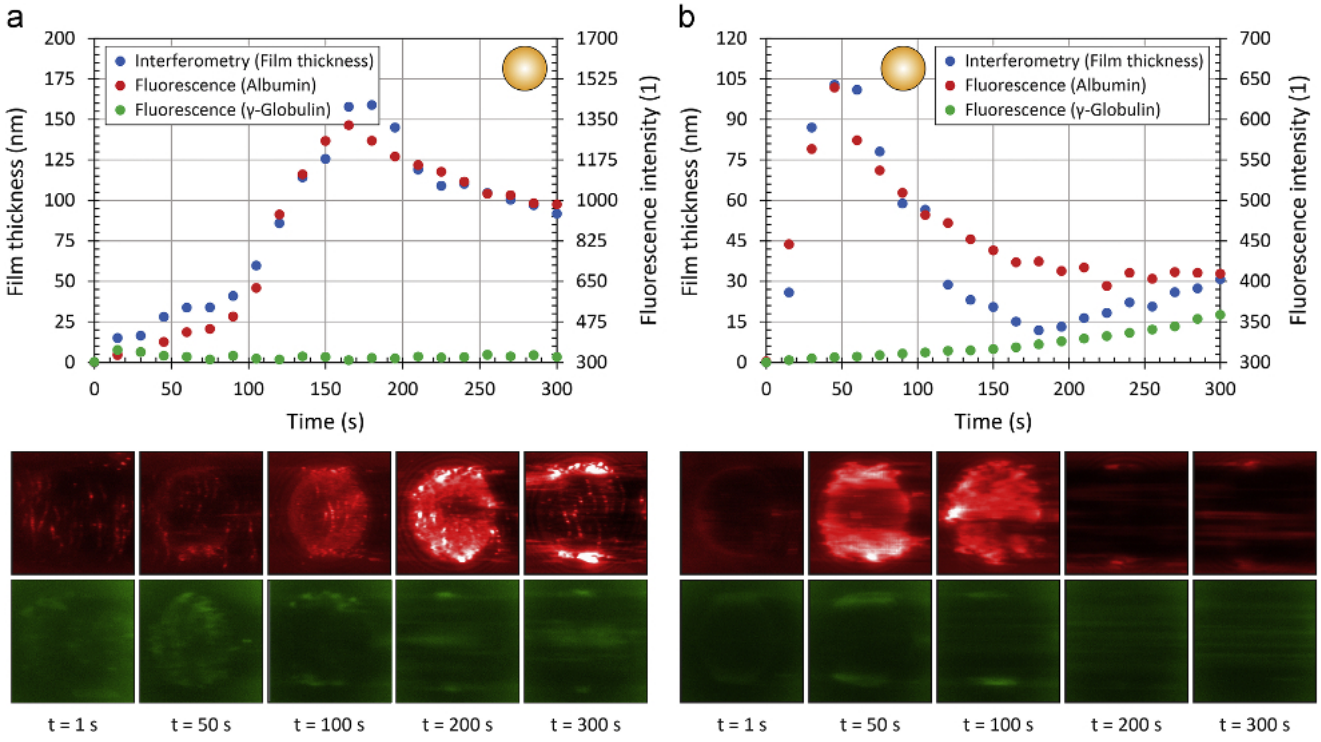

Fig. 6 – Sulox – development of film thickness and fluorescence intensity of labelled proteins as a function of time; fluorescent images of protein film in the contact zone (top – albumin, bottom – γ-globulin) under partial positive sliding for different mean speeds; a) 5.7 mm/s; b) 22 mm/s.

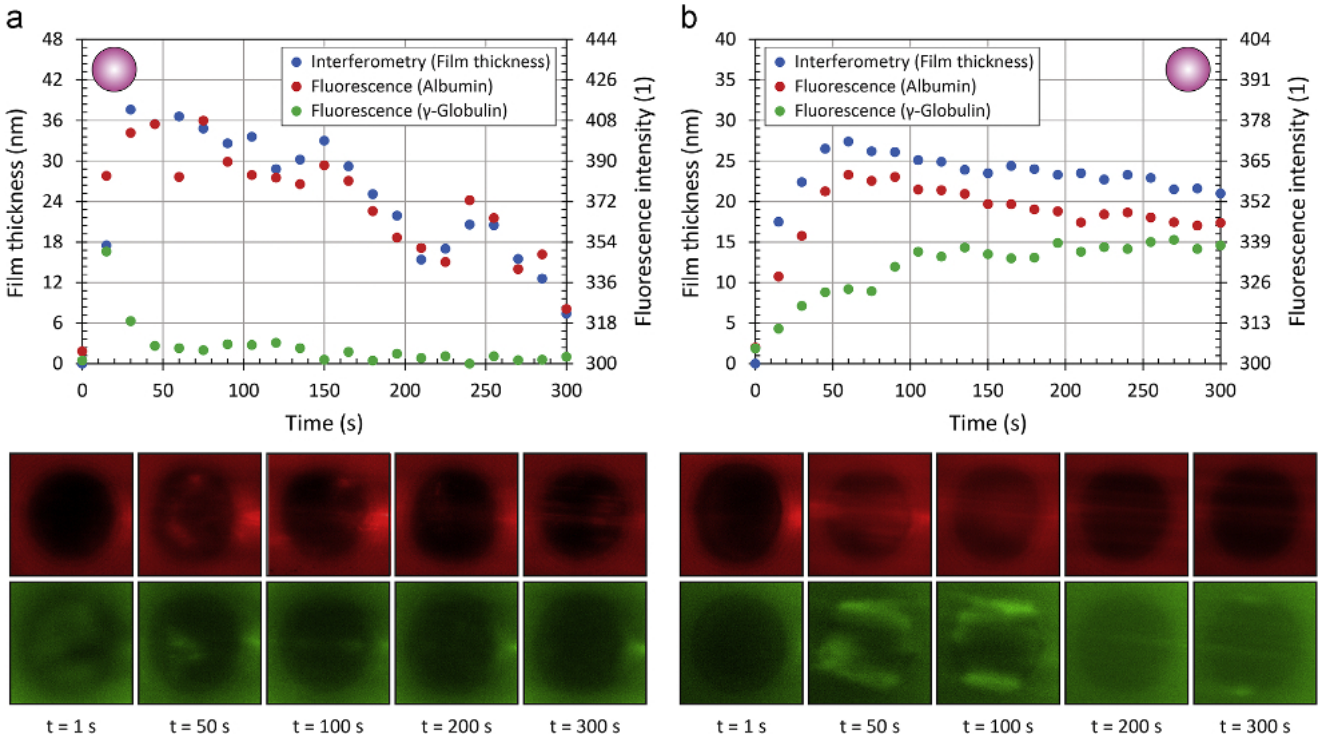

Fig. 7 – Biolox – development of film thickness and fluorescence intensity of labelled proteins as a function of time; fluorescent images of protein film in the contact zone (top – albumin, bottom – γ-globulin) under partial positive sliding for different mean speeds; a) 5.7 mm/s; b) 22 mm/s.

apparent from the images of the contact zone that the effect of γ-globulin on film thickness is negligible at lower speed. In general, the increase of speed did not have an effect on the protein film behaviour; however, the time before reaching the maximum value is significantly shorter. Maximum film thickness is not so high (≈ 100 nm), but still higher compared to other experimental conditions. The film thickness again decreases with increasing time; however, after some time, it again starts to slightly increase. From the graph in Fig. 6b, this is in a good correlation with proteins behaviour. Although the level of albumin intensity is almost stable during the second half of the test, γ-globulin starts to increase approximately in the middle of the experiment, causing the total thickness to increase.

Biolox ceramic showed the following character of film formation; at low speed, there is a rapid increase of film thickness in less than 30 s after the beginning of the test (Fig. 7a). Maximum film thickness is around 40 nm and the lubricant film gradually decreases for the rest of the experiment. Although the intensity of γ-globulin firstly shows a steep increase, it decreases to a very low and stable level from the second minute of the measurement. As in the case of Sulox, the albumin film corresponds very well with the development of film thickness. When the speed is 22 mm/s, formation of film thickness is similar compared to that at a lower speed, see Fig. 7b. However, the role of proteins is a different; in this case, even γ-globulin substantially contributes to film thickness. As the film has a tendency to a decrease (the same as that of albumin intensity), it can be concluded that the effect of albumin film is dominant in relation to the global behaviour of film thickness.

3.4. *Film thickness – summary*

In general, Sulox ceramic forms a thicker lubricant film under most conditions. While the maximum film thickness measured for Biolox ceramic was less than 40 nm, for Sulox ceramic, it was almost four times higher. As can be seen in Fig. 8, the film formation within artificial hip joints is strongly dependent on kinematic conditions. A rolling/sliding distance is also a crucial parameter. Under pure rolling conditions, the film thickness gradually increases independently of material with no significant scatter in results. When the ball speed is higher, there can be observed an increase of film thickness during the first half of the test followed by a decrease during the second half in most cases. The most significant difference in film formation was observed under positive sliding. For Sulox ceramic, a rapid increase of film followed by the gradual decrease was detected. As can be seen, especially at higher speed, in the case of Biolox (Fig. 7b), a decrease of film thickness after reaching the maximum was not as steep as that of Sulox (Fig. 6b); however, it should be mentioned that even the maximum film thickness was substantially lower compared to Sulox; approximately one fourth at lower and one third at higher speed.

4. Discussion

Under pure rolling conditions, the film thickness increased with time/rolling distance independently of ceramic type, as it is clear from Figs. 2 and 3 The maximum central film thickness varies in a range from 15 to 23 nm, which is in a very good agreement with the previously published results (Vrbka et al., 2013). The authors used BS as a test lubricant with the protein content equal to 22.4 mg/ml. In the present paper, the protein concentration was just 10.5 mg/ml. According to a good correlation of the data, it is evident that the protein content is not as significant as in the case of metal femoral head (Necas et al., 2015a). These phenomena can be attributed to the contribution of proteins. In the case of metal head, there was almost a negligible increment of γ-globulin. On the contrary, both ceramic heads showed that even if albumin is the dominant part of the fluid, the γ-globulin level also increased during the test. Dosing of the lubricant lasted for 180 s of the experiment while there is no clear effect of stopping the dosing on lubricant film. When the test was completed, the intensity of both proteins was very low. Therefore, it can be concluded that the adsorbed protein layer remaining on the surfaces is very thin, in the range of units of nm. Further increase of film during the experiment is caused especially by the hydrodynamic effect, while the layer is homogeneous with no gel-like protein clusters previously observed by Fan et al. (2011). The results of protein film do not fully agree with the data published by Myant et al. (2012) or Parkes et al. (2015), who used simple protein solutions to find out the lubrication mechanisms inside the metal-on-metal

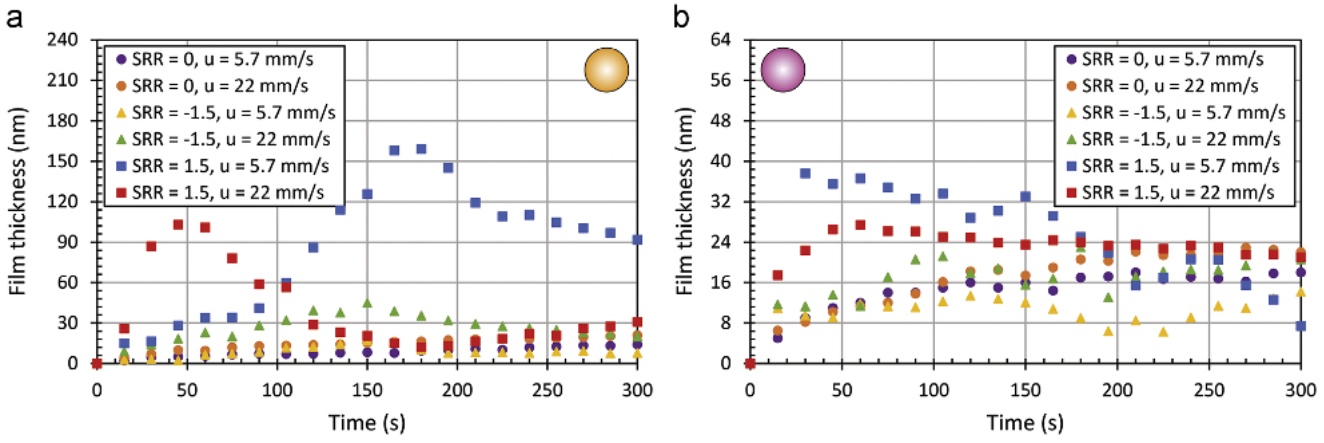

Fig. 8 – Comparison of film thicknesses under various operating conditions. a) Sulox; b) Biolox.

contact pair. It was found that γ-globulin solutions formed much thicker film compared to albumin solution. Although in the mentioned studies the authors employed a metal head, it generally supports the idea that it is essential to incorporate more constituents than just one specific protein into the lubricant.

Considering the slip between the surfaces led to different character of film formation. Under negative sliding, a sliding speed was an important parameter. Sulox ceramic exhibited a combined increasing/decreasing tendency while the film started to fall when the supplementation of the lubricant in front of the contact zone was stopped. The interesting fact is that the metal head showed an extremely thin protein film under the same operating conditions with the same lubricant (Necas et al., 2015a). Only when the speed increased, the lubricant film started to increase after some time as a consequence of adsorption of γ-globulin on the glass disc. This was attributed mainly to kinematic conditions; the speed of the head is higher compared to the disc speed causing the rotating head to disrupt the protein film and disable it to be fully developed (Necas et al., 2015a). Both ceramic heads showed a similar thickness compared to pure rolling with the exception of higher speed and the Sulox head, when the film thickness was almost two times higher, around 45 nm. It can be seen on the bottom part of Fig. 4a that the lubricant film is not homogeneous for Sulox. The film is formed especially due to protein clusters passing through the contact. The adsorbed layer detected at the end of the experiment was more than 10 nm; however, it was not uniformly attached to the rubbing surfaces; only the agglomerations of the proteins could be observed. From the above mentioned, it is expected that the ceramic surface shows stronger bonds with the proteins then metal. Although, in general, Vrbka et al. (2013) observed a thinner film for ceramic head, the authors used BS with unknown ratio of the contained proteins. If the content of γ-globulin in BS would be substantially lower than the content of albumin, the film could not be fully developed, since γ-globulin is, based on the current results, more important constituent. Even for Biolox ceramic, a similar behaviour could be observed for both tested speeds. The film increased immediately after the beginning of the experiment and reached around 10 nm. As can be seen in the graph in Fig. 5, this increase is caused by the presence of γ-globulin. Another increase of the lubricant film is attributed to the increment of albumin layer. After reaching the maximum, the thickness is around 10 nm for 5.7 mm/s and 18 nm for 22 mm/s, respectively. It is very complicated to assess the results of film thickness in terms of friction. However, Brockett et al. (2007) performed in vitro testing of friction rate using a hip simulator for different material combinations. The arrangement allowed rotation of the head while the cup was stationary. The results showed a remarkably lower friction for ceramic-on-ceramic than for metal-on-metal sliding pair. A similar trend of the coefficient of friction was introduced also by Vrbka et al. (2015a), who measured friction within hip replacements using the pendulum hip joint simulator, while the contact was lubricated by BS. The mentioned results are in a good correlation with the results of present and previous studies. When the metal head was investigated (Necas et al., 2015a), the lubricant film was negligible under negative sliding, which can cause an increase of friction. On the contrary, both ceramic heads showed the protein film from 15 to 45 nm ensuring a reduction of friction between the components.

Under positive sliding, a similar character of film formation, compared to the metal head (Necas et al., 2015a), was observed for Sulox. Moreover, the tendency corresponds to the results provided by Vrbka et al. (2013), who employed the head from the same material. As can be seen in Fig. 6, film thickness gradually increases, while the time before reaching the maximum is affected mainly by time/sliding distance. The total film thickness is considerably thicker compared to the previous results, more than 150 nm for lower and more than 100 nm for higher speed. Images of the contact zone representing the development of individual proteins corresponded very well to the film thickness curve (see the bottom of Fig. 6). At lower speed, the intensity of γ-globulin increased during the first 30–50 s and then it remained at very low level until the end of the test. The increase of albumin intensity correlates with the tendency of lubricant film, so it can be clearly concluded that albumin plays a dominant role. A very similar behaviour can be observed even for higher speed. The only difference is that during the second half of the experiment, γ-globulin starts to increase thus leading to a gradual increase of the film thickness. Biolox ceramic showed more scattered results under positive sliding with no significant effect of sliding speed. At lower speed, both proteins started to increase rapidly after the beginning of the test; γ-globulin dropped to a low level after very short time, see Fig. 7a. As in the case of Sulox, albumin development corresponded to the total lubricant film, indicating its importance during the film formation process. Increasing the sliding speed led to a higher importance of γ-globulin film. As can be seen in Fig. 7b, after approximately 50 s, proteins agglomerations start to pass the contact zone, while the film becomes homogeneous in the last third of the experiment. This process can be attributed to the adsorption of proteins on the bottom surface of the glass disc. Under positive sliding, the speed of the disc is higher compared to the ball speed. Therefore, mainly at higher speed, the same point on the disc passes through the contact many times enabling the protein film to continuously increase. Nakashima et al. (2007) showed that albumin adsorption onto the rubbing surfaces is not as strong as that of γ-globulin. This can help to better understand the development of albumin film, which starts to slightly decrease with time after reaching the maximum, indicating that the total thickness was caused mainly by the hydrodynamic effect rather than the adsorption process.

Although it is not clear from the contact images, we were not able to observe the gel-like protein substance in front of the contact zone. The same behaviour was also detected in the previous paper (Necas et al., 2015a). The inlet phase described in literature (Fan et al., 2011; Myant and Cann, 2013) apparently does not relate with the ball material, since there is no clear reason which would affect what happens before the lubricant passes through the contact. More probably, the inlet phase phenomenon is connected with the lubrication conditions. In both references (Fan et al., 2011; Myant and Cann, 2013), the authors were able to fully bath the surroundings of the components. In the present study,

the lubricant was dosed continuously for three minutes just in front of the contact while a non-adsorbed lubricant dropped to the dish below the ball after passing the contact.

In an effort to describe the development of lubricant film, the adsorption effect plays a very important role (Malmsten, 1998; Parkes et al., 2014). It was previously published that both proteins rather adsorb onto hydrophobic surfaces (Malmsten, 1998). The wettability of rubbing surfaces was checked, finding that it is rather hydrophobic; therefore, the proteins are able to adsorb onto it. Moreover, it was discussed by Nakashima et al. (2007) that the γ-globulin adsorption ability is stronger. According to the above information, in author's opinion, γ-globulin forms a relatively thin layer on the rubbing surfaces and it allows albumin to adsorb on it forming a layer structure leading to the increase of total film thickness in most cases.

When considering the impact of lubrication on hip implants, the squeaking effect should be discussed as well. It was reported several times that especially ceramic–ceramic pairs suffer from squeaking, while the incidence of this phenomena is in the range from 1% to 10% (Jarrett et al., 2009). Although one of the factors influencing the squeaking effect can be the geometry of components (Keurentjes et al., 2008), other factors must be taken into account, such as: impingement, component malposition, edge loading, third-body particles (Walter et al., 2010). Especially the last point is strongly associated with the lubrication inside the contact. It was clearly shown by Brockett et al. (2013) that the squeaking can be substantially affected by the particles released from the surfaces during the articulation. Further research about the effect of fluid composition on lubrication mechanisms in hip replacements is necessary; however, it seems that a sufficient protein film separating the surfaces can contribute to minimisation of the risk of squeaking.

It is obvious that the present paper suffers from several limitations. As was introduced by Vrbka et al. (2014, 2015b), conformity of rubbing surfaces clearly influences the formation of protein film. The main reason is the contact pressure since it was shown that a lower contact pressure leads to a thicker film (Mavraki and Cann, 2011). A conformal contact such as human joint exhibits a remarkably lower contact pressure compared to the ball-on-disc setup. Nevertheless, it was introduced in the literature review that the ball-on-disc apparatus was employed several times in an effort to describe some fundamental phenomena connected with hip joint lubrication. Moreover, the only one already published paper describing the lubricant film thickness measurement under real conformity (Vrbka et al., 2015b) dealt with metal femoral head. As there is a very limited amount of studies considering the ceramic heads in relation to lubrication mechanisms, it was decided to employ a ball-on-disc device to be able to compare the data with already published results (Vrbka et al., 2013, 2014).

Another area of interest is the motion character during the test. As the movement of the joint is multidirectional, it is very hard to conclude that the above described mechanisms can fully explain what actually happens within the real hip replacements. Myant and Cann (2014b) already introduced that a simple unidirectional motion showed different results compared to the reversing character of motion. One of the reasons why we applied the unidirectional motion is the ability to compare our results with the results presented by other authors. The second point is that it would be very complicated to dose the lubricant from both sides of the contact to ensure a precise synchronization of motion direction and lubricant supply.

In relation to the multidirectional motion, the load is also transient and is strongly dependent on the conditions such as walking, running, stance phase, etc. Therefore, the load should not be constant over the experiment; it should correspond to the actual arrangement of the components when simulating some specific movement conditions. The ball-on-disc device does not allow changing the load abruptly during the experiment since the load is applied by putting the weight on the lever. For this purpose, it is necessary to develop a new loading system which could be fully controlled by the user.

It was already discussed that the complexity of the model fluid is essential when trying to describe the lubrication mechanisms corresponding to particular constituents. Although we employed the mixture of albumin and γ-globulin in PBS, other constituents such as hyaluronic acid or lipids, should be taken into account (Sawae et al., 2008). More constituents contained in lubricant will lead to the increasing number of experiment repetition. As was pronounced, even now, each experiment is repeated three times (film thickness measurement, intensity of albumin measurement, intensity of γ-globulin measurement). Therefore, a better solution is to find a suitable combination of fluorescent markers which do not influence each other and to observe all the components at the same time by using appropriate fluorescent filters.

The next area, which should be discussed, is the difference between the mechanical properties of optical glass and real acetabular components. It is evident that one of the components must be transparent to enable in situ observation of the contact area. Nowadays, in general, two groups of replacements are implanted. One group is represented by hard-on-hard bearing couples (e.g. ceramic-on-ceramic or metal-on-metal), where the modulus of elasticity is in the range of hundreds of GPa. Another group can be described as hard-on-soft. In this case, the acetabular cup is made from polyethylene (PE). The modulus of elasticity of PE is just around 2–3 GPa. Optical glass has the elasticity modulus around 85 GPa. As the stiffness of glass is considerably higher than that of PE, it is apparent that the presented results relate rather to hard-on-hard implants.

From the images of the contact zone (Figs. 2–7), it can be seen that under some conditions, considerable protein inhomogeneities pass through the contact apparently influencing the thickness of the protein film. It should be highlighted that the exposure time during the experiment was 0.0064 s, therefore 156 images were taken per one second of the experiment. All the images were checked by the algorithm giving the average value of the fluorescent intensity inside the circle which radius is equal to one fifth of the contact zone radius. Although the protein clusters can cause strong peaks in the detected intensities, only the images which intensity was in a good correlation with the global tendency, were used for the final evaluation. Therefore, the local errors due to massive proteins clusters passing through the contact were minimised. The same evaluation procedure was applied even in the case of film thickness measurement by optical interferometry.

Finally, the limitation of the applied method should be mentioned. A main disadvantage of the applied experimental approach is that the experiments must be repeated three times under the same operating conditions. One of the solutions might be determining the film thickness directly by fluorescent microscopy (Myant et al., 2010; Necas et al., 2015b). In the present paper, a direct measurement of film thickness by using fluorescent method was not allowed due to several phenomena.

a. The surfaces of the tested materials are highly reflective which causes the interference of light, even if the glass disc is not covered with a chromium layer. The interference avoids processing a precise calibration. The problem with light interference was already published by Sugimura et al. (2000). For calibration, the authors substituted the tested sample by the sample made from glass. However, it was later pointed out by Myant et al. (2010) that the different reflectivity of calibration and test samples can cause some irregularities in results.
b. The second point disabling the film thickness measurement by fluorescent method was that both tested ceramic materials emit fluorescence. Even if there was no fluorescent marker in the excited area, the surface emitted a low level of fluorescence. This goes against the CoCrMo heads tested in the previous paper (Necas et al., 2015a). In that case, the fluorescence intensity was lowered by the quenching effect of chromium (Jie et al., 1998). As in the case of the quenching effect, the self-emitting fluorescence effect does not substantially influence the results. The intensity is only slightly higher; however, the absolute values of intensity are not decisive for evaluation as it is based on the increase/decrease of intensity compared to the initial state.

Both methods exhibit very satisfactory reproducibility. The optical interferometry provides accurate measurement of the film thickness with the resolution down to 1 nm (Hartl et al., 2001). The reproducibility of the fluorescent method was checked in a greater detail in our previous study (Košťál et al., 2015). The contact between the ball and the disc was lubricated by mineral oil, while 20 images were captured with 1 s delay under the constant speed of both components, indicating that the same film thickness expressed by the fluorescent intensity should be obtained. The results showed that the maximal deviations against the mean value were from −2.6% to 2.9%.

5. Conclusion

The conclusion can be summarised into the following points:

1. From the results, it is apparent that the combination of the mentioned methods can extend the knowledge about the protein film formation in artificial hip joints considering the contribution of particular proteins.
2. As both proteins play an important role under most conditions, it is not suitable to study only simple protein solutions.
3. The type of ceramic significantly influences the character of film formation, as well as the total film thickness.
4. Under pure rolling, the lubricant film is developed mainly by the presence of albumin, while the rolling speed does not substantially influence the film thickness. On the contrary, the effect of speed can be clearly seen when the ball rotates faster than the disc.
5. In most cases, the dominant protein is albumin; however, γ-globulin exhibits stronger adsorption to the rubbing surfaces; therefore, it can form a thin boundary layer enabling albumin to adsorb onto it and increase the total film thickness eventually.
6. The results clearly show that mainly slide-to-roll ratio is a fundamental parameter affecting the character of protein film formation. The effect of rolling/sliding distance corresponding to rolling/sliding speed is also substantial, since it influences the total film thickness in most cases. Therefore, further investigation should be performed under pure negative sliding (rotating ball, stationary counterpart) to approach the kinematic conditions inside the joints.

To be able to better simulate in vivo conditions, several points must be taken into account in the following study, such as real conformity of surfaces, transient character of motion and load, and more complex model fluid.

Acknowledgements

This research was carried out under the project CEITEC 2020 (LQ1601) with financial support from the Ministry of Education, Youth and Sports of the Czech Republic under the National Sustainability Programme II. The research was also supported by the project no. FSI-S-14-2336 with the financial support from the Ministry of Education, Youth and Sports of the Czech Republic. The authors express thanks to M. Švachová for her help with the experiments.

REFERENCES

Azushima, A., 2006. In situ 3D measurement of lubrication behavior at interface between tool and workpiece by direct fluorescence observation technique. Wear 260 (3), 243–248.
Brockett, C., Williams, S., Jin, Z., et al., 2007. Friction of total hip replacements with different bearings and loading conditions. J. Biomed. Mater. Res. Part B: Appl. Biomater. 81 (2), 508–515.
Brockett, C.L., Williams, S., Jin, Z., et al., 2013. Squeaking hip arthroplasties: a tribological phenomenon. J. Arthroplast. 28 (1), 90–97.
Dowson, D., 2006. Tribological principles in metal-on-metal hip joint design. Proc. Inst. Mech. Eng. Part H: J. Eng. Med. 220 (2), 161–171.
Dowson, D., Jin, Z.M., 2006. Metal-on-metal hip joint tribology. Proc. Inst. Mech. Eng. Part H: J. Eng. Med. 220 (2), 107–118.
Fan, J., Myant, C.W., Underwood, R., et al., 2011. Inlet protein aggregation: a new mechanism for lubricating film formation with model synovial fluids. Proc. Inst. Mech. Eng. Part H: J. Eng. Med. 225 (7), 696–709.
Goldsmith, A.A.J., Dowson, D., Isaac, G.H., et al., 2000. A comparative joint simulator study of the wear of metal-on-metal and alternative material combinations in hip replacements. Proc. Inst. Mech. Eng. Part H: J. Eng. Med. 214 (1), 39–47.

Hartl, M., Křupka, I., Poliščuk, R., et al., 2001. Thin film colorimetric interferometry. Tribol. Trans. 44 (2), 270–276.
Heisel, C., Silva, M., Schmalzried, T.P., 2003. Bearing surface options for total hip replacement in young patients. J. Bone Jt. Surg. 85 (7), 1366–1379.
Jarrett, C.A., Ranawat, A.S., Bruzzone, M., et al., 2009. The squeaking hip: a phenomenon of ceramic-on-ceramic total hip arthroplasty. J. Bone Jt. Surg. 91 (6), 1344–1349.
Jie, N., Zhang, Q., Yang, J., et al., 1998. Determination of chromium in waste-water and cast iron samples by fluorescence quenching of rhodamine 6G. Talanta 46 (1), 215–219.
Joshi, A.B., Porter, M.L., Trail, I.A., et al., 1993. Long-term results of Charnley low-friction arthroplasty in young patients. J. Bone Jt. Surg. Br. 75 (4), 616–623.
Keurentjes, J.C., Kuipers, R.M., Wever, D.J., et al., 2008. High incidence of squeaking in THAs with alumina ceramic-on-ceramic bearings. Clin. Orthop. Relat. Res. 466 (6), 1438–1443.
Košťál, D., Nečas, D., Šperka, P., et al., 2015. Lubricant rupture ratio at elastohydrodynamically lubricated contact outlet. Tribol. Lett. 59, 3.
Malmsten, M., 1998. Formation of adsorbed protein layers. J. Colloid Interface Sci. 207 (2), 186–199.
Mavraki, A., Cann, P.M., 2009. Friction and lubricant film thickness measurements on simulated synovial fluids. Proc. Inst. Mech. Eng. Part J: J. Eng. Tribol. 223 (3), 325–335.
Mavraki, A., Cann, P.M., 2011. Lubricating film thickness measurements with bovine serum. Tribol. Int. 44 (5), 550–556.
Myant, C., Cann, P., 2013. In contact observation of model synovial fluid lubricating mechanisms. Tribol. Int. 63, 97–104.
Myant, C., Cann, P., 2014a. On the matter of synovial fluid lubrication: implications for metal-on-metal hip tribology. J. Mech. Behav. Biomed. Mater. 34, 338–348.
Myant, C., Cann, P., 2014b. The effect of transient conditions on synovial fluid protein aggregation lubrication. J. Mech. Behav. Biomed. Mater. 34, 349–357.
Myant, C., Reddyhoff, T., Spikes, H.A., 2010. Laser-induced fluorescence for film thickness mapping in pure sliding lubricated, compliant, contacts. Tribol. Int. 43 (11), 1960–1969.
Myant, C., Underwood, R., Fan, J., et al., 2012. Lubrication of metal-on-metal hip joints: the effect of protein content and load on film formation and wear. J. Mech. Behav. Biomed. Mater. 6, 30–40.
Nakashima, K., Sawae, Y., Murakami, T., 2007. Effect of conformational changes and differences of proteins on frictional properties of poly (vinyl alcohol) hydrogel. Tribol. Int. 40 (10), 1423–1427.
Nečas, D., Vrbka, M., Urban, F., et al., 2015a. The effect of lubricant constituents on lubrication mechanisms in hip joint replacements. J. Mech. Behav. Biomed. Mater. 55, 295–307.
Nečas, D., Šperka, P., Vrbka, M., et al., 2015b. Film thickness mapping in lubricated contacts using fluorescence. MM Sci. J. (04), 821–824.
Parkes, M., Myant, C., Cann, P.M., et al., 2014. The effect of buffer solution choice on protein adsorption and lubrication. Tribol. Int. 72, 108–117.
Parkes, M., Myant, C., Cann, P.M., et al., 2015. Synovial fluid lubrication: the effect of protein interactions on adsorbed and lubricating films. Biotribology 1–2, 51–60.
Pramanik, S., Agarwal, A.K., Rai, K.N., 2005. Chronology of total hip joint replacement and materials development. Trends Biomater. Artif. Organs 19 (1), 15–26.
Reddyhoff, T., Choo, J.H., Spikes, H.A., et al., 2010. Lubricant flow in an elastohydrodynamic contact using fluorescence. Tribol. Lett. 38 (3), 207–215.
Sawae, Y., Yamamoto, A., Murakami, T., 2008. Influence of protein and lipid concentration of the test lubricant on the wear of ultra high molecular weight polyethylene. Tribol. Int. 41 (7), 648–656.
Smith, S.L., Dowson, D., Goldsmith, A.A.J., 2001. The effect of femoral head diameter upon lubrication and wear of metal-on-metal total hip replacements. Proc. Inst. Mech. Eng. Part H: J. Eng. Med. 215 (2), 161–170.
Scholes, S.C., Unsworth, A., 2006. The effects of proteins on the friction and lubrication of artificial joints. Proc. Inst. Mech. Eng. Part H: J. Eng. Med. 220 (6), 687–693.
Sugimura, J., Hashimoto, M., Yamamoto, Y., 2000. Study of elastohydrodynamic contacts with fluorescence microscope. Tribol. Ser. 38, 609–617.
Vrbka, M., Návrat, T., Křupka, I., et al., 2013. Study of film formation in bovine serum lubricated contacts under rolling/sliding conditions. Proc. Inst. Mech. Eng. Part J: J. Eng. Tribol. 227 (5), 459–475.
Vrbka, M., Křupka, I., Hartl, M., et al., 2014. In situ measurements of thin films in bovine serum lubricated contacts using optical interferometry. Proc. Inst. Mech. Eng. Part H: J. Eng. Med. 228 (2), 149–158.
Vrbka, M., Nečas, D., Bartošík, J., et al., 2015a. Determination of a friction coefficient for THA bearing couples. Acta Chir. Orthop. Traumatol. Cechoslov. 82 (5), 341–347.
Vrbka, M., Nečas, D., Hartl, M., et al., 2015b. Visualization of lubricating films between artificial head and cup with respect to real geometry. Biotribology 1–2, 61–65.
Walter, W.L., Yeung, E., Esposito, C., 2010. A review of squeaking hips. J. Am. Acad. Orthop. Surg. 18 (6), 319–326.
Wang, A., Essner, A., Schmidig, G., 2004. The effects of lubricant composition on in vitro wear testing of polymeric acetabular components. J. Biomed. Mater. Res. Part B: Appl. Biomater. 68 (1), 45–52.

6 CONCLUSIONS

The present dissertation deals with the lubrication mechanisms within hip replacements. Although total hip arthroplasty became one of the most successful and most applied surgery; the service life of implants is still limited. As the main attention of the researchers was paid to the quantification of wear rate previously, so far, little is known about the lubrication mechanisms inside the contact. However, such a knowledge can help to better understand the mechanisms leading to implant failure. Recently, the protein film development was studied in a model ball-on-disc configuration, while several effects were extensively investigated. One of the most important factor seems to be the composition of model SF. Nevertheless, none of the performed studies could explain the role of particular proteins contained in SF in relation to the protein film formation. When focusing on individual constituents, only simple protein solutions were used; which does not correspond to the behaviour of complex fluids. To be able to distinguish the constituents in lubricant, optical method based on fluorescent microscopy was developed as a part of the PhD thesis.

The first part of the thesis discusses potential experimental approaches for in situ analysis of film thickness inside the contact. A fluorescent method is described in a greater detail, presenting the possibilities of the method published in the last 40 years. Consequently, the studies focusing on the protein film formation in hip replacements are introduced, giving the general overview of the parameters apparently influencing the protein film. The defined aim of the thesis comes from the critical analysis of the current state of the art in the field. The latter part deals with the employed experimental devices and applied measurement methods.

The main goal of the thesis was to perform an experimental analysis of protein film formation focusing on the role of the particular proteins. For this purpose, fluorescent method was developed and verified by the measurement of film thickness in EHL and i-EHL contact. The ability of the method is later demonstrated as a tool for the quantification of the lubricant division at EHL contact outlet. As the method was supported by optical interferometry, the use of the method for the measurement of film thickness considering real conformity of rubbing surfaces is also presented. Finally, the methodological approach for the assessment of the role of proteins while the simultaneous presence of another protein on lubrication mechanisms within hip replacements is widely presented.

The current thesis contains original results extending the knowledge in the area of hip joint replacements lubrication. The results are confronted with the previous studies. The further step is to employ a developed methodology approaching the real conditions in joints such as conformity, multidirectional motion, transient loading conditions and higher complexity of model SF.

The main contribution of the thesis can be summarized into the following points:

- For the first time, protein film formation under real conformity of rubbing surfaces was analysed in situ.
- An optical method based on fluorescent microscopy was developed, enabling direct measurement of film thickness in both, rigid and compliant contacts.

- The ability of the fluorescent method was demonstrated investigating lubricant division at EHL contact outlet.
- Analysis of protein film formation within hip joint replacements with respect to implant material and various operating conditions was conducted, focusing on the role of particular SF proteins, considering complex model fluids.

Regarding to scientific question, the obtained knowledge can be summarized to the following concluding remarks:

- Contrary to previously published results, it was found that under most conditions, albumin protein is responsible for film thickness development. This proves that it is necessary to study complex model fluids, not just the simple protein solutions, since the interaction of the constituents can substantially affect the formation of the protein film (**HYPOTHESIS WAS FALSIFIED**).
- Under pure rolling conditions, film formation was similar for metal and ceramic heads, while the total film thickness was higher in the case of metal (especially at higher rolling speed), confirming the effect of surface wettability. However, when rolling/sliding conditions were taken into account, the character of film formation was completely different, dependent on implant material, sliding speed, and positivity/negativity of the slippage, while the thickness was higher in the case of ceramic heads, in general (**HYPOTHESIS WAS FALSIFIED**).
- From the investigated factors, the main parameter influencing the protein formation is indisputably the level of slippage between the surfaces (**HYPOTHESIS WAS CONFIRMED**).
- With the exception of partial positive sliding, film thickness was always higher at higher rolling/sliding speed (**HYPOTHESIS WAS FALSIFIED**).

7 LIST OF PUBLICATIONS

7.1 Papers published in journals with impact factor

KOŠŤÁL, D.; NEČAS, D.; ŠPERKA, P.; SVOBODA, P.; KŘUPKA, I.; HARTL, M. Lubricant rupture ratio at elastohydrodynamically lubricated contact outlet. *Tribology Letters*, 2015, 59(3), 1-9.
(Journal impact factor = 1.74)

VRBKA, M.; NEČAS, D.; BARTOŠÍK, J.; HARTL, M.; KŘUPKA, I.; GALANDÁKOVÁ, A.; GALLO, J. Determination of a friction coefficient for THA bearing couples. *Acta chirurgiae orthopaedicae et traumatologiae Cechoslovaca*, 2015, 82(5), 341-347.
(Journal impact factor = 0.39)

TKACHENKO, S.; NEČAS, D.; DATSKEVICH, O.; ČUPERA, J.; SPOTZ, Z.; VRBKA, M.; KULAK, L.; FORET, R. Tribological performance of Ti–Si based in situ composites. *Tribology Transactions*. 2016, 59(2), 340-351.
(Journal impact factor = 1.35)

NEČAS, D.; VRBKA, M.; URBAN, F.; KŘUPKA, I.; HARTL, M. The effect of lubricant constituents on lubrication mechanisms in hip joint replacements. *Journal of the Mechanical Behavior of Biomedical Materials*, 2016, 55, 295-307.
(Journal impact factor = 2.88)

NEČAS, D.; VRBKA, M.; KŘUPKA, I.; HARTL, M.; GALANDÁKOVÁ, A. Lubrication within hip replacements – Implication for ceramic-on-hard bearing couples. *Journal of the Mechanical Behavior of Biomedical Materials*, 2016, 61, 371-383.
(Journal impact factor = 2.88)

NEČAS, D.; VRBKA, M.; URBAN, F.; GALLO, J.; KŘUPKA, I.; HARTL, M. In situ observation of lubricant film formation in THR considering real conformity: The effect of diameter, clearance and material. *Journal of the Mechanical Behavior of Biomedical Materials*.
UNDER REVIEW (after first revision)
(Journal impact factor = 2.88)

NEČAS, D.; VRBKA, M.; REBENDA, D.; GALLO, J.; WOLFOVÁ, L.; KŘUPKA, I.; HARTL, M. In situ observation of lubricant film formation in THR considering real conformity: The effect of model synovial fluid composition. *Journal of the Mechanical Behavior of Biomedical Materials*.
UNDER REVIEW
(Journal impact factor = 2.88)

7.2 Papers published in peer-reviewed journals

NEČAS, D.; ŠPERKA, P.; VRBKA, M.; KŘUPKA, I.; HARTL, M. Film thickness mapping in lubricated contacts using fluorescence. *MM Science Journal*, 2015, 2015(4), 821-824.

VRBKA, M.; NEČAS, D.; HARTL, M.; KŘUPKA, I.; URBAN, F.; GALLO, J. Visualization of lubricating films between artificial head and cup with respect to real geometry. *Biotribology*, 2015, 1-2, 61-65.

7.3 Papers in conference proceedings

NEČAS, D., VRBKA, M.; ŠPERKA, P.; DRUCKMÜLLER, M.; SKLÁDAL, P.; ŠTARHA, P.; KŘUPKA, I.; HARTL, M. Qualitative analysis of film thickness in rolling EHD contact by fluorescence technique. *Lecture Notes in Mechanical Engineering*, 2014, 615-622.

TKACHENKO, S.; NEČAS, D.; DATSKEVICH, O.; ČUPERA, J.; SPOTZ, Z.; VRBKA, M.; KULAK, L.; FORET, R. Tribological behavior of Ti– Si based in situ composites under sliding. *Metal 2014*, 2014, 2704-2709.

NEČAS, D., VRBKA, M.; YARIMITSU, S.; NAKASHIMA, K.; SAWAE, Y.; ŠPERKA, P.; KŘUPKA, I.; HARTL, M. Frictional properties of PVA hydrogel. *The Latest Methods of Construction Design*, 2016, 159-164.

7.4 Conference abstracts

VRBKA, M.; NEČAS, D.; URBAN, F.; KŘUPKA, I.; HARTL, M.; GALLO, J. A novel approach for in situ observation of lubricant film at the interface between artificial head and cup of THA. *EORS 22nd Annual Meeting*, 2014, Nantes, France.

SAWAE, Y.; VRBKA, M.; URBAN. F.; NEČAS, D.; YARIMITSU, S.; NAKASHIMA, K.; MURAKAMI, T.; HARTL, M. Friction characterization of ceramic-on-hydrogel hip joint in pendulum test. *2nd International Conference on Biotribology*, 2014, Toronto, Canada.

NEČAS, D.; SAWAE, Y.; YARIMITSU, S.; NAKASHIMA, K.; VRBKA, M.; HARTL, M.; MURAKAMI, T. Protein adsorbed film formation and frictional characteristics of CoCrMo-on-UHMWPE sliding pair in reciprocating sliding test. *2nd International Conference on Biotribology*, 2014, Toronto, Canada.

NEČAS, D.; VRBKA, M.; URBAN, F.; KŘUPKA, I.; HARTL, M.; GALLO, J. Observation of lubricant film between artificial head and cup. *Tribology Frontiers Conference*, 2014, Chicago, USA.

KOŠŤÁL, D.; NEČAS, D.; ŠPERKA, P.; SVOBODA, P.; KŘUPKA, I.; HARTL, M. Lubricant division in EHL contact outlet. *Tribology Frontiers Conference*, 2014, Chicago, USA.

URBAN, F.; NEČAS, D.; VRBKA, M.; KŘUPKA, I.; HARTL, M.; GALLO, J. In Situ Observation of Lubricant Film within Artificial Hip Joints. *International Tribology Conference*, 2015, Tokyo, Japan.

NEČAS, D.; VRBKA, M.; URBAN, F.; KŘUPKA, I.; HARTL, M.; GALLO, J. An experimental investigation of lubricant film formation in artificial hip joints. *The 8th International Biotribology Forum, The 36th Biotribology Symposium*, 2015, Yokohama, Japan.

NEČAS, D.; ŠVACHOVÁ, M.; VRBKA, M.; KŘUPKA, I.; HARTL, M. The effect of albumin and γ-globulin on lubricant film formation in artificial hip joints. *The 17th Nordic Symposium on Tribology - NORDTRIB 2016*, 2016, Hämeenlinna, Finland.

8 LITERATURE

[1] OECD (2015), Health at a Glance 2015: OECD Indicators, OECD Publishing, Paris.

[2] PRAMANIK, S.; AGARWAL, A.K.; RAI, K.N. Chronology of total hip joint replacement and materials development. *Trends in Biomaterials & Artificial Organs*, 2005, 19(1), 15-26.

[3] JOSHI, A.B.; PORTER, M.L.; TRAIL, I.A.; HUNT, L.P.; MURPHY, J.C.M.; HARDINGE, K. Long-term results of Charnley low-friction arthroplasty in young patients. *Journal of Bone and Joint Surgery-British Volume,* 1993, 75(4), 616-623.

[4] GOLDSMITH, A.A.J.; DOWSON, D.; ISAAC, J.H., LANCASTER, J.G. A comparative joint simulator study of the wear of metal-on-metal and alternative material combinations in hip replacements. *Proceedings of the Institution of Mechanical Engineers, Part H: Journal of Engineering in Medicine*, 2000, 214(1), 39-47.

[5] SMITH, S.L.; DOWSON, D.; GOLDSMITH, A.A.J. The effect of femoral head diameter upon lubrication and wear of metal-on-metal total hip replacements. *Proceedings of the Institution of Mechanical Engineers, Part H: Journal of Engineering in Medicine*, 2001, 215(2), 161-170.

[6] WANG, A.; ESSNER, A.; SCHMIDIG, G. The effects of lubricant composition on in vitro wear testing of polymeric acetabular components. *Journal of Biomedical Materials Research Part B: Applied Biomaterials*, 2004, 68(1), 45-52.

[7] HEISEL, C.; SILVA, M.; SCHMALZRIED, T.P. Bearing surface options for total hip replacement in young patients. *The Journal of Bone & Joint Surgery*, 2003, 85(7), 1366-1379.

[8] JIN, Z.M.; STONE, M.; INGHAM, E.; FISHER, J. (v) Biotribology. *Current Orthopaedics*, 2006, 20(1), 32-40.

[9] DOWSON, D. Tribological principles in metal-on-metal hip joint design. *Proceedings of the Institution of Mechanical Engineers, Part H: Journal of Engineering in Medicine*, 2006, 220(2), 161-171.

[10] JALALI-VAHID, D.; JIN, Z.M.; DOWSON, D. Effect of start-up conditions on elastohydrodynamic lubrication of metal-on-metal hip implants. *Proceedings of the Institution of Mechanical Engineers, Part J: Journal of Engineering Tribology*, 2006, 220(3), 143-150.

[11] DOWSON, D.; JIN, Z.M. Metal-on-metal hip joint tribology. *Proceedings of the Institution of Mechanical Engineers, Part H: Journal of Engineering in Medicine*, 2006, 220(2), 107-118.

[12] MAVRAKI, A.; CANN, P.M. Lubricating film thickness measurements with bovine serum. *Tribology International*, 2011, 44(5), 550-556.

[13] MYANT, C.; CANN, P. In contact observation of model synovial fluid lubricating mechanisms. *Tribology International*, 2013, 63, 97-104.

[14] PARKES, M.; MYANT, C.; CANN, P.M.; WONG, J.S.S. Synovial Fluid Lubrication: The Effect of Protein Interactions on Adsorbed and Lubricating Films. *Biotribology*, 2015, 1-2, 51-60.

[15] SCHOLES, S.C.; UNSWORTH, A. The effects of proteins on the friction and lubrication of artificial joints. *Proceedings of the Institution of Mechanical Engineers, Part H: Journal of Engineering in Medicine*, 2006, 220(6), 687-693.

[16] WIMMER, M.A.; SPRECHER, C.; HAUERT, R.; TAGER, G.; FISCHER, A. Tribochemical reaction on metal-on-metal hip joint bearings: a comparison between in-vitro and in-vivo results. *Wear*, 2003, 255(7), 1007-1014.

[17] POLL, G.; GABELLI, A. Formation of Lubricant Film in Rotary Sealing Contacts: Part II: A New Measuring Principle for Lubricant Film Thickness. *Journal of Tribology*, 1992, 114(2), 290-296.

[18] SPIKES, H.A. Thin films in elastohydrodynamic lubrication: the contribution of experiment. *Proceedings of the Institution of Mechanical Engineers, Part J: Journal of Engineering Tribology*, 1999, 213(5), 335-352.

[19] ALBAHRANI, S., PHILIPPON, D.; VERGNE, P.; BLUET, J. A review of in situ methodologies for studying elastohydrodynamic lubrication. *Proceedings of the Institution of Mechanical Engineers, Part J: Journal of Engineering Tribology*, 2015, 230(1), 86-110.

[20] DOWSON, D.; MCNIE, C.M.; GOLDSMITH, A.A.J. Direct experimental evidence of lubrication in a metal-on-metal total hip replacement tested in a joint simulator. *Proceedings of the Institution of Mechanical Engineers, Part C: Journal of Mechanical Engineering Science*, 2000, 214(1), 75-86.

[21] SMITH, S.L., DOWSON, D.; GOLDSMITH, A.A.J. Direct evidence of lubrication in ceramic-on-ceramic total hip replacements. *Proceedings of the Institution of Mechanical Engineers, Part C: Journal of Mechanical Engineering Science*, 2001, 215(3), 265-268.

[22] HARTL, M., KŘUPKA, I.; POLIŠČUK, R.; LIŠKA, M.; MOLIMARD, J.; QUERRY, M.; VERGNE, P. Thin Film Colorimetric Interferometry. *Tribology Transactions*, 2001, 44(2), 270-276.

[23] SMART, A.E.; FORD R.A.J. Measurement of thin liquid films by a fluorescence technique. *Wear*, 1974, 29(1), 41-47.

[24] FORD, R.A.J.; FOORD, C.A. Laser-based fluorescence techniques for measuring thin liquid films. *Wear*, 1978, 51(2), 289-297.

[25] GABELLI, A.; POLL, G. Formation of Lubricant Film in Rotary Sealing Contacts: Part I: Lubricant Film Modeling. *Journal of Tribology*, 1992, 114(2), 280-287.

[26] POLL, G.; GABELLI, A.; BINNINGTON, P.G.; QU, J. Dynamic mapping of rotary lip seal lubricant films by fluorescent image processing. *Fluid Sealing*, 1992, 55-77, Springer Netherlands.

[27] GOHAR, R. A ball-and-plate machine for measuring elasthoydrodynamic oil films. *Proceedings of the Institution of Mechanical Engineers, Conference Proceedings*, 1967, 182(37), 43-45.

[28] SUGIMURA, J., HASHIMOTO, M.; YAMAMOTO, Y. Study of elastohydrodynamic contacts with fluorescence microscope. *Tribology series*, 2000, 38, 609-617.

[29] HIDROVO, C.H.; HART, D.P. Dual emission laser induced fluorescence technique (DELIF) for oil film thickness and temperature measurement. *AMSE/JSME Fluids Engineering Decision Summer Meeting*, 2000, 23-28.

[30] HIDROVO, C.H.; HART, D.P. Emission reabsorption laser induced fluorescence (ERLIF) film thickness measurement. *Measurement Science and Technology*, 2001, 12(4), 467-477.

[31] AZUSHIMA, A. In lubro 3D measurement of oil film thickness at the interface between tool and workpiece in sheet drawing using a fluorescence microscope. *Tribology International*, 2005, 38(2), 105-112.

[32] AZUSHIMA, Akira. In situ 3D measurement of lubrication behavior at interface between tool and workpiece by direct fluorescence observation technique. *Wear*, 2006, 260(3), 243-248.

[33] REDDYHOFF, T.; CHOO, J.H.; SPIKES, H.A.; GLOVNEA, R.P. Lubricant Flow in an Elastohydrodynamic Contact Using Fluorescence. *Tribology Letters*, 2010, 38(3), 207-215.

[34] PONJAVIC, A.; CHENNAOUI, M.; WONG, J.S.S. Through-Thickness Velocity Profile Measurements in an Elastohydrodynamic Contact. *Tribology Letters*, 2013, 50(2), 261-277.

[35] QIAN, S.; GUO, D.; LIU, S.; LU, X. Experimental Investigation of Lubrication Failure of Polyalphaolefin Oil Film at High Slide/Roll Ratios. *Tribology Letters*, 2011, 44(2), 107-115.

[36] QIAN, S.; GUO, D.; LIU, S.; LU, X. Experimental Investigation of Lubricant Flow Properties Under Micro Oil Supply Condition. *Journal of Tribology*, 2012, 134(4), 041501.

[37] XIAO, H.; GUO, D.; LIU, S.; XIE, G.; PAN, G.; LU, X.; LUO, J. Direct observation of oil displacement by water flowing toward an oil nanogap. *Journal of Applied Physics*. 2011, 110(4), 044906.

[38] MYANT, C.; REDDYHOFF, T.; SPIKES, H.A. Laser-induced fluorescence for film thickness mapping in pure sliding lubricated, compliant, contacts. *Tribology International,* 2010, 43(11), 1960-1969.

[39] BONGAERTS, J.H.H.; DAY, J.P.R.; MARRIOTT, C.; PUDNEY, P.D.A.; WILLIAMSON, A.M. In situ confocal Raman spectroscopy of lubricants in a soft elastohydrodynamic tribological contact. *Journal of Applied Physics*, 2008, 104(1), 014913.

[40] MYANT, C.; FOWELL, M.; CANN, P. The effect of transient motion on Isoviscous-EHL films in compliant, point, contacts. *Tribology International*, 2014, 72, 98-107.

[41] FOWELL, M.T.; MYANT, C.; SPIKES, H.A.; KADIRIC, A. A study of lubricant film thickness in compliant contacts of elastomeric seal materials using a laser induced fluorescence technique. *Tribology International*, 2014, 80, 76-89.

[42] HAMROCK, B.J.; DOWSON, D. Elastohydrodynamic Lubrication of Elliptical Contacts for Materials of Low Elastic Modulus I—Fully Flooded Conjunction. *Journal of Lubrication Technology*, 1978, 100(2), 236-245.

[43] NIJENBANNING, G.; VENNER, C.H.; MOES, H. Film thickness in elastohydrodynamically lubricated elliptic contacts. *Wear*, 1994, 176(2), 217-229.

[44] MAVRAKI, A.; CANN, P.M. Friction and lubricant film thickness measurements on simulated synovial fluids. *Proceedings of the Institution of Mechanical Engineers, Part J: Journal of Engineering Tribology*, 2009, 223(3), 325-335.

[45] FAN, J.; MYANT, C.W.; UNDERWOOD, R.; CANN, P.M.; HART, A. Inlet protein aggregation: a new mechanism for lubricating film formation with model synovial fluids. *Proceedings of the Institution of Mechanical Engineers, Part H: Journal of Engineering in Medicine*, 2011, 225(7), 696-709.

[46] MYANT, C.; UNDERWOOD, R.; FAN, J.; CANN, P.M. Lubrication of metal-on-metal hip joints: the effect of protein content and load on film formation and wear. *Journal of the mechanical behavior of biomedical materials*, 2012, 6, 30-40.

[47] MYANT, C.; CANN, P. In contact observation of model synovial fluid lubricating mechanisms. *Tribology International*, 2013, 63, 97-104.

[48] MYANT, C.; CANN, P. On the matter of synovial fluid lubrication: Implications for Metal-on-Metal hip tribology. *Journal of the Mechanical Behavior of Biomedical Materials*, 2014, 34, 338-348.

[49] VRBKA, M.; NÁVRAT, T.; KŘUPKA, I.; HARTL, M.; ŠPERKA, P.; GALLO, J. Study of film formation in bovine serum lubricated contacts under rolling/sliding conditions. *Proceedings of the Institution of Mechanical Engineers, Part J: Journal of Engineering Tribology*, 2013, 227(5), 459-475.

[50] VRBKA, M., KŘUPKA, I.; HARTL, M.; NÁVRAT, T.; GALLO, J.; GALANDÁKOVÁ, A. In situ measurements of thin films in bovine serum lubricated contacts using optical interferometry. *Proceedings of the Institution of Mechanical Engineers, Part H: Journal of Engineering in Medicine*, 2014, 228(2), 149-158.

[51] MYANT, C.W.; CANN, P. The effect of transient conditions on synovial fluid protein aggregation lubrication. *Journal of the Mechanical Behavior of Biomedical Materials*, 2014, 34, 349-357.

[52] STANTON, T.E. Boundary lubrication in engineering practice. *Engineer*, 1923, 135, 678–680.

[53] CRISCO, J.J.; BLUME, J.; TEEPLE, E.; FLEMING, B.C.; JAY, G.D. Assuming exponential decay by incorporating viscous damping improves the prediction of the coefficient of friction in pendulum tests of whole articular joints. *Proceedings of the Institution of Mechanical Engineers, Part H: Journal of Engineering in Medicine*, 2007, 221(3), 325-333.

[54] HAUGLAND, R.P.; SPENCE, M.T.Z.; JOHNSON, I.D. Handbook of fluorescent probes and research chemicals. 6th ed. Eugene, OR, USA (4849 Pitchford Ave., Eugene 97402): Molecular Probes, c1996. ISBN 0965224007.

[55] JIE, N.; ZHANG, Q.; YANG, J.; HUANG, X. Determination of chromium in waste-water and cast iron samples by fluorescence quenching of rhodamine 6G. *Talanta*, 46(1), 215-219.

[56] VARNES, A.W.; DODSON, R.B.; WEHRY, E.L. Interactions of transition-metal ions with photoexcited states of flavines. Fluorescence quenching studies. *Journal of the American Chemical Society*. 1972, 94(3), 946-950.

[57] ZHANG, L.; XU, C.; LI, B. Simple and sensitive detection method for chromium(VI) in water using glutathione—capped CdTe quantum dots as fluorescent probes. *Microchimica Acta*. 2009, 166(1-2), 61-68.

[58] HAMROCK, B.J.; DOWSON, D. Isothermal elastohydrodynamic lubrication of point contacts: part III—fully flooded results. *Journal of Lubrication Technology*, 1977, 99(2), 264-275.

[59] HAMROCK, B.J.; DOWSON, D. Elastohydrodynamic lubrication of elliptical contacts for materials of low elastic modulus I—fully flooded conjunction. *Journal of Lubrication Technology*, 1978, 100(2), 236-245.

[60] BRUYERE, V.; FILLOT, N.; MORALES-ESPEJEL, G.E.; VERGNE, P. A Two-Phase Flow Approach for the Outlet of Lubricated Line Contacts. *Journal of Tribology*, 2012, 134(4), 041503.

[61] BROCKETT, C.; WILLIAMS, S.; JIN, Z.; ISAAC, G.; FISHER, J. Friction of total hip replacements with different bearings and loading conditions. *Journal of Biomedical Materials Research Part B: Applied Biomaterials*, 2007, 81B(2), 508-515.

LIST OF FIGURES AND TABLES

LIST OF SYMBOLS, PHYSICAL CONSTANTS AND ABBREVIATIONS

η	Pa·s	Dynamic viscosity
λ	nm	Wavelength

BS	Bovine serum
CMOS	Complementary metal-oxide-semiconductor
COF	Coefficicent of friction
DELIF	Dual emission laser induced fluorescence
EHD	Elastohydrodynamic
EHL	Elastohydrodynamic lubricated
ERLIF	Emission reabsorption laser induced fluorescence
FITC	Fluorescein-5-isothiocyanate
FKM	Fluorocarbon rubber
FRAP	Fluorescence recovery after photobleaching
HXPE	Highly cross-linked polyethylene
i-EHL	Isoviscous-elastohydrodynamic lubricated
LIF	Laser induced fluorescence
IMID	Institute of Machine and Industrial Design
MTM	Mini traction machine
PAL	Protein aggregation lubrication
PBS	Phosphate-buffered saline
PDMS	Polydimethylsiloxane
RBITC	Rhodamine-B-isothiocyanate
sCMOS	Scientific complementary metal-oxide-semiconductor
SF	Synovial fluid
SRR	Slide-to-roll ratio
UHMWPE	Ultra-high molecular weight polyethylene